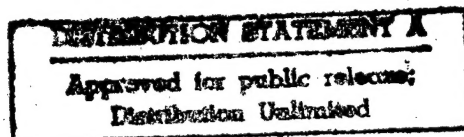


188025

JPRS-UMS-87-005

11 MAY 1987



USSR Report

MATERIALS SCIENCE AND METALLURGY

COMPLEX SUBSATELLITE OCEANOGRAPHIC EXPERIMENT
OF THE USSR AND GDR ON THE BALTIC SEA

19980811 172

SPECIAL NOTICE INSIDE

FBIS

FOREIGN BROADCAST INFORMATION SERVICE

REPRODUCED BY
U.S. DEPARTMENT OF COMMERCE
NATIONAL TECHNICAL
INFORMATION SERVICE
SPRINGFIELD, VA 22161

9
102
A06

SPECIAL NOTICE

Effective 1 June 1987 JPRS reports will have a new cover design and color, and some reports will have a different title and format. Some of the color changes may be implemented earlier if existing supplies of stock are depleted.

The new cover colors will be as follows:

CHINA.....aqua
EAST EUROPE.....gold
SOVIET UNION.....salmon
EAST ASIA.....yellow
NEAR EAST & SOUTH ASIA...blue
LATIN AMERICA.....pink
WEST EUROPE.....ivory
AFRICA (SUB-SAHARA).....tan
SCIENCE & TECHNOLOGY.....gray
WORLDWIDES.....pewter

The changes that are of interest to readers of this report are as follows:

All science and technology material will be found in the following SCIENCE & TECHNOLOGY series:

CHINA (CST)
CHINA/ENERGY (CEN)
EUROPE & LATIN AMERICA (ELS)
JAPAN (JST)
USSR: COMPUTERS (UCC)
USSR: EARTH SCIENCES (UES)
USSR: MATERIALS SCIENCE (UMS)
USSR: LIFE SCIENCES (ULS)
USSR: CHEMISTRY (UCH)
USSR: ELECTRONICS & ELECTRICAL ENGINEERING (UEE)
USSR: PHYSICS & MATHEMATICS (UPM)
USSR: SPACE (USP)
USSR: SPACE BIOLOGY & AEROSPACE MEDICINE (USB)
USSR: SCIENCE & TECHNOLOGY POLICY (UST)
USSR: ENGINEERING & EQUIPMENT (UEQ)

The USSR REPORT: MACHINE TOOLS AND METALWORKING EQUIPMENT (UMM) will no longer be published. Material formerly found in this report will appear in the SCIENCE & TECHNOLOGY/USSR: ENGINEERING & EQUIPMENT (UEQ) series.

If any subscription changes are desired, U.S. Government subscribers should notify their distribution contact point. Nongovernment subscribers should contact the National Technical Information Service, 5285 Port Royal Road, Springfield, Virginia 22161.

NOTE

JPRS publications contain information primarily from foreign newspapers, periodicals and books, but also from news agency transmissions and broadcasts. Materials from foreign-language sources are translated; those from English-language sources are transcribed or reprinted, with the original phrasing and other characteristics retained.

Headlines, editorial reports, and material enclosed in brackets [] are supplied by JPRS. Processing indicators such as [Text] or [Excerpt] in the first line of each item, or following the last line of a brief, indicate how the original information was processed. Where no processing indicator is given, the information was summarized or extracted.

Unfamiliar names rendered phonetically or transliterated are enclosed in parentheses. Words or names preceded by a question mark and enclosed in parentheses were not clear in the original but have been supplied as appropriate in context. Other unattributed parenthetical notes within the body of an item originate with the source. Times within items are as given by source.

The contents of this publication in no way represent the policies, views or attitudes of the U.S. Government.

PROCUREMENT OF PUBLICATIONS

JPRS publications may be ordered from the National Technical Information Service (NTIS), Springfield, Virginia 22161. In ordering, it is recommended that the JPRS number, title, date and author, if applicable, of publication be cited.

Current JPRS publications are announced in Government Reports Announcements issued semimonthly by the NTIS, and are listed in the Monthly Catalog of U.S. Government Publications issued by the Superintendent of Documents, U.S. Government Printing Office, Washington, D.C. 20402.

Correspondence pertaining to matters other than procurement may be addressed to Joint Publications Research Service, 1000 North Glebe Road, Arlington, Virginia 22201.

Soviet books and journal articles displaying a copyright notice are reproduced and sold by NTIS with permission of the copyright agency of the Soviet Union. Permission for further reproduction must be obtained from copyright owner.

11 MAY 1987

USSR REPORT
MATERIALS SCIENCE AND METALLURGY
COMPLEX SUBSATELLITE OCEANOGRAPHIC EXPERIMENT
OF THE USSR AND GDR ON THE BALTIC SEA

Leningrad KOMPLEKSNIY PODSPYTNIKOVYY OKEANOGRAFICHESKIY EKSPERIMENT
SSSR I GDR NA BALTIYSKOM MORE in Russian 1985, pp 1-105

[Book "Complex Subsatellite Oceanographic Experiment of the USSR and
GDR na Baltiyskom More" edited by S. V. Viktorov, Gidrometeoizdat,
690 copies, 105 pages]

CONTENTS

Foreword (p 3).....	1
Editor's Note (p 5).....	3
1. The Role of Subsatellite Research in the Development of Methods of Remotely Sensing the Earth and the World Ocean (p 7).....	4
1.1. Structure of the System of Subsatellite Measurements and Observations (p 7).....	4
1.2. Subsatellite Information Bank (p 8).....	5
1.3. Airborne Means for Gathering Reference Oceanographic Information (p 10).....	7
1.4. Collection of Surface-Level Reference Data (p 16).....	13
2. Basic Information on the Complex Subsatellite Oceanographic Experiment (p 18).....	15
2.1. Goals and Tasks of the Experiment (p 18).....	15
2.2. Content of Technical Means, Measurements and Observations (p 20).....	17
2.3. General Concept of Experiment Organization. Experiment Control (p 24).....	19
2.4. Execution of the Experiment. Brief Description of the Information Obtained (p 29).....	25
2.5. Weather Conditions During the Experiment (p 33).....	29

3.	Accumulation of Satellite and Reference Oceanographic Data in the Format of a Regional Information Bank (p 37).....	32
3.1.	Data Bank Structure (p 37).....	34
3.2.	List of Operations Performed (p 41).....	38
4.	Complex Hydrooptical Research in the Central Baltic Sea (p 42)....	39
4.1.	Distribution of Suspended Matter and Chlorophyll in the Experiment Region Based on Vessel Measurements (p 42)	39
4.2.	Several Results of Vessel Research on the Surface Spectral Brightness of the Baltic Sea (p 49)	43
4.3.	Determination of the Sea Color Index From Measurements Made Through the Atmosphere (p 52).....	49
4.4.	Relationships Between Atmosphere Optical Thickness and a) the Horizontal Visibility Range and b) the Sky Radiation Brightness Under Various Atmospheric Conditions Above the Baltic Sea (p 56).....	52
4.5.	Investigation of the Radiation Brightness Field of the Water+Atmosphere System From Satellite Images of the Baltic Sea (p 60).....	58
4.6.	Conclusion (p 64).....	61
5.	Complex Research of the Baltic Sea Temperature Field (p 65).....	62
5.1.	Distribution of Thermodynamic Temperature of the Water in the Experiment Region According to Measurements Made on the Vessel A. v. Humboldt (p 65).....	62
5.2.	Analysis of Sea Surface Layer Temperature (TSSL) in the Test Areas (p 69).....	65
5.3.	Analysis of TSS Measurements by Airborne IR Radiometer on the Sea Test Area (p 75).....	71
5.4.	Analysis of the Influence of the Atmosphere on the Measurements of the Baltic Sea Surface Temperature According to Aerological Sounding Data and Climatic Data (p 80).....	76
5.5.	Analysis of Satellite Measurements of the Temperature Field of the Baltic Sea Surface with an Evaluation of the Atmospheric Corrections (p 83).....	79
5.6.	Conclusion (p 91).....	85
6.	Basic Results of the Experiment (p 94).....	89
	Bibliography (p 98).....	92

UDC 551.46.0 : 629.78

COMPLEX SUBSATELLITE OCEANOGRAPHIC EXPERIMENT OF THE USSR AND GDR IN THE
BALTIC SEA

Leningrad KOMPLEKSNIY PODSPUTNIKOVYY OKEANOGRAFICHESKIY EKSPERIMENT SSSR I
GDR NA BALTIYSKOM MORE in Russian 1985 (signed to press 02 Apr 85) pp 1-105

[Book edited by S.V. Viktorov, candidate of physico-mathematical sciences,
Gidrometeoizdat, 690 copies, 105 pages]

[Text] Annotation

Problems of preparing and executing the first joint complex subsatellite
experiment of the USSR and GDR in the Baltic Sea (April, 1982) are
discussed.

This collection was prepared by scientists from both countries.

Present views on the role of subsatellite experiments in the development of
satellite oceanography are presented. Information is given on the goals of
the international experiment and on the complement of satellite measurement
devices, airplane laboratories and research vessels. The general concept
of organizing the synchronous measurement of radiative and thermodynamic
sea temperatures and water-mass optical characteristics, as well as
additional oceanographic and meteorological characteristics synchronously
with measurements from satellites in the visible and infrared bands is
presented.

The complex-experiment control system and the distinguishing features of
experiment execution are described.

This collection is of interest to specialists in remote sensing of the
earth and to students in relevant disciplines.

Foreword

The traditional friendly relations between oceanographers in the USSR and
GDR began many years ago, practically from the moment that the GDR Academy
of Sciences [AS] Institute of Oceanography in Rostock-Warnemünde was
established. In 1983, the institute celebrated its 25th anniversary.
Specialists from both countries have participated in many joint expeditions
over the oceans and seas, in the analysis of experimental information etc.

A new stage in the cooperation came in the early 1980s, when joint research between USSR and GDR scientists on satellite oceanography began. The prerequisites for this were: 1) the logic of the development of modern oceanography, which is more and more based on new remote methods of obtaining information about the ocean medium, in addition to traditional methods, and 2) the presence of steady scientific contacts based on mutual respect and trust. Cooperation in this new direction would be impossible without a solid foundation of friendly relations between the peoples of the USSR and GDR in all areas: political, economic and cultural.

From the very beginning, the arena for bilateral cooperation was the Baltic Sea, which borders both countries. The study of this "little sea with its big problems" is of great interest to both countries, which intensively use the Baltic Sea and its shores for shipping, fishing and other economic activities, as well as for recreational purposes.

Satellite oceanography is a comparatively new scientific field, with a number of unsolved problems. Synchronous measurements of sea-surface parameters from satellites, airplanes and ships should aid in developing and perfecting methods of interpreting satellite data.

In April, 1982, the First Joint Complex Subsatellite Oceanographic Experiment was carried out in the central part of the Baltic Sea by specialists from the USSR and GDR. A large volume of synchronous data was obtained from several satellites, airplane laboratories, a special research vessel, vessels of opportunity and shore stations. These data characterize the hydrological and hydrobiological state of the waters in the subsatellite site and the surrounding water area of the Baltic Sea.

The preparation and successful execution of this complicated experiment, the first such experiment for the Baltic Sea, are the result of the combined work of collectives of scientists and specialists from the Leningrad Branch, State Oceanographic Institute [LO GOIN] of the State Committee for Hydrometeorology and Environmental Control [Goskomgidromet] and the GDR AS Institute of Oceanography [IM]; each organization coordinated the work of several establishments in its own country. The following contributed to the organization of the experiment: in the USSR, the State Scientific-Research Center for the Study of Natural Resources [GosNITsIPR], the Main Center for Receiving and Processing Satellite Information and the Klaypeda Marine Hydrometeorological Observatory; in the GDR, the Lindenberg Aerological Observatory of the GDR Meteorological Service.

Special note should be made of the important work performed by the directors of the joint research, S.V. Viktorov (LO GOIN) and H.-J. Brosin (IM) in preparing the experiment.

The present collection, prepared by USSR and GDR scientists, is the result of the first joint step in the difficult path of developing methods for the oceanographic use of satellite remote-sensing data about the earth in the interests of our countries' economies and the study of the environment.

(signed) V.A. Pozhkov, doctor of physico-mathematical sciences,
Director, Leningrad Branch, State Oceanographic Institute

K. Voigt, corresponding member, GDR Academy of Sciences,
Director, Institute of Oceanography, GDR Academy of Sciences

Editor's Note

In ocean expedition work, measurement and observation data have been the basis for various types of oceanographic research for many years. The results of processing and analyzing data from individual expeditions and joint experiments are published, as a rule, for several years after the data collection is completed.

The First Joint Subsatellite Experiment of the USSR and GDR in the Baltic Sea was completed not long ago. Since then, specialists of both countries have been able to analyze only some of the experimental data.

The first to be processed were data needed to verify the concept of complex vessel-aviation oceanographic subsatellite experiments and data which characterize the changeability of the investigated marine characteristics. The results obtained during the processing of these data are necessary for planning further experimental work to study the possibilities of using satellite information in regional oceanographic research. The experimental results are not limited by the information in the present collection. Scientists of both countries will continue to publish individual and joint articles based on the information from this expedition.

In accordance with the agreement, the present collection was prepared at the Leningrad Branch, State Oceanographic Institute based on materials presented by USSR and GDR specialists.

The first section of the book presents current views on the role of subsatellite research in the development of remote methods of studying the earth, including satellite oceanography. The contents of this section were prepared by USSR specialists (1.1, 1.2 and 1.4 by I.F. Berestovskiy, Goskomgidromet, and S.V. Viktorov, LO GOIN, and 1.3 by S.V. Viktorov).

The second section contains information on the goals and tasks of the international experiment, the complement of measurement devices on the satellites, airplane laboratories and the research vessel. This section presents the overall concept of the organization of synchronous measurement of radiative and thermodynamic sea temperatures and water-mass optical characteristics, as well as additional oceanographic and meteorological characteristics in the visible and infrared bands synchronously with the satellite measurements. The control system of the complex experiment is described, and the distinguishing features of executing the experiment are discussed. The authors of this section are I.F. Berestovskiy, S.V. Viktorov, V.V. Vinogradov and V.A. Gashko (LO GOIN); H.-J. Brosin (IM GDR AS) and Yu.A. Doronina (2.5) (LO GOIN).

The third section is devoted to the problem of using the primary data obtained from the complex subsatellite research. The problems discussed involve the accumulation, storage, preliminary processing and presentation of the oceanographic information in the format of the LO GOIN data bank, in

which some data obtained from the experiment were entered. This section was prepared by I.A. Bychkova, S.V. Viktorov, V.V. Vinogradov, Yu.A. Doronina, V.Yu. Lobanov, Ye.V. Polyakov and O.V. Reshetova (LO GOIN).

The results of the complex research on the suspended-matter and chlorophyll contents and on the hydrooptical characteristics of the waters of the central Baltic Sea are presented in the fourth section. This section also includes data on the optical characteristics of the atmosphere during the experiment. This section is presented by GDR and USSR specialists (4.1, H.-J. Brosin and H. Siegel, IM GDR AS; 4.2, H. Siegel and H.-J. Brosin; 4.3, V.A. Gashko, LO GOIN; 4.4, M. Weller and U. Leiterer, Lindenberg Aerological Observatory, and 4.5, S.V. Viktorov).

The fifth section presents the results of the complex investigation of the Baltic Sea temperature field, based on the joint use of satellite, aircraft and vessel data obtained during the joint experiment. The following people prepared this section: H.-J. Brosin (5.1); I.A. Bychkova, S.V. Viktorov, and V.V. Vinogradov (5.2, 5.3, 5.5 and 5.6); Yu.A. Doronina (5.3) and L.I. Koprova, GosNITsIPR (5.4, 5.6).

A summary of the First Subsatellite Oceanographic Experiment of the USSR and GDR in the Baltic Sea is given in the concluding section, prepared by S.V. Viktorov.

The authors wish to thank GosNITsIPR, the crew of the research vessel A. v. Humboldt (captain G. Herzig), the crew of the Il-14 airplane (commander O.V. Sotnikov) and the crew of the An-30 airplane (commander F.R. Vishnevskiy), as well as to the collectives of a number of organizations which took part in preparing the complex subsatellite experiment and which assisted in its successful execution.

1. The Role of Subsatellite Research in the Development of Methods of Remotely Sensing the Earth and the World Ocean

The present stage of development of satellite natural science (earth science) is characterized by the need to use auxiliary (reference and apriori) information in the processing and interpretation of satellite data. Therefore, a satellite system of studying the natural resources of the earth and the world ocean must include a subsystem for collecting this auxiliary information. Since this subsystem is itself quite complicated, we will also refer to it below as a system.

1.1. Structure of the System of Subsatellite Measurements and Observations

The satellite data for each individual sample unit (or some combination of these units) contains information both on the type of the natural subject linked with this unit and on the characteristics of its physical state. The task of interpretation is reduced to finding a data-transformation function which has as its values the unknown characteristics of the subject. The arguments of these functions, besides the spectral brightnesses measured by satellite, in the overwhelming majority of cases also are either: 1) certain values of the characteristics of the subjects themselves or of the surrounding environment or 2) values specified apriori

or collected from special platforms while the satellite survey is in progress.

Thus, the tasks of interpreting the data of remote measurements are most often malposed problems. This situation necessitates that additional data, different for different processing tasks, must be obtained. For example, for precise spatial location, one must have the geodesic coordinates of the contour points; for taking into account the influence of the atmosphere, certain parameters of atmospheric conditions; for solving recognition tasks, data on test areas, etc.

Compared with other directions of satellite earth science, the use of information from airborne and seaborne reference-data platforms in satellite oceanography is very specific in nature. Presently, the organization and execution of complex experimental research on special sites overflowed by satellites is important from the point of view of developing methods of thematically interpreting satellite information and determining the conditions which limit or prevent the obtaining of information of specified precision. The primary task of this research is to develop the optimum methodology for performing observations on subsatellite routes using airborne, vessel and fixed test-site means, including research on the problem of the combined use of different-scale measurements. Once the methodology has been developed and accepted, regular complex reference measurements can be made.

In the general case, the system of subsatellite measurements and observations must include a bank of reference and apriori information and the technical means for collecting airborne and surface-level reference data, as well as communications lines between the system components. To a certain degree, these elements are also present in the structure of the complex subsatellite experiments.

1.2. Subsatellite Information Bank

The bank of reference and apriori information consists of a data bank [DB] and its control system.

Here, apriori information is understood to be information obtained outside the satellite system, as a rule, before the satellite survey. Reference information is the combined results of synchronous (or quasisynchronous) measurements auxiliary to the satellite survey and taken from airplanes, vessels or other mobile measurement-device platforms and from stationary means located on or near the water surface. The DB can contain: cartographic data, statistical data, measurement-device characteristics; aerial photographic surveys and selected satellite photographs, actual measurements (made synchronously with the satellite survey) of environmental parameters at individual points on the earth's surface etc.

A characteristic of the bank of apriori and reference data is the interaction of two information flows: satellite and auxiliary. Naturally, the DB must consist of fixed and transient (operational) parts. The data-bank structure must permit both rapid exchange of information between DB parts and rapid access to the DB by the main processor of the processing

subsystem, including in the interactive mode, based on "interpreter-computer" interaction.

For specificity, we will discuss the DB information content using the example of processing satellite IR radiometric information for determining the sea-surface temperature field [13]. The fixed part of the DB might contain:

data of laboratory calibrations of onboard equipment;

information corresponding to the coastline chart, the degree of detail of which depends on how precisely the satellite measurement data, the water-body region etc. are geographically located;

tables of radiation corrections corresponding to various atmospheric models and depending on the season, time period and region of the measurement;

the levels of discrimination of the cloud cover;

information on the temperature measured during the previous session; data on the cloudiness trend; a set of histograms corresponding to various cloudiness situations for the given set of measurement points, as well as elements of the videoinformation structure for the given region;

tables of average seasonal (monthly) temperatures, data on measured temperatures during previous sessions and data on temperature trends and gradients;

a set of formulas for converting from the sea surface temperature T_{ss} to the sea surface-layer temperature T_{ssl} , corresponding to various seasons, measurement periods and regions;

the coordinates of sites where, in particular, reference measurements of T_{ss} and T_{ssl} are being made and

contour maps of various regions of the world ocean, blanks of output-information tables, the numbers of conditional colors (in the case of information presented in this form) as well as conditional addresses of the consumers receiving the information in various forms.

The operational part of the DB might contain the results of measurements of T_{ss} and T_{ssl} made by buoys and vessels synchronously with the satellite overflight, aerological atmosphere-sounding data etc. The arbitrary nature of the division of the DB into two parts is based on the fact that some of the information over time is transferred from the operational part into the fixed part. For example, data on the temperature after the n -th session is transferred from the operational part of the DB into the fixed part before the information of the $(n+1)$ -th session is processed.

The effectiveness of overall satellite-system operation is greatly determined by the fullness of the cartographic information provided in the DB. The DB cartographic information consists of: general geographic maps, bathymetric charts, hydrological (hydrographic) characteristics etc. This

involves such complicated problems as: 1) determining the types and content of the cartographic data, 2) determining the precision, as well as the amount of detail, used to represent the thematic load on the maps, 3) developing forms of map representation suitable for storage and use in digital form and 4) developing new types of charts, for example, reflecting the distinguishing spectral features of the surface in various frequency bands.

The establishment of banks of satellite and reference information is a complicated scientific-technical and production task. It is possible that one of the main ways to establish these banks for oceanographic data is to organize banks on a regional basis. In this case, the banks must be standardized to ensure the exchangeability of data between the regional banks. Chapter 3 describes the format of such a data bank developed by LO GOIN for the Baltic Sea.

1.3. Airborne Means for Gathering Reference Oceanographic Information

In accordance with the concept developed at the Laboratory of Satellite Oceanography and Aerial Methods of LO GOIN, airborne equipment systems for measuring oceanographic characteristics must be considered, on the one hand, as part of the system of gathering subsatellite reference information and, on the other hand, as an independent instrument for determining the condition of the sea surface.

Main Types of Airborne Information Measurement Systems. The following types of airborne information-measurement systems for determining oceanographic characteristics can be distinguished with respect to purpose, content and distinguishing features: 1) experimental systems, 2) operating systems and 3) satellite auxiliary systems.

Experimental airborne systems are designed to develop new means and methods of obtaining oceanographic information. Experimental systems must be constructed on the basis of a universal information-processing system with flexible programs which permit various sensors to be connected to the system and which permit various sensor arrangements. These systems are characterized by: broad ranges of sensor characteristics, a certain redundancy of measurement means and excessive volumes of information. The airborne platforms for experimental systems must be aircraft with wide ranges of altitude and speed.

Research using airborne information-measurement systems of this type involves: 1) determining the spatial, temporal and spectral characteristics of the research subjects; 2) developing methods of taking measurements; 3) selecting the optimum sensors and spectral ranges etc. There cannot be a great number of such airborne oceanographic laboratories: by nature, these are unique systems. The research results are used to develop measurement means and automated information-storage and -preprocessing devices for operating systems.

Operating airborne systems are designed to obtain operational and long-term information on the sea state for direct use in various economic sectors and environmental-monitoring organizations. The types, volumes and forms of

representation of this information are determined on the basis of agreements with specific consumers. The airborne platforms for this type of system are specially equipped standard airplanes and helicopters.

Satellite auxiliary airborne systems must be a satellite-system component designed to determine oceanographic parameters. It should be noted that a number of works [3, 21, 27] are devoted to general problems of using aircraft to solve problems of remote sensing of the earth from space. However, several problems specific to satellite oceanography have not been sufficiently investigated. The exceptional dynamic nature of the subject (namely, the world ocean), the wide ranges of its characteristics and the difficulties of organizing subsatellite measurements manifoldly complicate the overall interaction scheme and the measurement-means structure in the satellite-airplane-test area system for satellite oceanography. Moreover, in our opinion, it is namely in this application that the role of airborne information-measurement systems is most significant.

Because of the novelty of the task of integrating airborne and spaceborne means of measuring the characteristics of the world-ocean surface and the atmosphere, satellite auxiliary airborne systems are closer to experimental systems than to operating systems with respect to their tactical-technical characteristics.

The use of satellite auxiliary airborne systems can be arbitrarily divided into a number of stages. In the first stage, using airborne platforms, measurement means are developed which can be used as individual sensors in the on-satellite equipment. In the second stage, airborne information-measurement systems perform mass measurements on the satellite tracks (sites) in various synoptic situations, for various sea states, for various water areas and during different seasons.

This same procedure is used to accumulate synchronous and quasisynchronous information and to establish data banks for the development of decoding algorithms and the interpretation of satellite information by different economic sectors. For airborne systems to effectively function in this stage, they and the onboard satellite systems must have a reasonable compatibility of frequency, spatial and temporal characteristics. The main requirement for airborne satellite auxiliary systems in this stage is to make it possible to restore values of primary oceanographic parameters most adequately to their true values at the moment (interval) of satellite measurement.

Using the information obtained from airborne systems, the satellite information is critically analyzed, spurious measurements are rejected, the algorithms for processing and interpreting the information are refined, corrections are introduced etc. As the system of surface-level processing means is developed and as satellite onboard measurement means are improved, the role of airborne auxiliary systems probably will decline. In future stages, airborne auxiliary means, presumably, will be used to collect information in a limited number of test areas in ground-truth sites and to solve "supplemental-investigation problems."

This last term requires explanation. A situation can be envisioned in which the system of satellite onboard measurement means and the ground system of processing and interpreting the information do not permit a unique judgment on the nature of one or another anomaly on the world ocean surface. In this situation, additional, more detailed measurements must be made using an independent equipment system. This supplemental investigation should be done using airborne information-measurement systems.

Requirements for Aircraft Platforms for Oceanographic Research. Due to the nature of the task of modern aerial oceanography, taking into account the tasks of supporting satellite oceanographic systems, aircraft platforms have the following requirements:

flight range: sea version, 3000-5000 km; ocean version, 10,000-20,000 km;

working altitude range, 200-2000 m;

stable operating speed, 250-400 km/h;

payload, 5-10 t;

available power-supply capacity, 10-20 kW;

working area in cabin, 30-40 m²;

the presence of additional hatches, in particular, with plane-parallel optical windows which permit a pressure drop to be maintained;

in order to protect equipment and glass from contamination and damage during takeoff, landing and taxiing, the hatches must have external protective doors;

some hatches must have windows transparent in the infrared and radio frequency bands;

the presence of special devices for ejecting floats, buoys and disposable in situ sensors of oceanographic characteristics;

the presence of a special room for a photographic darkroom and

in order to improve the precision of determining the current coordinates in the absence of ground beacons in flight over open ocean, the aircraft platform must have special equipment, including an inertial navigation system, a navigation computer and long-distance navigation-system displays.

Researchers presently have no universal platforms which fully satisfy all these requirements.

Three types of airplanes are used in joint natural-resource research programs using airborne laboratories; each type solves a limited sphere of tasks (Table 1.1) in accordance with its classification [33].

Table 1.1. Classification of Airplanes Used for Natural-Resource Research

<u>Parameter</u>	<u>Type of airplane</u>		
	<u>medium</u>	<u>heavy</u>	<u>high-altitude</u>
Ceiling, km	8-12	10-14	20-25
Endurance, h	4-6	8-10	4-6
Load, t	2-3	6-10	1
Equipment power consumption, kW	4-5	8-10	2-4
Number of operators	5-8	15-20	1-2

The medium-type airplane mainly is called upon to solve the sphere of tasks involving the development of opticophysical and to some extent radiophysical methods and means of remote sensing and to perform experiments at low altitudes (300-500 m) over limited areas or limited test-area lengths.

Heavy airborne laboratories are designed for the practical solution of all scientific-experimental tasks performed by aircraft in aerial-satellite research. Such an airplane must be equipped with all types of scientific equipment, be able to provide for testing and development of this equipment and provide for the execution of complex research over a wide range of wavelengths.

High-altitude airplanes must be able to provide for experimental measurements and photographs throughout practically the entire atmospheric layer [33].

Foreign and Domestic Aircraft Systems for Studying the Earth's Natural Resources. The characteristics of several foreign airborne systems used for studying the earth's natural resources (including those of the world ocean) are given in Table 1.2, which was constructed from information given in [33]. The data in this table show the wide variety of characteristics of aircraft platforms, special equipment and scientific equipment.

In our country, the main aircraft platforms for equipment systems to study the earth's natural resources are the Il-14, Il-18 and An-30 [1, 2, 12]. The aerial-photography and special versions of the An-30 have the most modern equipment.

Main Characteristics of the An-30 Airplane [35]

Maximum takeoff weight	23,000 kg
Cruising speed	430 km/h
Practical range	2360 km
Practical ceiling	8000 m
Stall speed	195 km/h
Takeoff distance (to an altitude of 15 m)	1240 m
Landing run	660 m

Table 1.2. Characteristics of Several Foreign Aircraft Systems for Studying the Earth's Natural Resources [33]

(1) Тип самолета	(2) Полная полезная масса, кг	(3) Масса научного оборудования, кг	(4) Минимальная высота, км	(5) Дальность, км	(6) ЭКП, км	(7) Состав научного оборудования	(8) Продолжительность полета, ч	(9) Примечание
(10) «Грумман ОИ-1 Мо-гавк»	6 820	2 250	110, 490**	2 260	9 000	АФС-МЗ, РЛС БО (19)		Парк 365 шт. (25)
(11) «Леарджет-36-А»	8 160	1 250	750**	5 030	13 700	—	6,5—10	5 модификаций (26)
(12) «Суперкинг ЭПР-200»	6 350	—	150	3 100—4 320	—	Комплекс АФС (20)		Специальный вариант для Географического института (27)
(13) «Фоккер 27 МК-400»	17 500	—	(290—180)**	3 700	9 100	Комплекс АФС (21)	12	Автоматизированный навигационный инерционный комплекс (28)
(14) «НАСА-927 Локхид»	51 400	9 000	280, 610**	3000—3700	9 100	АФС-МЗ (4), РЛС (22) 1,8 см, спектрометр, ИК-спектрометр, ИК-радиометр, СВЧ-сканеры	7	—
(15) «НАСА-929 Локхид»*	61 400	9 230	590**	4 000	12 000	АФС-МЗ (4), РЛС (22) 1,8 см, спектрометр, ИК-спектрометр, ИК-радиометр, СВЧ-сканеры	9	
(16) «Е-Системе Л-450»	2 140	160—320	170**	9 700	15 200	АФС-МЗ (6), АФС (23) сканер с углом зрения 130°, ИК-спектрометр 6—13 мкм, ИК-радиометр 10—12 мкм АФС (24)	24—30	Самолет-планер с дистанционным управлением в радиусе 400 км (29)
(17) РБ-57-Ф	26 000	—	145, 740**	5 300	14 900		6—8	Оборудование в гонимом (30)
(18) «Локхид У-2»	7 850		790**	3 550 (4 200)	21 300		5	Гиростабилизированная платформа для АФС (31)

(в скобках указано число зон).

(32) Примечание. АФС-МЗ — аэрофотосъемочная аппаратура многозональная
 (33) * Этот тип самолета известен также как НС-130 В (РС-130).
 (34) ** Указана крейсерская скорость.

[Key on following page]

Key:

1. Type of airplane
2. Total flying weight, kg
3. Weight of scientific equipment, kg
4. Minimum speed, km/h
5. Range, km
6. Practical ceiling, m
7. Scientific equipment
8. Flight duration, h
9. Notes
10. Grumman OV-1 Mohawk
11. Learjet-36-A
12. Superking AIR-200
13. Fokker 27 MK-400
14. Lockheed NASA-927
15. Lockheed NASA-929*
16. E-Systems L-450
17. RB-57-F
18. Lockheed U-2
19. MAC, airborne radar
20. aerial-camera system
21. aerial-camera system
22. MAC (4), airborne radar 1.8 cm, optical spectrometers, IR spectrometers, IR radiometers, 3 scatterometers, microwave scanners
23. MAC (6), camera, IR scanner with capture angle of 130° , IR spectrometer 6-13 μm , IR radiometer 10-12 μm
24. aerial camera
25. Fleet of 365 planes
26. 5 versions
27. Special version for Geographic Institute
28. Automated navigation inertial system
29. Remote-controlled glider with a radius of 400 km
30. Equipment in gondola
31. Gyrostabilized platform for aerial camera
32. Note. MAC stands for multispectral aerial camera (number in parentheses indicates the number of bands)
33. *This type of airplane is also known as the NS-130 V (RS-130).
34. **Cruising speed

There are three glass-covered photographic hatches for plane aerial photography and two photographic hatches for perspective aerial photography. The fuselage has external sliding covers to protect the glass. The airplane is equipped with a darkroom. The aerial camera has a gyro-stabilized mounting.

There is a specially developed piloting-navigation equipment system consisting of a directional system with an astrocompass, a Doppler navigator, a navigational digital computer and an autopilot with an automatic turn device. This system can be used to automate a flight route and also to automate the approaches to subsequent routes [33].

In a number of cases, helicopters are convenient for collecting subsatellite reference data. While airplanes are mainly used to collect

instantaneous characteristics of various types of natural subjects over large areas, the helicopter, due to its capability of hovering over a natural subject, when equipped with measurement equipment can be used to collect either instantaneous or dynamic characteristics of a limited area from various altitudes.

In all cases, the set of measured parameters, the volume of data and the content of the measurement equipment are determined by the contents of the specific remote-sensing task. For example, the equipment on GosNITsIPR's An-30 laboratory airplane contains an MKF-6 multispectral camera, a television, various spectrometers and radiometers, a set of aerial cameras and other equipment.

The Il-14 airplane which is part of LO GOIN's specialized oceanographic equipment system has several aerial cameras with various focal lengths; a set of IR radiometers for determining the water surface temperature; a thermohygrometer, which determines the air temperature and humidity at the flight altitude; an IR lidar for mapping oil slicks on the sea surface; a spectrophotometer for determining the spectral brightness of the sea and other equipment. A television system is used for observation and operational documentation of water-surface phenomena.

1.4. Collection of Surface-Level Reference Data

The value of surface measurements is their reliability and precision. However, they can cover only small areas of the earth's surface. As a rule, surface measurements are made on constant, preselected test areas of surface-truth sites [STSs], and the latter have special requirements. With regard to land research, the STS is a limited area which is physico-geographically representative of a given zone. The site contains a typical range of natural systems both in the natural state and altered by man. The STS territory must be easily accessible for examination by expeditions and must be well documented with cartographic information and aerial photographs. A necessary requirement for any site is that it contain so-called test areas, in which detailed stationary or semistationary research on natural subjects can be carried out. These test areas serve as the basis for performing the necessary methodological work of identifying natural subjects and studying their properties based on comparing various types of remote-sensing data with direct surface measurement data. Test areas must be representative of the physico-geographic conditions for a given STS so that the results obtained can be extrapolated to the entire site. These areas must have the optimum dimensions: on the one hand, so that their characteristic features can be reflected on the small-scale satellite photographs used in the work and, on the other hand, so that detailed surface investigation can be carried out. The specific dimensions of each test area in each specific case depend on the task posed in the subsatellite experiment.

In light of the great temporal variability of oceanographic characteristics, the problems of collecting reference information at sea have distinguishing features. The general principles of organizing oceanographic aerial-satellite sites have been discussed, in particular, in [5, 6, 9, 10, 17]. Information obtained from sites and stored in data

banks should be used primarily for developing and improving methods of thematically interpreting satellite information. Moreover, the large volume of regularly obtained natural-resource and hydrometeorological information makes it possible to consider subsatellite sites as independent means of collecting long-term information.

It should be kept in mind that the statement itself of the problem of executing subsatellite (airborne and surface) measurements is correct only in that case when the airborne and surface-level information is "compatible" with the satellite information and can be effectively used in the analysis and interpretation of the latter.

In order to ensure this compatibility, a number of requirements must be fulfilled:

synchronism (or quasi-synchronism) of obtaining all types of information;

metrological unity of all types of measurements;

representativeness of surface and airborne measurements with regard to the territory covered by the satellite survey;

comparability of scales and resolution of all types of measurements and

timeliness of delivering airborne and surface information to the satellite-information processing centers.

The requirement of synchronism is important in the study of dynamic (rapidly changing) parameters of natural formations and phenomena. The requirements for synchronism of information collection are especially strict in research on sea and ocean surfaces, due to their great temporal variability.

Great attention must be given to problems of metrological control of all in situ and remote measurements, including satellite and on-site measurements. In order to ensure the unity, reliability and precision of measurements, the theoretical metrological fundamentals of the remote determination of natural-medium parameters must be developed. Metrological control of measurements made by surface, airborne and satellite equipment is one of the basic and most complicated requirements. In order to fulfill this requirement, the electrical scales and spectral channels of the equipment must be mutually coordinated using standardized test stands and standards with standardized methodology. The failure to fulfill this requirement leads to a situation where the satellite, airborne and surface measurements are only qualitatively comparable in a number of cases, and some of the collected information is not used.

Standard automated information-measurement systems, described in [22], provide for: 1) proper operation of the system of collecting and preprocessing the measurements on surface-truth sites and test areas and 2) the transmission of these data to regional processing centers. These systems can perform regular measurements, quasi-synchronous with the airborne/satellite measurements, of parameters of a natural medium on test

areas and transmit these data by radio through satellites or standard communications channels to the processing centers. In the future, the wide use of standard systems consisting of several local observation nodes, a ground station and an airborne observation station during complex subsatellite experiments should make it possible to better fulfill the above requirements for airborne and ground-level observations.

In April, 1982, USSR and GDR specialists conducted a complex subsatellite oceanographic experiment on a region of Baltic Sea. This experiment used airplanes at medium and low altitudes for determining the oceanographic parameters. Sea and atmospheric characteristics were measured from a research vessel. The data of coastal stations and aerological sounding stations were used. Synchronous satellite photographs and subsatellite measurements and observations obtained as a result of the experiments were used, in particular, to develop a methodology for collecting reference oceanographic information.

2. Basic Information on the Complex Subsatellite Oceanographic Experiment

2.1. Goals and Tasks of the Experiment

Goals of the Experiment

1. To develop elements of the technological system of interaction between the airborne, vessel and satellite means within the framework of the complex oceanographic subsatellite experiment.
2. To obtain data of synchronous and quasi-synchronous airborne, vessel and satellite measurements and observations necessary for the development of preliminary methodological recommendations to determine the content of suspended matter in the seawater and to refine the methods for determining the sea surface temperature from satellite measurements.
3. To perform methodological work on the comparative analysis of sea surface images obtained from Meteor-Priroda satellites (medium- and high-resolution) and images obtained from an airplane laboratory using an MKF-6M multispectral camera.

Basic Tasks of the Experiment

1. To experimentally develop a method of making vessel and airborne measurements within the framework of the synchronous complex subsatellite experiment.
2. To evaluate the suitability of the selected working region and time interval for performing the complex subsatellite experiment, taking into account the actual organizational-technical conditions of experiment execution.
3. To prepare the staff of the operating experiment-control group, the crews of the ship and airplane and the operators of the vessel and airborne scientific equipment to make the synchronous subsatellite measurements and observations within the framework of the complex experiment.

4. To make complex synchronous and quasi-synchronous measurements of hydrooptical characteristics of the Baltic Sea waters in the experiment region and the atmospheric characteristics from the vessel and the airplanes, including the taking of aerial photographs of the sea surface using a multispectral camera. The measurement results will be used in the following research and development:

developing, verifying and perfecting methodological recommendations for determining the content of suspended matter in seawater based on airborne and satellite measurements;

performing methodological work on comparing the information content of sea surface images obtained from a satellite and images obtained from an airplane using an MKF-6M multispectral camera;

studying the space-time variability and spectrum variability of the radiation brightness of the sea in the region being studied;

studying the correlations between the hydrooptical parameters affecting the formation of sea radiation (irradiance from above and below, attenuation index, scattering index in a given direction and brightness coefficient of the sea layer);

determining the color indexes and spectral brightness contrasts of the sea surface in the region being studied; determining the factors affecting the variability of these values;

studying the influence of atmospheric factors on the variability of the brightness spectrum of the radiation ascending from the sea surface;

obtaining correlations between the concentrations of mineral and organic suspended matter and the ascending-radiation spectrum; and

studying the variability of the chlorophyll and suspended-matter contents and the link between this variability and water-mass dynamics.

5. To make complex synchronous and quasi-synchronous measurements of Baltic Sea water temperature in the experiment region and of atmospheric characteristics from vessel and airplane. The measurements will be used to perform the following research and development:

developing, verifying and perfecting methodological recommendations for determining the sea surface temperature from airborne and satellite measurements;

interpreting satellite digital maps and analog images of the surface temperature of the Baltic Sea, including an investigation of the precision and reliability of this information;

investigating the link between the sea-surface radiative temperature measured by satellite and the radiative temperature measured by vessel; determining the influence of atmospheric factors on the vessel and satellite radiation measurements;

investigating the link between the sea-surface radiative temperature measured by vessel and the temperature measured by in situ methods, including measurements from the surface to the bottom;

studying the daily variation in sea-surface temperature based on in situ and remote measurements and

studying the spatial variability of the sea-surface temperature distribution in the experiment region.

Thus, it is easy to distinguish the two component parts of the complex experiment: an optical and a temperature part, which are to a certain degree independent.

2.2. Content of Technical Means, Measurements and Observations

In accordance with the goals and tasks of the experiment, the following basic types of measurements and observations were made: satellite, airborne and vessel.

Content of Satellite Information. In order to fulfill the optical part of the experiment for the region in which airborne and vessel work was performed, radio-television survey data were obtained from a two-channel medium-resolution camera and a Fragment high-resolution camera on Meteor-Priroda satellites.

To fulfill the temperature part of the experiment, digital charts and IR images of the sea surface were obtained on the basis of information from Meteor-2 and NOAA satellites.

Technical Means of the Subsatellite Experiment. The following USSR equipment was used in the experiment:

GosNITsIPR's An-30 airplane laboratory, b/n 30023, with an MKF-6M multispectral aerial camera and an AFA-TE-200 standard aerial camera (flight director, V.V. Drabkin; flight operators, V.A. Gashko and L.L. Sukhacheva, and person responsible for MKF-6M survey, M.A. Afanasov);

LQ GOIN's Il-14 airplane laboratory, b/n 91611, with an MIR-3 IR radiometer (Table 2.1) and an AFA-41 standard aerial camera (flight director, Yu.A. Doronina, and flight operators, O.N. Frantsuzov and R.I. Goncharova).

The GDR contribution to the experiment was the use of the A. v. Humboldt expedition vessel of the GDR AS, equipped with: a bathometer probe (temperature, salinity and water samples, including samples for determining chlorophyll), an instrument for continuous determination of chlorophyll, an instrument for determining the angular function of light scattering, an instrument for measuring light attenuation, an instrument for measuring irradiance, a spectrometer and a system for standard meteorological observations. The above equipment was operated by GDR specialists headed by H.-J. Brosin. Also on the vessel were two USSR specialists, Ye.P. Belkov and A.B. Zhuravlev, who operated an equipment system consisting of a spectrophotometer and an IR radiometer with a calibrating device.

Table 2.1. Technical Characteristics of the MIR-3 IR Radiometer

	<u>Radiometer used</u> <u>on vessel</u> <u>(modernized)</u>	<u>Standard radiometer</u> <u>used on airplane</u>
Measured temperature range, °C	(-10)-(+32)	(-2)-(+32)
Basic measurement error (with simulated water surface, standard error), °C	0.1	0.4
Time constant, s	0.5	1.0
Angle of vision, °	2.5	10
Spectral range, μm	8-12	8-12
Filter type	Interference	Band-pass

Content of the Airborne Measurements and Observations. The content of the measurements and observations made on the An-30 airplane is as follows:

aerial photography of the sea surface in the experiment region using an MKF-6M camera;

same, using a standard aerial camera and

aerial visual observations of the sea-surface, atmospheric and cloud conditions.

The content of measurements and observations made on the Il-14 airplane is as follows:

IR measurements of the sea-surface radiative temperature along routes in the experiment region using an MIR-3 radiometer;

measurements of the temperature and humidity of the outside air using a thermohygrometer and

aerial visual observations of the sea-surface, atmospheric and cloud conditions.

Content of Vessel Measurements and Observations. During the experiment, a series of two basic types of measurements and observations was performed: specialized hydrooptical measurements and water-temperature measurements, as well as auxiliary and standard measurements and observations.

Hydrooptical Measurements:

spectral flux density and irradiance from above and below in the range 0.4-1.0 μm ;

spectral brightness of the sea;

radiation attenuation index in the band 0.38-0.725 μm ;

scattering index in water of light with a wavelength of 0.633 μm ;

underwater irradiance at 0.435 μm or 0.545 μm and spectral values of atmospheric absorption.

Water-Temperature Measurements:

radiative temperature of the sea surface and thermodynamic temperature of the water surface layer.

Auxiliary and Standard Measurements and Observations:

For the correct interpretation of the results of the specialized hydrooptical and temperature measurements, the following were performed:

measurements of the seston and chlorophyll contents or of the phaeopigment content;

meteorological and oceanographic measurements and observations (presence and type of cloud cover, wind direction and speed, air temperature and humidity and sea state) and

oceanographic work to determine the vertical temperature distribution, salinity and density of the water, as well as taking samples from various depths for subsequent laboratory determination of the suspended-particle content.

The integrated nature of the synchronous measurements and observations made for the temperature and optical parts of the experiment is described in Tables 2.2 and 2.3.

2.3. General Concept of Experiment Organization. Experiment Control.

The present state of development of satellite oceanography is characterized by the necessity of performing complex synchronous subsatellite measurements of a large number of parameters of sea-surface and atmospheric conditions. This is due to the incomplete development of methods of determining oceanographic parameters from satellite measurement data, as well as to the necessity of calibrating and periodically monitoring the onboard equipment.

The execution of subsatellite ocean and sea experiments involves considerable organizational and technical difficulties. These include: the necessity of taking into account the different spatial coverages of the satellite, airborne and vessel equipment, the considerable difference in speeds of the equipment platforms, problems of operational control of aircraft and vessels etc. At present, extremely few complex vessel-airborne subsatellite experiments have been performed in the world; in some experiments, vessels of opportunity were used rather than special vessels. There is no generally accepted ideology or technological scheme for performing oceanographic subsatellite experiments.

Table 2.2. Summary of Measurement Information and Observations of Various Levels for the Temperature Part of the Experiment

<u>Level</u>	<u>Experimental Program</u>	<u>Auxiliary</u>
Satellite	Digital maps of sea-surface temperature according to data from scanning IR radiometers of the Nos 5 and 7 Meteor-2 satellites	NOAA-6, NOAA-7
	Sea-surface images according to data from scanning IR radiometers of the Nos 5, 7 and 8 Meteor-2 satellites	NOAA-6, NOAA-7
Airborne	Route measurements (maps) of the sea-surface temperature according to data from an MIR-3 IR radiometer (Il-14)	Images of sea surface in the IR band from television data (An-30)
	Air temperature and humidity measurements (Il-14)	
	Aerial visual observations of the atmospheric and sea-surface conditions, including oil slicks	
Vessel A. v. Humboldt	Measurements of the sea radiative temperature using an IR radiometer. Measurements of the surface-layer thermodynamic temperature using a thermistor sensor. Measurements of the water thermodynamic temperature at a depth of 4.5 m	
	Measurements of the water thermodynamic temperature from the surface to the bottom	
	Standard meteorological measurements. Standard oceanographic and meteorological observations. Special observations of oil slicks on the sea surface	
Hydro- graphic Vessels and Vessels of Opportunity	Measurements of thermodynamic temperature of the sea	
	Standard meteorological measurements and observations	
Shore	Aerological atmospheric sounding data made by near-shore GMS's	
	Sea temperature measurements at coastal stations and observation posts	
	Standard meteorological measurements at coastal stations and observation posts	

Table 2.3. Summary of Measurement Information and Observations of Various Levels for the Optical Part of the Experiment

<u>Level</u>	<u>Experimental Program</u>	<u>Auxiliary</u>
Satellite	Sea-surface images obtained using medium-resolution scanners of the Nos 30 and 31 Meteor-2 satellites	Low resolution: No 8 Meteor-2 satellite
	Sea-surface images obtained using the Fragment high-resolution camera of the No 30 Meteor satellite	
Airborne	Sea-surface images obtained using MKF-6M and AFA-TE-200 cameras (An-30)	
	Aerial visual observations of atmospheric and sea-surface conditions, including oil slicks	
Vessel A. v. Humboldt	Integrated hydrooptical measurements of sea and atmospheric parameters	
	Measurements of the chlorophyll and suspended-particle contents	
	Standard meteorological measurements	
	Standard oceanographic and meteorological observations	

Scientists of the Baltic countries, including the USSR and GDR, have produced only a few publications discussing individual problems relating to the use of satellite and airborne measurement data for studying the hydrological and hydrochemical conditions of the Baltic Sea [14, 62, 64].

USSR and GDR organizations are performing separate methodological work on using remote methods of studying the Baltic Sea from vessels and airplanes. However, there is no regular series of synchronous vessel-airborne subsatellite measurements of the Baltic Sea.

In connection with this, it was feasible that USSR and GDR organizations perform a series of joint synchronous complex subsatellite experiments to develop the technological elements for the interaction of airborne and vessel equipment and to obtain experimental data for the development and improvement of methods of determining oceanographic parameters based on aerial and satellite measurements.

When organizing such an experiment, it is necessary above all to provide synchronous (quasi-synchronous) measurements and observations of sea and atmospheric parameters by all types of equipment platforms: satellite, airborne and vessel.

The following factors were considered in selecting the region for the first joint experiment: 1) previous oceanographic studies, 2) mutual interest of specialists of both countries in studying the region, 3) accessibility for research using Soviet airplanes based in the USSR and 4) relative proximity to the homeport of the GDR vessel (Rostock).

The USSR and GDR agreed on the region in the vicinity of point 9A (international classification) with coordinates of lat. $56^{\circ}06'$ N, long. $19^{\circ}10'$ E as the experiment location. This station is located in the central Baltic Sea, in the southern part of the Gotland Depression (Fig 2.1). This station is one of the stations of the International Baltic Year 1969-1970. International research in the BOSEX experimental program was also conducted in the area of this point in autumn 1977. The station is included in the regular long-term oceanographic observation programs of various scientific establishments in Baltic countries.

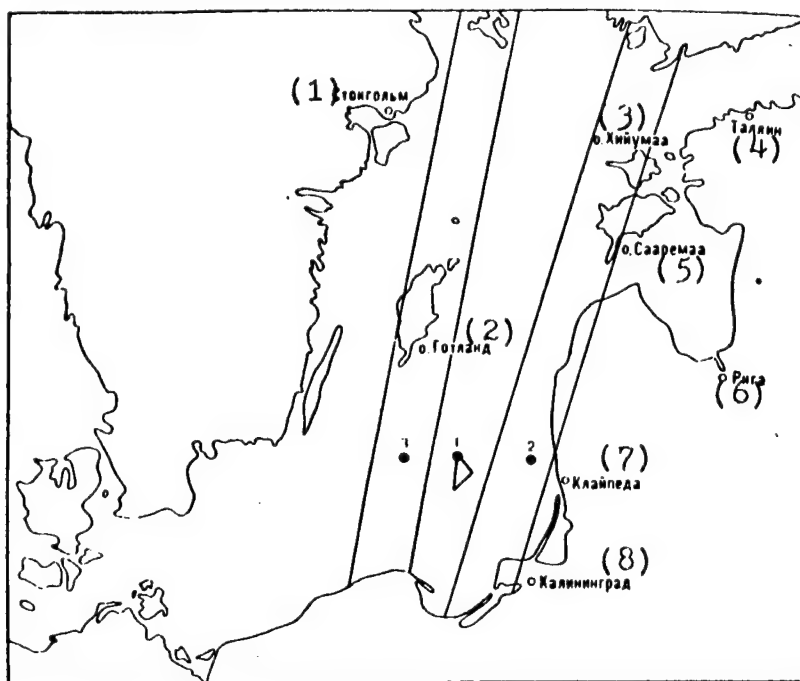


Figure 2.1. Region of the Subsatellite Experiment:

1. vessel site
- 2, 3. position of the vessel on 23 April 1982 (2) and 24 April 1982 (3)

Key:

- | | |
|-------------------|--------------------|
| 1. Stockholm | 5. Saaremaa Island |
| 2. Gotland | 6. Riga |
| 3. Hiiumaa Island | 7. Klaypeda |
| 4. Tallinn | 8. Kaliningrad |

The Institute of Oceanography, GDR AS, has been performing regular oceanographic measurements at this point in March, May, August and late

October (early November) since 1969. Also, the Swedish Institute of Oceanography (Göteborg), BaltNIRKh [Baltic Scientific-Research Institute of Fisheries] in the USSR (Riga) and other institutions make regular measurements at this station.

The conditions at this station are considered characteristic of this part of the Baltic Sea. Thus, taking into account the previous study and representativeness of this area, as well as the fact that the position of the station satisfies the above organizational requirements, the region of station 9A was selected as the site of the first joint complex subsatellite experiment.

The methodology for performing the vessel measurements synchronously with satellite overflight is based on the principle of independent movement of the vessel over a predetermined route with precise recording of the time of passage over various sections.

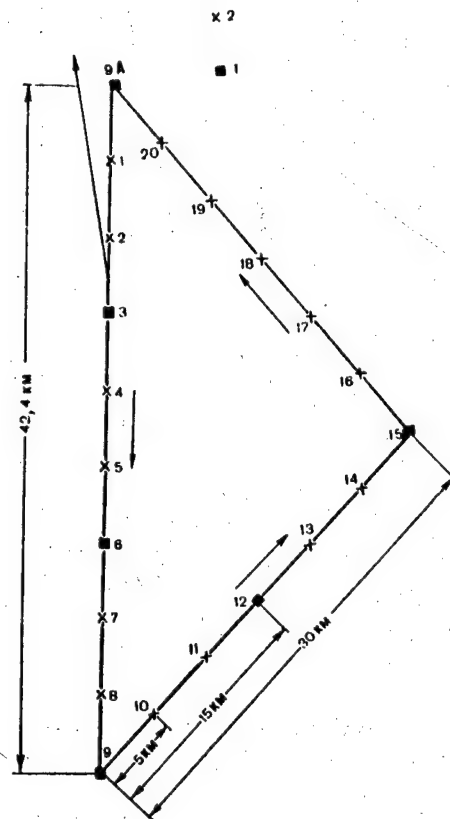


Figure 2.2. General Diagram of the Site and Location of the Vessel Stations:

1. hydrooptical station
 2. oceanographic and hydrooptical station
- arrows indicate the direction of vessel travel

When planning the time interval of the measurements, the requirements of space-time resolution of the vessel data were taken into account. These

requirements stem from the spatial resolution of the remote sensors and from the expected space-time variability of the measured parameters. Additionally, the organizational-technical capabilities were taken into account (the vessel speed, the necessity of performing special maneuvers to provide for special measurement conditions, the actual time needed for measurements etc.). With these conditions, taking into account the orbital characteristics of the satellite, the research-region configuration shown in Fig 2.2 was adopted.

The measurements were organized so that the vessel traveled over the research region at the same time every day. The vessel position at any moment was determined with a precision of 250 m.

The hypotenuse of the daily triangular route of the vessel coincides with the direction of movement of the subsatellite point for the Meteor-series satellites.

The vessel is the most conservative element in the satellite-airplane-vessel system. In this experiment, the vessel route was determined for each day of the experiment and, as a rule, was not subject to change regardless of the presence or absence on a given day of one or both airplanes in the experiment region. Every day, the vessel starts from point 9A, as shown in Fig 2.2. The time needed to complete section 1 (including 4 hydrooptical stations and 10 oceanographic stations at points 0-9) is about 8 h. The time for completing section 2 (including 2 hydrooptical stations at points 12 and 15 and 6 oceanographic stations at points 10-15) is about 5 h. The time needed to complete section 3 (including 6 oceanographic stations) is 3 h.

Thus, the total working time of the vessel is 16 h per day. As calculated, the An-30 airplane is located in the experiment region for 3 h, while the Il-14, for 4-5 h.

With one flight per day, the An-30 airplane with the MKF-6M camera must operate in two modes: 1) at large solar zenith angles (morning and evening version) and 2) at small solar zenith angles (midday version).

The flight altitude is from 1 to 6 km, while the flight patterns are along and perpendicular to the vessel route. Line-of-flight aerial photography is performed.

With one flight per day, the Il-14 airplane operated over a special network of route legs covering the entire experiment region (Fig 2.3). The sea-surface radiative temperature was continuously recorded with an IR radiometer. The network of legs is constructed so as to ensure maximum coverage of the test area and its environs, as well as to ensure synchronism of the measurements with satellite overflight and coincidence of individual legs with the vessel route. The flight altitude is less than 1 km.

Spatial location of the airborne measurements was performed independently on each airplane. The vessel was used as an auxiliary navigational reference. This circumstance should make it much easier to perform subsequent space-time location of measurements during integrated data

processing. Therefore, the precision of determining the vessel position at any moment must be no less than 250 m. All the moments of vessel operation (beginning and end of movement, change of course, beginning and end of hydrooptical and hydrological measurements) were recorded. All moments of airplane overflight above the vessel were also recorded.

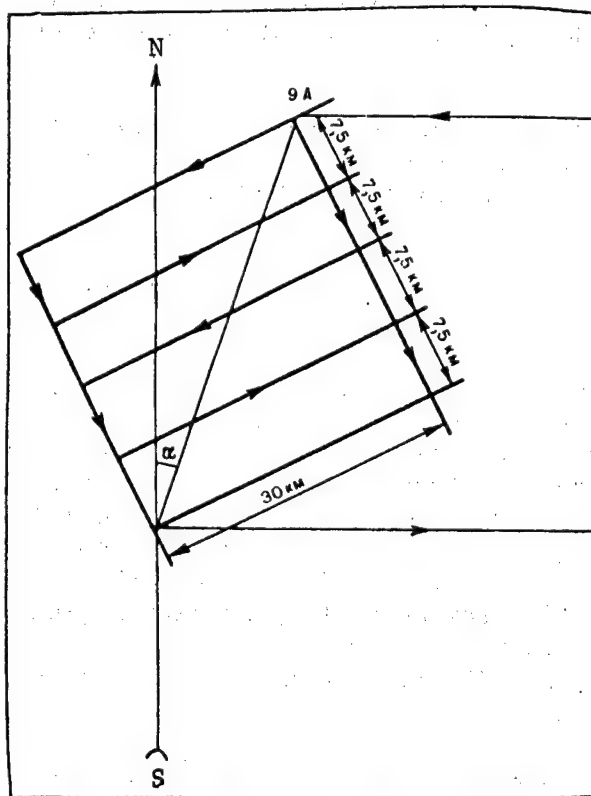


Figure 2.3. Diagram of Airplane Route Legs Over the Site

The Control Group, made up of Soviet specialists, supervised the experiment operations. The group's tasks were: operational monitoring of the execution of the complex-experiment program by all participants, maintaining regular communications between individual groups and, if necessary, changing the work of individual groups with respect to the time, location or nature of measurements (Fig 2.4).

2.4. Execution of the Experiment. Brief Description of the Information Obtained

The program of the First Complex Subsatellite Oceanographic Experiment of the USSR and GDR in the Baltic Sea was realized within the planned time period. The experiment began on 18 April 1982 with the arrival of the GDR vessel A. v. Humboldt at the port of Klaypeda to take on two LO GOIN specialists and cargo and for installation and adjustment of the USSR-supplied equipment. The experiment ended on 27 April 1982 with the return of the vessel to Klaypeda. The operational phase of the experiment was from 19 through 26 April 1982.

The vessel positions during the subsatellite experiment are shown in Fig 2.1 and in Tables 2.4 and 2.5.

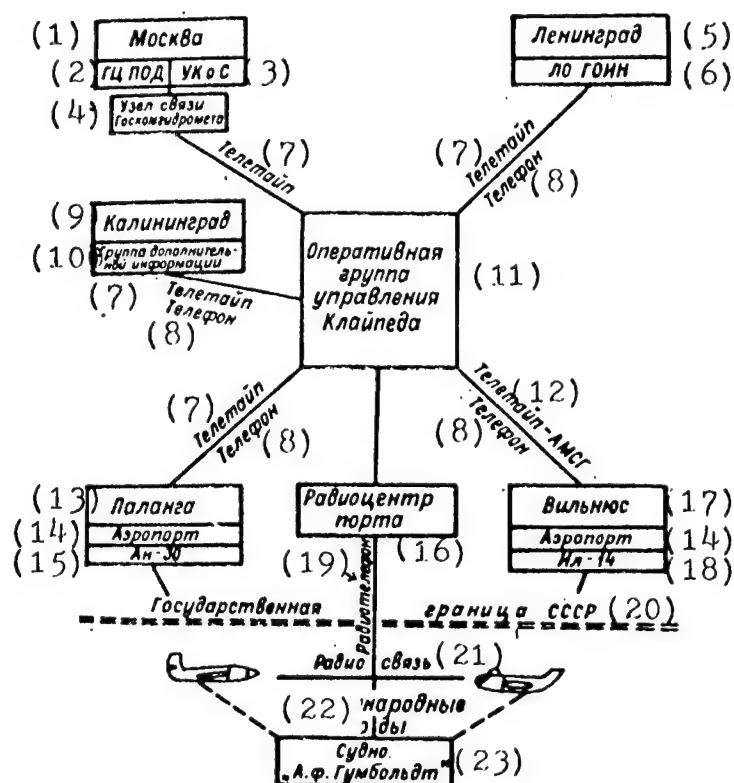


Figure 2.4. Diagram of Experiment Control

Key:

- | | |
|--|--|
| 1. Moscow | 12. Teletype of Aviation Weather Station |
| 2. Main Center for Receiving and Processing Data | 13. Palanga |
| 3. UK o S [not further identified] | 14. Airport |
| 4. Goskomgidromet Communications Center | 15. An-30 |
| 5. Leningrad | 16. Port Radio Communications Center |
| 6. LO GOIN | 17. Vilnius |
| 7. Teletype | 18. Il-14 |
| 8. Telephone | 19. Radiotelephone |
| 9. Kaliningrad | 20. USSR border |
| 10. Auxiliary Information Group | 21. Radio link |
| 11. Operational Control Group, Klaypeda | 22. International waters |
| | 23. Vessel A. v. Humboldt |

Table 2.4. Position of the Vessel During the Subsatellite Experiment.
April, 1982.

Date	Ship Position	Station
19-22, 25, 26	Triangle with peak at point lat 56°06' N, long 19°10' E	975-995
23	lat 56°00' N, long 20°42' E	974
24	lat 56°00' N, long 18°15' E	973

Table 2.5. Coordinates of Site Stations

(1) Номер станции (см. рис. 2.2)	(2) Станция	(3) Глубина, м	Координаты (4)	
			с. ш. (5)	в. д. (6)
0	995(9A)	130	56°06,0'	19°10,0'
1	994	127	56 03,2	19 09,8
2	993	119	56 00,6	19 09,0
3	992	112	55 57,9	19 08,2
4	991	110	55 55,2	19 07,9
5	990	95	55 52,5	19 07,1
6	989	89	55 50,0	19 06,9
7	988	90	55 48,0	19 06,0
8	987	88	55 45,7	19 05,3
9	986	90	55 43,5	19 05,0
10	985	80	55 45,0	19 08,0
11	984	72	55 46,7	19 12,5
12	983	70	55 48,4	19 16,6
13	982	65	55 50,0	19 20,3
14	981	60	55 51,5	19 24,0
15	980	58	55 53,2	19 27,8
16	979	55	55 55,2	19 25,0
17	978	70	55 57,4	19 22,0
18	977	75	55 59,0	19 19,0
19	976	84	56 01,9	19 16,0
20	975	122	56 03,9	19 13,0

Key:

- | | |
|---------------------------------|----------------|
| 1. Station number (see Fig 2.2) | 4. Coordinates |
| 2. Station | 5. lat N |
| 3. Depth, m | 6. long E |

Of special interest both scientifically and organizationally is the successful fulfillment of the complicated operational maneuvers to synchronize the vessel optical measurements with the overflight of the No 30 Meteor satellite carrying the Fragment camera. With a spatial resolution of 80 m, the width of the field of view of this camera in this region is only 85 km, which causes considerable difficulties in collecting synchronous reference information. During the experiment, the field of view of the Fragment camera passed through the Baltic Sea only twice, on 23 and 24 April. The day before, upon receiving the revised forecast of satellite movement, the Control Group performed calculations and ordered the vessel A. v. Humboldt to shift from the initial working region (1, see Fig 2.1) on 23 April to point 2, and on 24 April, to point 3 (Table 2.4). These shifts ensured that the vessel would be located in the field of view during both satellite overflights. Afterwards, the vessel was returned to the initial working region (Table 2.5).

A general representation of the success which the vessel and airplanes had in executing the subprograms is given in Table 2.6. The USSR and GDR specialists performed the full volume of hydrooptical measurements in the vessel subprogram. Sea-surface temperatures were measured using an IR radiometer at the stations; continuous measurements during vessel travel were not made. The temperature of the water surface layer was measured using thermistor sensors only at individual stations.

Table 2.6. Summary of Execution of the Experimental Program. April, 1982

	(2)	(3)	(4)	(5)	(6)			
(1) Дата	Сушко, А. ф. Гумбольдт*		Самолет Ил-14		Самолет Ан-30	5, 7, 8-й ИСЗ „Метеор-2“	30, 31-й ИСЗ „Метеор“	(7) Аэрологическое зондиров.
	(8) температура	(9) гидрооптические измерения	(8) температура	(10) температура и влажность воздуха	(11) МКФ-6м	(12) температура	(13) изображения	
18			+			+		+
19	+		+		+	+		+
20	+					+	+	+
21	+	+	+	+		+	+	+
22	+	+				+	+	+
23	+	+	+	+	+	+	+	+
24	+	+	+	+	+	+	+	+
25	+	+	+	+	+	+	+	+
26	+	+	+	+		+	+	+

Key:

- | | |
|---------------------------------------|----------------------------------|
| 1. Date | 8. temperature |
| 2. Vessel A. v. Humboldt | 9. hydrooptical measurements |
| 3. Il-14 airplane | 10. air temperature and humidity |
| 4. An-30 airplane | 11. MKF-6M |
| 5. Nos 5, 7 and 8 Meteor-2 satellites | 12. water temperature |
| 6. Nos 30 and 31 Meteor satellites | 13. images |
| 7. Aerological sounding | |

The Il-14 airplane performed 50 hours of flight work. Data were obtained on the sea surface temperature in the vessel operating region and over the approach from the coast to the site. Data were also obtained on the air temperature and humidity at the flight altitude (usually 300 m). The aerial work (Figs 2.5 and 2.6) was done synchronously (or quasi-synchronously) with the Meteor-2 satellite measurements of sea-surface radiative temperature and with the vessel measurements of water temperature. In addition, soundings were taken: successive measurements of the air temperature above the vessel at altitudes of 100, 200, 300 and 400 m.

The An-30 aircraft performed 30 flight hours of aerial work. A large volume of photographic data was obtained using the MKF-6M under various weather conditions and from various altitudes (from 1000 to 6000 m) at various times of the day.

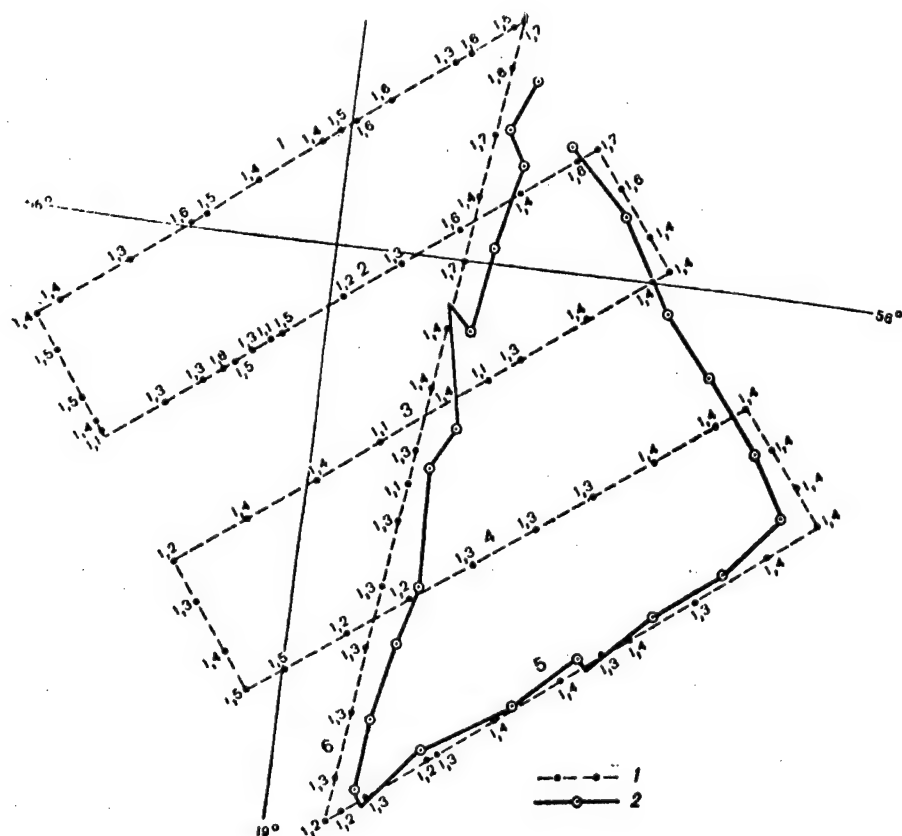


Figure 2.5. Actual Routes of the Il-14 Airplane (1) and the Vessel A. v. Humboldt (2) Over the Site on 19 April 1982:

The radiative temperatures ($^{\circ}\text{C}$) from aerial measurements are shown. The numbers indicate the number of the aircraft route leg.

2.5. Weather Conditions During the Experiment

The weather conditions in the Baltic Sea during the subsatellite experiment were marked by rapid changing of the atmospheric processes at the beginning and end of the period and by relative stability during the middle.

The weather in the test sites at the beginning and very end of the joint work was determined by the activation of cyclonic activity and the formation of front boundaries with a rapid alternation of cyclones and anticyclones (sometimes within several hours during the joint observations). During the middle period of the joint work, the weather was anticyclonic.

In general, the weather was predominantly clear and sunny, with either calm (in two cases) or moderate winds (7-8 m/s). On the next-to-last day of the experiment, a steady strong north wind of 10-12 m/s and tending to strengthen was recorded. The maximum wind speed of 16 m/s was recorded on 16 April.

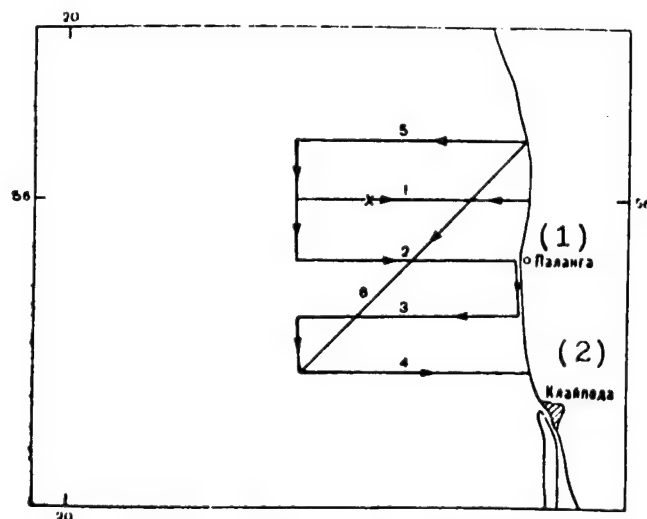


Figure 2.6. Actual Route of the Il-14 Airplane in the Nearshore Zone on 23 April 1982:

The numbers indicate the number of the flight leg. The cross indicates the vessel position.

Key:

1. Palanga

2. Klaypeda

The work was carried out when the spring warmup of the water masses was starting. During clear sunny weather, with radiation heating and without advection of cold air masses, the air temperature increased, reaching 8-10° C. In the presence of advection of cold air masses, the air temperature decreased by several degrees and, as a rule, was below the mutliyear average daily air temperature (for example, on 25 April 1982).

Overall, for the entire period, the predominant air temperature was below the multiyear average daily temperature, due to the distinguishing features of atmospheric circulation in the Baltic Sea during that period.

Air-temperature fluctuations were noted during the entire working period. Below is a description of the weather conditions for individual days of the experiment.

18 April. On the first day of the experiment (when only airborne measurements were made) the weather over the site in early morning was determined by the northwest boundary of an anticyclone centered above Minsk, which caused sunny weather and mid-level clouds at the very beginning of the measurements. By 10 am, a cyclone approached the working region from Scandanavia. The weather began to be determined by the southeast periphery. A secondary cold front passed through the region. All of this caused the weather to change from sunny to cloudy. Altocumulus clouds were replaced by continuous low-level stratocumulus clouds with a ceiling of 600-700 m, which very rapidly descended to 400 m, with some cloud accumulations dropping to 250 m and with individual clouds noted at altitudes of 100-150 m. At the end of the aerial observations, rain and

snow was observed at water level (as the front passed). At first, the visibility deteriorated insignificantly from 40-50 km; then in the second half of the aerial working period, it decreased very quickly, reaching a minimum of 3 km by the end of the aerial observations.

There was a change in the wind field, both in terms of strength (from 5 to 12 m/s) and direction (from 340 to 0°), which was also linked with the passage of the cold front.

19 April. In the first half of the day, as during the day before, the weather was determined by the influence of the periphery of the same cyclone. During the second half of the day, the weather over the entire Baltic Sea was determined by a high-pressure region centered above England.

The restructuring of atmospheric processes also caused a change in the weather conditions right during the synchronous observations. On this day, continuous nimbostratus clouds were replaced by stratocumulus clouds, which disappeared altogether by the end of the joint work. The weather then became sunny and the steady precipitation ceased during the first half of the measurement period.

The visibility increased to 20 km. A moderate northerly wind of 8-10 m/s was observed. After the end of the joint work, the wind strengthened and cloudiness increased close to the shore because a new cyclone with a front approached from the Atlantic. The air temperature decreased because of cold advection.

21 April. The work region was located in a barometric trough. The weather conditions were: unbroken low-level cloudiness (stratocumulus and nimbostratus) with a ceiling of 400 m. The wind was northerly and moderate (10°, 10 m/s). The visibility was 5-8 km.

23 and 24 April. For the next two days of the joint work, the weather was determined by a low-gradient high-pressure field, which produced calm and clear, sunny weather. The air temperature was 8° C.

25 April. In the next-to-last day of the work, the weather was determined by the southwest boundary of an anticyclone. During the entire day, the weather was sunny and clear; the wind speed was 12-14 m/s and wind direction was 350°. The air temperature was 6° C.

26 April. The Baltic-Sea weather was determined by a trough. A cold front passed through the working region. This produced continuous (occasionally broken) low-level cloudiness (stratocumulus and nimbostratus) with a ceiling of 450-500 m. When the front passed, the cloudiness was continuous with a ceiling of 150-200 m, with the altitude of individual clouds not exceeding 80-100 m.

During the entire measurement period, rain, sometimes heavy, was noted, along with strong northerly winds (14-16 m/s). The air temperature decreased to 4° C.

Overall, during the subsatellite working period, the most favorable days for satellite observations were 22 through 25 April, when stable, relatively clear weather predominated, produced by a low-gradient high-pressure field (Figs 2.7 and 2.8). The wind was weak and of variable direction.

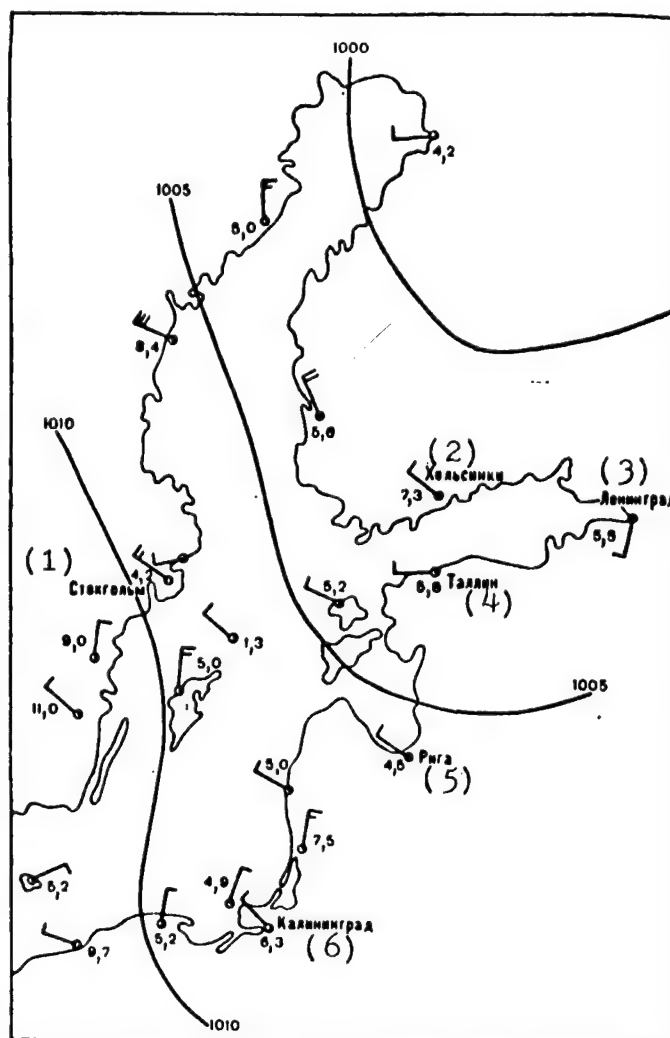


Figure 2.7. Weather Map for the Baltic Sea Region on 17 April 1982 at 1600 GMT

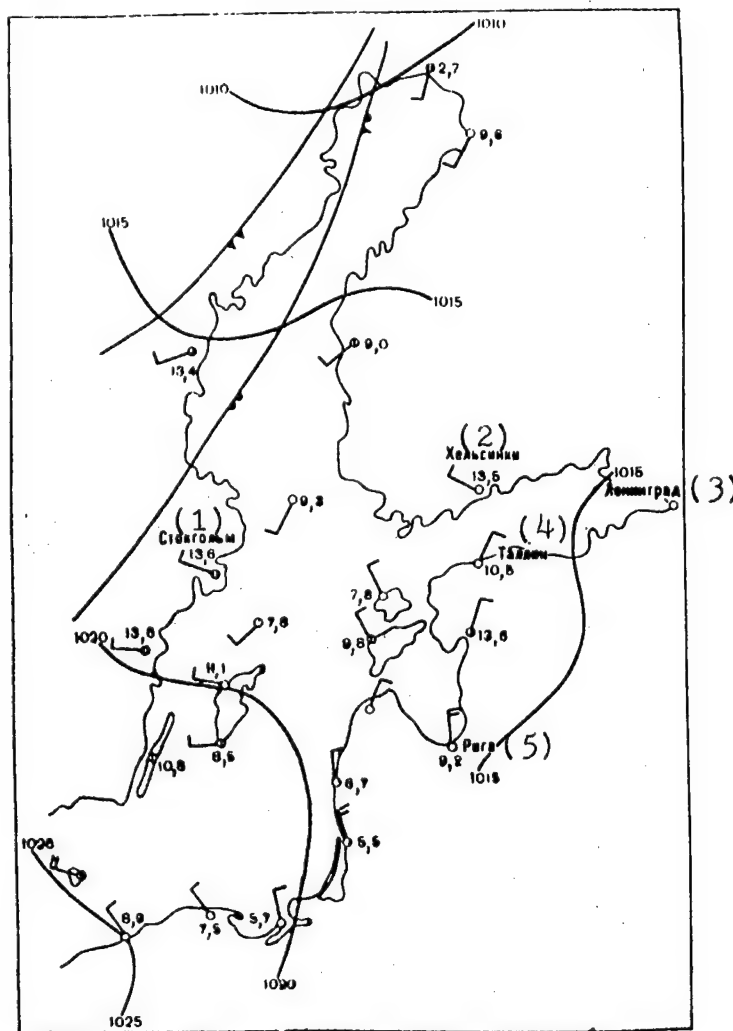
Key:

- | | |
|--------------|----------------|
| 1. Stockholm | 4. Tallinn |
| 2. Helsinki | 5. Riga |
| 3. Leningrad | 6. Kaliningrad |

3. Accumulation of Satellite and Reference Oceanographic Data in the Format of a Regional Information Bank

In recent years, the volume of oceanographic information obtained by observations from various platforms has increased greatly. The use in oceanography of data from satellite platforms leads to ever greater volumes of initial data, which exceed by several orders of magnitude the volumes of

1. *Chlorophyll a* and *Chlorophyll b* were determined by the method of Lichtenthaler and Whistler (1973). The total chlorophyll content was determined by the method of Arar and Cook (1977). The carotenoid content was determined by the method of Lichtenthaler and Whistler (1973). The total carotenoid content was determined by the method of Arar and Cook (1977). The total carotenoid content was determined by the method of Arar and Cook (1977).



•

- | | |
|--------------|------------|
| 1. Stockholm | 4. Tallinn |
| 2. Helsinki | 5. Riga |
| 3. Leningrad | |

interests of oceanography on the basis of a limited number of files of synchronous satellite and reference measurements without the inevitable, at this stage, constant and frequent references to a centralized archive of satellite data.

While retaining the main features of the conceptual data bank [13] for an interactive satellite-information processing system, the format of the regional satellite and reference oceanographic data bank developed by LO GOIN has a number of distinguishing features.

3.1. Data Bank Structure

The bank consists of a data base [DB] and a data base control system [DBCS] with programs for processing and presenting the information.

The software of the bank must perform the following functions:

receive and arrange data on machine carriers;

permit the editing of data;

present the information for applications;

present the information for reference purposes;

provide information on the data base contents and

output the data in numerical or graphic form.

The link between user and data bank can be either in a packet or in an interactive mode.

The structure of the data base makes considerable use of the formats of the oceanographic data: vectors (oceanographic station, airplane route leg) or matrices (satellite observations, calculated fields of various parameters). This makes it possible to economically and effectively use index addressing of records in files, since the volume of records greatly exceeds the volume of indexes. The index-random addressing method is used. In this system, a multilevel indexing scheme was selected. The inputs to the indexes are the component keys, while the outputs are the absolute addresses of the records.

Information is inputted into the data base by the input module (Fig 3.1). Information can be entered from punched tape [PT], from an automated aerial-observation system, from punched cards and from external carriers: magnetic tape [MT] and magnetic disks [MD].

The information is outputted on an alphanumeric printer, a plotter or a display.

The development of programs to provide for an interactive operating mode is planned. The system will output answers on the terminal screen or through the output module to various information-display devices.

The data base uses two index levels (Fig 3.2). If necessary, additional indexing levels can be provided.

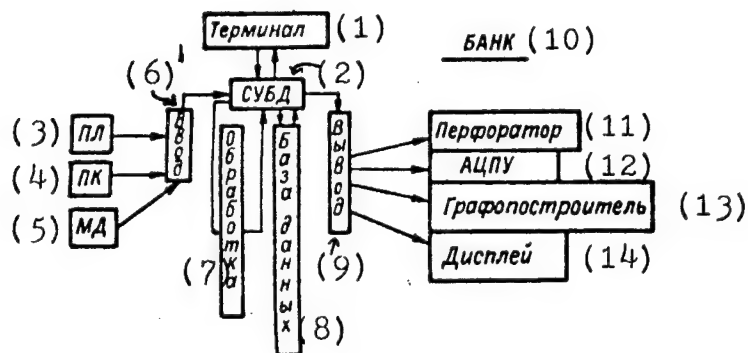


Figure 3.1. Diagram of Bank Interfaces

Key:

- | | |
|---------------|--------------------------|
| 1. Terminal | 8. Data base |
| 2. DBCS | 9. Output |
| 3. PT | 10. Bank |
| 4. PC | 11. Perforator |
| 5. MD | 12. Alphanumeric printer |
| 6. Input | 13. Plotter |
| 7. Processing | 14. Display |

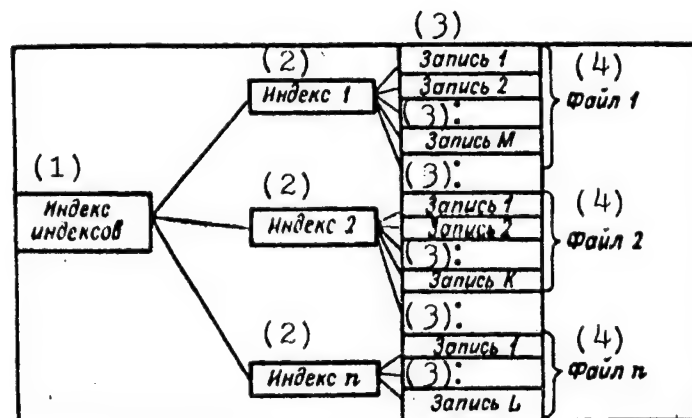


Figure 3.2. Principles of the Logical Organization of the Data Base

Key:

- | | |
|---------------------|-----------|
| 1. Index of indexes | 3. Record |
| 2. Index | 4. File |

At present, three files have been established: satellite information (KOSM), airborne observations (AVIA) and vessel observations (SUDNO). There can be any number of files. The procedure for creating a new file is simple and can be performed by either an administrator or by a bank user. The administrator can register the users.

The records are arranged in random order on the carrier as they arrive, without separation by file (Fig 3.3). Records from different files follow one after another. The order is determined only by means of the indexes. Blank sections appear because records are eliminated after their respective expiration dates. This organization of records greatly simplifies the processes of updating and supplementing the data. A record of the KOSM file contains the observational data from one satellite overflight. Multichannel information can be stored. The record of an airplane file contains the data of one flight; i.e., a set of data from several legs, which is combined and organized inside the record by service information (number and length of legs and frequency of observations). The organization of vessel observations is more complicated due to the many different types of data (individual oceanographic parameters), their spatial position (horizons) and methods of measurement (remote and in situ).

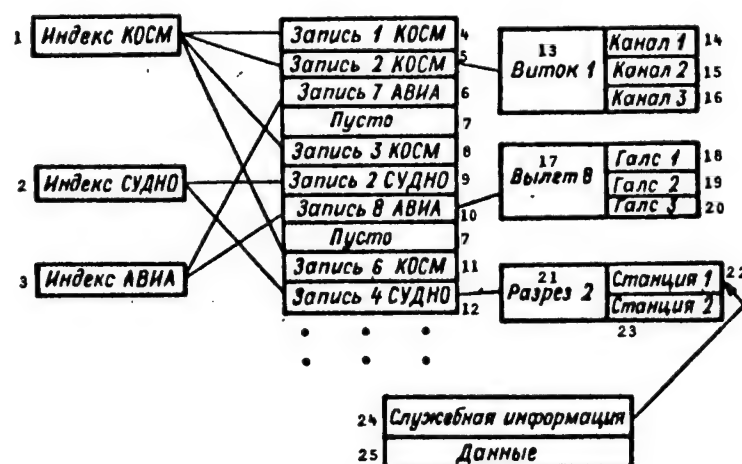


Figure 3.3. Physical Organization of Data

Key:

- | | |
|--------------------|-------------------------|
| 1. KOSM index | 14. Channel 1 |
| 2. SUDNO index | 15. Channel 2 |
| 3. AVIA index | 16. Channel 3 |
| 4. KOSM record 1 | 17. Flight 8 |
| 5. KOSM record 2 | 18. Leg 1 |
| 6. AVIA record 7 | 19. Leg 2 |
| 7. Blank | 20. Leg 3 |
| 8. KOSM record 3 | 21. Cross section 2 |
| 9. SUDNO record 2 | 22. Station 1 |
| 10. AVIA record 8 | 23. Station 2 |
| 11. KOSM record 6 | 24. Service information |
| 12. SUDNO record 4 | 25. Data |
| 13. Pass 1 | |

We will now discuss the structure of the records and indexes (Fig 3.4). Each record is preceded by a record title and concludes with a start-of-record indicator, for example, an absolute or relative address.

The record title, along with the word definition of the data, also can contain service information on the distinguishing features of data organization in the record. In this case, the record title partially fulfills the function of an index, which simplifies the structure of the index itself. The start-of-record indicator, put at the end of the record, is a data-protection element. These indicators, along with the record titles, make it possible to restore the indexes if they are destroyed. The index is a table of keys and indicators, and complex keys are used. The record identifier is generated by the system and serves as the primary key. The aggregate of several other key components is also a primary key, while each component is a secondary key. This organization of keys makes it possible, on the one hand, to easily obtain various inverted files (according to sets of secondary keys) and, on the other hand, to promptly work with the selected information according to the record identifiers. As this figure shows, secondary keys are: space-time coordinates of the observation; the channel, leg or cross section number; the author and date of information entry into the data base; the expiration date and several other attributes. The key defines the indicator which is used to end the record in the external memory. The indicator also contains some necessary information on data organization in the record.

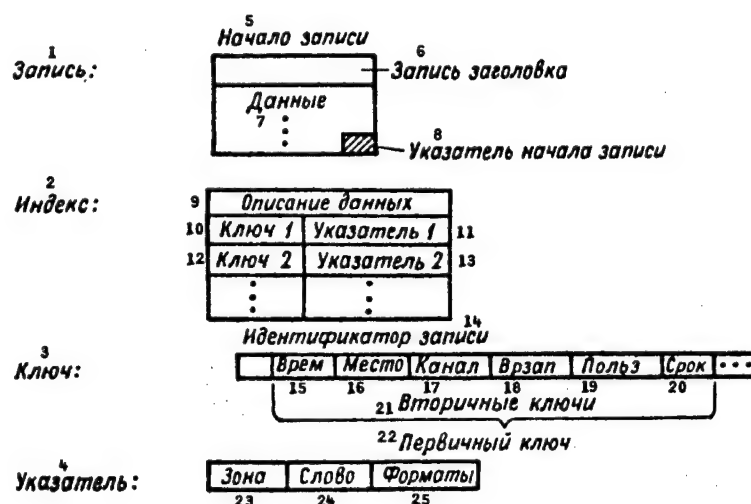


Figure 3.4. Structure of Records and Indexes

Key:

- | | |
|------------------------------|-----------------------|
| 1. Record: | 14. Record identifier |
| 2. Index: | 15. Time |
| 3. Key: | 16. Place |
| 4. Indicator: | 17. Channel |
| 5. Beginning of record | 18. Time of recording |
| 6. Record title | 19. Use |
| 7. Data | 20. Expiration |
| 8. Start-of-record indicator | 21. Secondary keys |
| 9. Description of data | 22. Primary key |
| 10. Key 1 | 23. Zone |
| 11. Indicator 1 | 24. Word |
| 12. Key 2 | 25. Formats |
| 13. Indicator 2 | |

The data-description language is a modified set of Fortran format specifications.

3.2. List of Operations Performed

The data-manipulation language [DML] is a set of Fortran operators for calling up subroutines. In order to make work in the packet mode easier, the list of subroutine parameters was reduced as much as possible. This was achieved by putting auxiliary information in the indexes and directly in the records.

In the interactive mode, the parameters are entered sequentially upon inquiry from the screen after giving the name of the DML subroutine-statement. The scheme used in the CODASYL language is realized. The following operations are provided:

creating (or opening) a file; i.e., referring to the index of one of the files; further interpretation of the DML statements will occur with the use of parameters of the selected index;

searching for data in the base, without transmitting them to the working area of the magnetic on-line memory;

transferring data to the working area;

changing and editing data (inside a record);

recording new data; the record is entered with modification;

eliminating a record; i.e., erasing the key of the corresponding record in the index; although the record remains, it becomes "transparent" to the user, and it becomes a "blank" section;

organizing the file, collecting the "trash"; the records are physically transferred to new addresses, "blank" sections are eliminated and the indexes are reorganized and

quitting a file, ending contact with the bank; this is necessary to remove the bank programs from the magnetic on-line memory.

The processing module contains the following operations: averaging and placing the information in a regular network of a given spacing, adding (subtracting) fields, comparing two fields, calculating histograms, calculating functions along a given cross section or along a broken line and several other operations.

The bank format was tested, in particular, on information obtained during the joint subsatellite experiment of the USSR and GDR in April 1982. The water temperatures at standard horizons, obtained by the research vessel A. v. Humboldt, and the sea surface temperatures measured by the IR radiometers from the airplane and satellite were entered into the data base.

The implementation of the bank format into daily use will greatly simplify and speed the processing of synchronous satellite and reference measurement data.

4. Complex Hydrooptical Research in the Central Baltic Sea

4.1. Distribution of Suspended Matter and Chlorophyll in the Experiment Region Based on Vessel Measurements

Generalized data on the distribution of suspended matter in the Baltic Sea can be found in [18]. At an average value of 3 mg/liter, the concentration of suspended matter in the Baltic Sea is 2-5 times higher than the average concentration in other seas of the Atlantic Ocean and in the ocean itself (Table 4.1). High concentrations of suspended matter occur in surface layers; the suspended-matter concentrations decrease below the thermocline and in layers below the discontinuity layer. Only in the bottom layers (0-5 m above the sea floor) is there a noticeable increase in the suspended-matter content.

Table 4.1. Concentration of Suspended Matter in the Baltic Sea [18]

<u>Layer, m</u>	<u>Average value, mg/liter</u>	<u>Range, mg/liter</u>
Surface	3.3	0.6-12.4
10-20	2.8	1.5-5.4
25	2.4	0.2-8.0
50	1.9	0.4-8.1
100	1.9	0.4-4.8
At the bottom	3.0	0.4-12.4

The maximum concentrations are observed primarily near the sources of the suspended matter: abrasion coasts, estuaries, straits and shallow sections of the sea with active bottom erosion. The suspended matter entering the sea moves along the coasts and out to the deep sea. The zones of maximum suspended-matter content vary in width from 3 to 60 km. High concentrations of suspended matter linked with plankton activity are also observed in regions of high biological activity. Published maps indicate that the suspended-matter concentration is 2-3 mg/liter in the surface layer of the site near international station 9A. At a distance of 40 km toward the coast, there is a 33-km-wide band of increased concentrations (over 4 mg/liter). This band includes station 974. High concentrations, from 3 to 4 mg/liter, were also noted in regions east of Rügen Island and in Pomeranian Bay, investigated by the vessel A. v. Humboldt during a trip made as part of the subsatellite-experiment program.

The suspended matter is terrigenous in most layers near abrasion coasts, but in the open sea, biological materials predominate. In [19] it was established that in samples taken from surface layers in the open part of the Baltic Sea, 76.9-99.6 percent of all the suspended particles were organic. At the surface in the Gotland Basin, organic particles (especially diatoms) make up 77 percent. The overall quantity of particles is about $0.6 \cdot 10^6$ per liter; the maximum values of $1.2 \cdot 10^6$ particles/liter were observed at the discontinuity layer and in bottom layers ($1.0 \cdot 10^6$ particles/liter). The particle sizes are mainly less than $2.5 \mu\text{m}$ [19].

During the preparatory research for the joint experiment (August 1981) and during the experiment (April 1982), the measured concentrations of suspended matter were mainly in the range 0.4-2.0 mg/liter. Concentrations exceeding 2.0 mg/liter were noted only at a few stations and at a few horizons. The data at nearshore stations also do not coincide with the values given in [18]. One of the possible reasons is the use of different analytic methods. Significant differences can occur when the suspended-matter content is determined by filtration methods, depending on the type of filters used and the methods of processing them [48].

Generalized information on the occurrence of chlorophyll and on the extent of phytoplankton in the Baltic Sea can be found in [20, 23, 24, 42, 48, 49].

The spatial distribution and temporal development of phytoplankton are determined by various natural factors. Spatial changes in the phytoplankton content are strongly dependent on water salinity. The most important parameters for plankton growth are light and biogenous elements. In addition, water temperature, stratification and turbulent mixing also affect phytoplankton growth.

The dominant forms of phytoplankton in the Baltic Sea are diatoms, blue-green algae and dinoflagellates. The Baltic Sea has several characteristic temporal maximums for the growth of phytoplankton biomass. Massive phytoplankton growth ("blooming") depends on the following conditions:

a sufficient amount of solar energy reaching the sea surface;

sufficient reserves of biogenous elements and

the presence of phytoplankton in a layer with sufficient light for primary production (euphotic zone). This condition means that vertical convection must not exceed the depth of the euphotic zone.

Due to the fact that the optimum conditions for phytoplankton blooming occur in different regions of the Baltic Sea at different times, there are regional differences in the periods and intensity of blooming. The spring phytoplankton bloom is the most intense. In the eastern and northern parts of the Baltic Sea, the spring bloom begins 1-3 months later than in the western parts.

Approximate Times for the Start of Blooming for Several Characteristic Regions of the Baltic Sea

Mecklenburg Bay	before mid-March
Arkona and Gdansk Basins	late March-early April
Bornholm Basin	mid-April
Southern Gotland Basin	late April-early May
Gotland Depression	mid-May

The second phytoplankton bloom, which is mainly represented by blue-green algae, occurs in summer (late July-early August) and is particularly

manifested in the west and central Baltic Sea. The fall peak of phytoplankton biomass in the Arkona, Bornholm and Gotland Basins (late September-October) is less significant than the spring peak.

The chlorophyll concentration per unit volume of water (mg/m^3) or the concentration in the euphotic-zone water column (mg/m^2) is often a measure of phytoplankton biomass. If that is insufficient, then an additional chlorophyll determination is used to establish phytoplankton temporal changes and horizontal and vertical distribution; a determination of the phaeopigments (decomposition products of chlorophyll) permits the physiological state of the phytoplankton to be determined.

The Oceanography Institute, GDR AS, has been conducting chlorophyll distribution research in the Baltic Sea since 1969, usually regularly four times a year. In order to determine the average chlorophyll concentrations in the experiment region, data were used from the following stations characteristic of the southern part of the Gotland Basin:

9A	lat $56^{\circ}06'$ N,	long $19^{\circ}10'$ E
8A	lat $55^{\circ}38'$ N,	long $18^{\circ}36'$ E
259	lat $53^{\circ}33'$ N,	long $18^{\circ}24'$ E

The average (for 1969-1982) chlorophyll concentrations were determined at these stations for the euphotic zone from 0 to 30 m (Table 4.2).

Table 4.2. Average Chlorophyll Concentrations in the Experiment Region

<u>Time</u>	<u>Concentration,</u> <u>mg/m^3</u>	<u>Concentration in</u> <u>column, mg/m^2</u>
Late March	0.57	17.2
Mid-May	2.03	61.0
Early August	1.65	49.4
Late October	1.17	35.1

It should be noted that the maximum values at a given depth can be much higher than these data, since the distribution of phytoplankton in the upper 30-m layer is not always homogeneous. For example, in the eastern Gotland Basin in May 1970, chlorophyll concentrations above $153 \text{ mg}/\text{m}^2$ were determined, while at the mouth of the Gulf of Finland in May 1972, the concentration was even above $350 \text{ mg}/\text{m}^2$ (at a depth of 5 m, above $30 \text{ mg}/\text{m}^2$).

On the basis of available data, a plankton bloom in the experiment area can be considered as occurring when the chlorophyll concentration exceeds $3 \text{ mg}/\text{m}^3$. We emphasize that due to the small number of measurements and the absence of appropriate models, it is impossible at this time to make any specific forecasts of the time, duration or activity of phytoplankton blooms for a particular small region of the Baltic Sea on the scale of the subsatellite site in 1982.

With regard to seston, there are only a few measurements in the experiment site, giving the following minimum and maximum seston concentrations:

October 1978	0.3-1.2 mg/liter
August 1980	0.6-1.5 mg/liter
August-September 1982	0.6-1.5 mg/liter

During the subsatellite experiment, the concentrations of suspended matter (seston), chlorophyll a and phaeopigments were determined in the site near international station 9A from 19 through 22 and from 25 through 26 April 1982. Additionally, the attenuation of light at a wavelength of 380 nm (α_{380}) by filtered water samples was studied as an additional measure of the dissolved absorbing substances. Besides taking into account horizontal inhomogeneities by taking surface samples every 5 km, the dissolved- and suspended-matter contents in the 10-m-thick surface layer were determined at stations 995, 992, 989, 986 and 983 (distance between stations, 15 km) simultaneously with the optical measurements (an attempt at continuous recording of the chlorophyll content failed for technical reasons). At stations 974 and 973, the dissolved- and suspended-matter contents were determined every 2 h on 23 and 24 April 1982.

During the subsatellite experiment, the concentrations of seston, chlorophyll a and phaeopigments at a depth of 0 m were determined (Table 4.3). The maximum chlorophyll concentrations were not always in the top surface layer, due to light obstruction of phytoplankton products [23].

Table 4.3. Range of Suspended-Matter and Chlorophyll Contents at the 0 m Horizon

	<u>Site</u>	<u>Station 974</u>	<u>Station 973</u>
Seston, mg/liter	0.4-1.5	0.5-1.9	0.9-2.0
Chlorophyll a, mg/m ³	1.3-4.3	3.1-8.0	1.2-5.0
Phaeopigments, mg/m ³	0.1-2.0	0-0.7	0.6-1.6

An example of the horizontal distribution of chlorophyll and phaeopigment concentrations at the sea surface is shown in Fig 4.1. The greatest concentrations almost always were observed at the most northerly stations and in the southwest part of the site. During the repeat survey on 25 and 26 April, the concentration distribution at a depth of 0 m was more homogeneous. The distribution of pigments in the upper 10-m layer presents a similar picture (Fig 4.2). During the entire research period, the highest maximums of chlorophyll (over 5 mg/m³) occurred at stations 995 and, especially, 989. The distance between pigment-concentration maximums was about 25-30 km (according to measurements made at separate points). These distinguishing features observed in the pigment distribution are not so clearly manifested in the distributions of seston or dissolved organic matter.

The temporal changes in concentrations of dissolved and suspended matter during the measurements on 23 and 24 April are shown in Fig 4.3. Both the dissolved organic matter concentrations (the figure shows the light attenuation, α , at a wavelength of 380 nm) and the chlorophyll concentrations are much higher at nearshore station 974 (distance from the coast, about 35 km) than at station 973 in the open sea. At station 974,

a water mass with lower seston and chlorophyll concentrations arrived at about 1100 GMT, but after noon, it was followed by a water mass with higher concentrations.

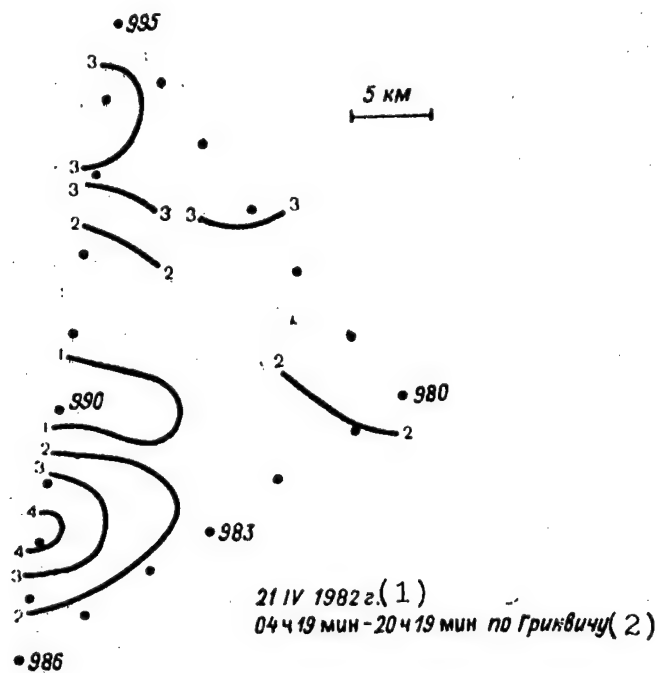


Figure 4.1. Horizontal Distribution of Chlorophyll a and Phaeopigments at a Depth of 0 m, mg/m^3

Key:

1. 21 April 1982

2. 0419-2019 GMT

Significant changes in the concentrations of suspended matter and, especially, chlorophyll were observed on 24 April. Additional research on the phytoplankton volumes and a determination of the dominant types at a depth of 0 m emphasize these changes (Table 4.4).

Based on the fact that the dominant types of phytoplankton varied considerably, it can be concluded that the observed changes in pigment concentrations apparently are primarily caused by advective processes.

4.2. Several Results of Vessel Research on the Surface Spectral Brightness of the Baltic Sea

Within the framework of the joint subsatellite oceanographic experiment on the Baltic Sea in April 1982, research was conducted on the spectral brightness of the sea surface and functions were obtained of the dissolved- and suspended-matter concentrations vs. the spectral brightness coefficients in selected visible-wavelength bands. In preparation for the joint experiment, similar research was done by specialists of the Oceanography Institute, GDR AS, on the vessel A. v. Humboldt in August 1981.

The work was performed mainly on the site near international station 9A, as well as in Pomeranian Bay and in the Arkona and Bornholm Basins (Fig 4.4).

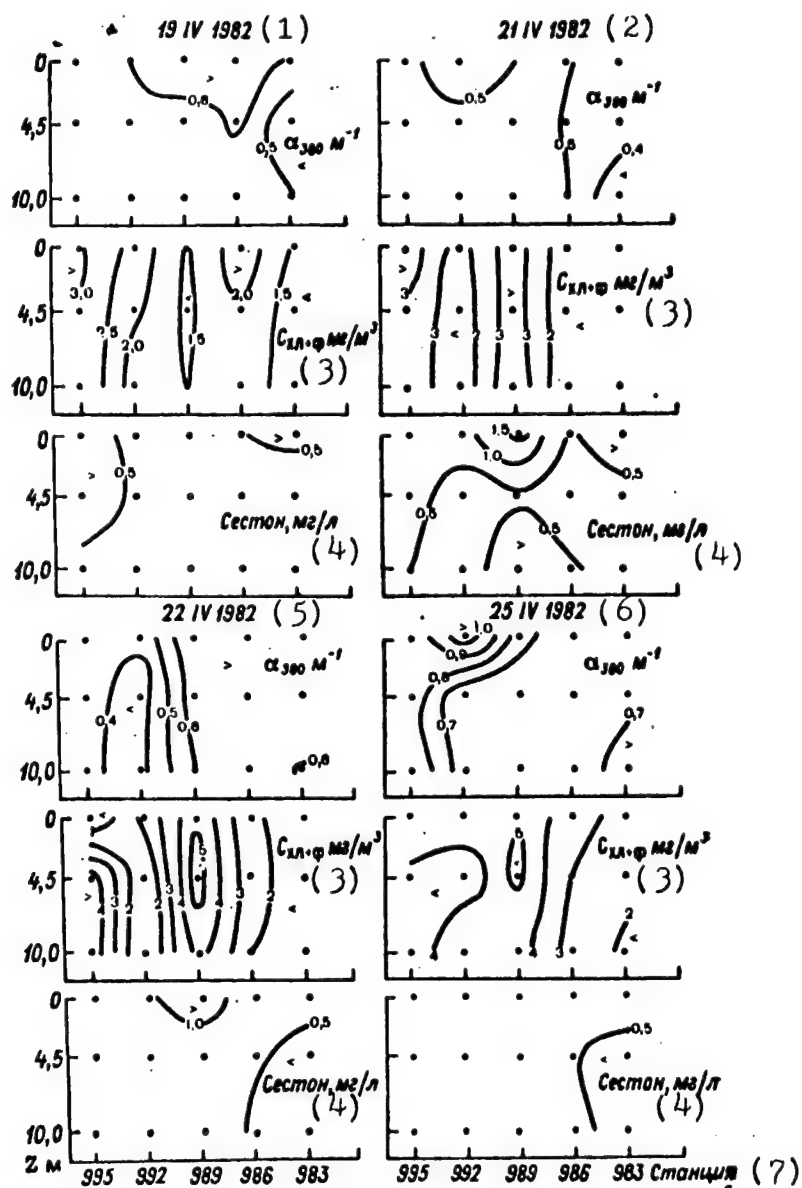


Figure 4.2. Spatial Distribution of Concentrations of Seston, Pigments and Dissolved Organic Matter, α_{380} .

Key:

- | | |
|-----------------------------------|------------------|
| 1. 19 April 1982 | 5. 22 April 1982 |
| 2. 21 April 1982 | 6. 25 April 1982 |
| 3. C_{ch+p} , mg/m ³ | 7. Station |
| 4. Seston, mg/liter | |

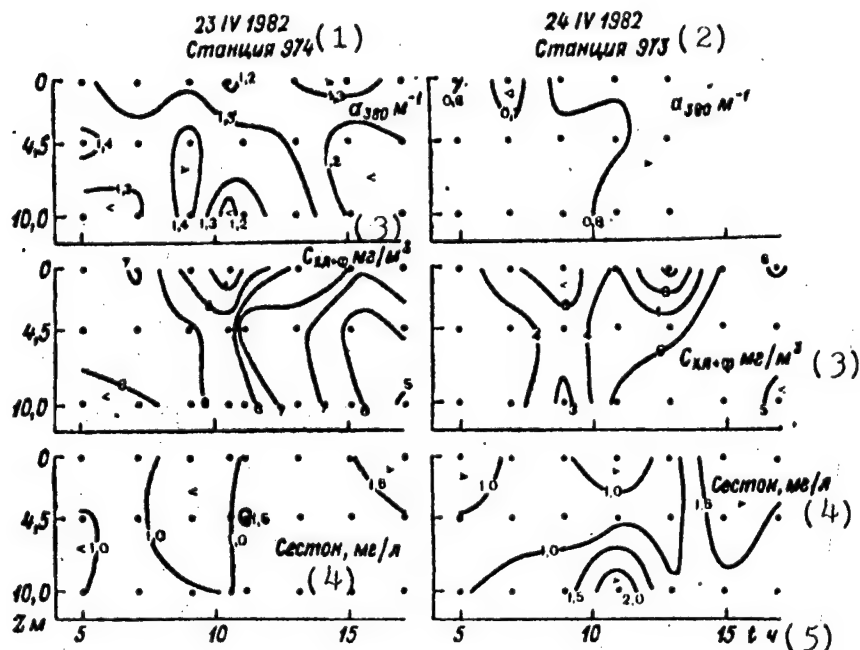


Figure 4.3. Temporal Changes of the Concentrations of Dissolved and Suspended Matter, α_{380} .

Key:

- | | |
|------------------------------|---------------------|
| 1. 23 April 1982 Station 974 | 4. Seston, mg/liter |
| 2. 24 April 1982 Station 973 | 5. t, h |
| 3. C_{ch+p} , mg/m^3 | |

Table 4.4. Volumes and Types of Phytoplankton Determined on 24 April 1982

Время по Гринвичу, ч мин (1)	Объем вытеснения, mm^3/l (2)	Доминирующие виды (3)
4 55	154,0	<i>Aphanizomenon flos-aquae</i> <i>Eutreptia lanowii</i>
7 11	74,6	<i>Chaetoceros ceratosporus</i> <i>Carteria cordiformis</i>
8 58	83,4	<i>Achuanthes taeniata</i> <i>Aphanizomenon flos-aquae</i>
10 00	97,7	<i>Chaetoceros ceratosporus</i> <i>Carteria cordiformis</i>
10 30	72,3	<i>Chaetoceros spp.</i> <i>Aphanizomenon flos-aquae</i>
11 00	117,5	<i>Aphanizomenon flos-aquae</i> <i>Chaetoceros spp.</i>
13 00	70,7	<i>Aphanizomenon flos-aquae</i> <i>Chaetoceros spp.</i>

Key:

- | | |
|--------------------------------------|-------------------|
| 1. GMT, h min | 3. Dominant types |
| 2. Displacement volume, $mm^3/liter$ | |

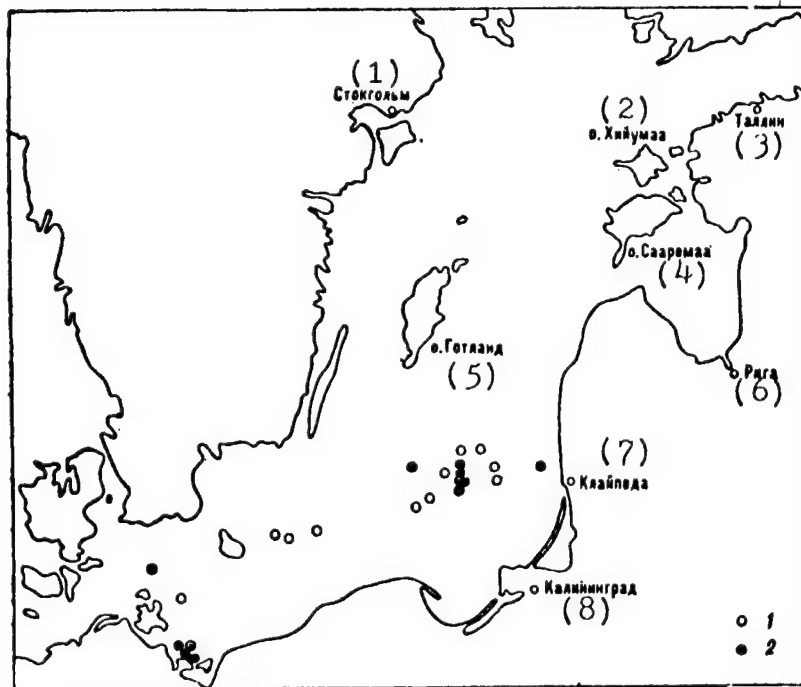


Figure 4.4. Location of Stations at Which Hydrooptical Measurements Were Made in August 1981 (1) and April 1982 (2)

Key:

- | | | |
|-------------------|--------------------|----------------|
| 1. Stockholm | 4. Saaremaa Island | 7. Klaypeda |
| 2. Hiiumaa Island | 5. Gotland | 8. Kaliningrad |
| 3. Tallinn | 6. Riga | |

The spectral brightness coefficients, ρ_λ , (Fig 4.5) were determined using measurements of the descending spectral irradiance, E_λ^{\downarrow} , and the spectral brightness of the ascending radiation, L_λ , above the sea surface

$$\rho_\lambda = L_\lambda \pi / E_\lambda^{\downarrow} \quad (4.1)$$

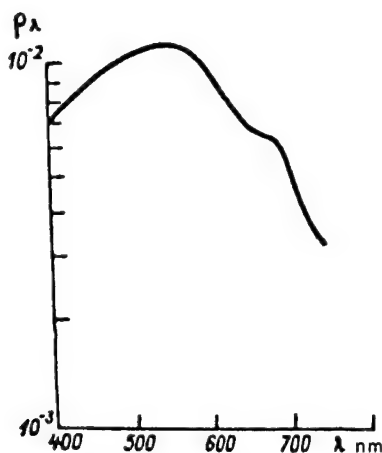


Figure 4.5. Spectral Brightness Coefficients for Subsatellite Station 974, 0900 h

The spectrometer described in [46, 47] was used for these measurements (Tables 4.5 and 4.6).

Table 4.5. Spectral Brightness of Ascending Radiation, L_λ , $W/(cm^2 \cdot nm \cdot sr)$. April 1982

(1) Станция	(2) Дата	(3) Время по Гринвичу, ч мин	L_{440}	L_{480}	L_{520}	L_{560}	L_{600}
987	20	11 30	0,230	0,313	0,300	0,160	0,123
986	20	13 30	0,250	0,280	0,290	0,145	0,114
984	20	15 00	0,215	0,288	0,270	0,184	0,160
993	22	08 00	0,175	0,240	0,270	0,150	0,130
991	22	10 45	0,210	0,268	0,270	0,143	0,112
989	22	14 20	0,185	0,245	0,250	0,153	0,134
974	23	05 00	0,240	0,298	0,320	0,280	0,187
974	23	09 00	0,285	0,367	0,420	0,272	0,180
974	23	15 00	0,235	0,296	0,310	0,225	0,190
973	24	06 50	0,255	0,292	0,300	0,190	0,176
973	24	10 17	0,270	0,358	0,375	0,245	0,156
973	24	14 20	0,260	0,327	0,325	0,225	0,171

Key:

1. Station 2. Date 3. GMT, h min

Table 4.6. Spectral Brightness Coefficient, $\rho_\lambda \cdot 10^2$. April 1982

(1) Стан- ция	(2) Дата	(3) Время по Гринвичу, ч мин	ρ_{440}	ρ_{480}	ρ_{520}	ρ_{560}	ρ_{600}
987	20	11 30	0,74	0,84	0,85	0,57	0,42
986	20	13 00	0,90	0,90	0,93	0,72	0,445
984	20	15 00	1,23	1,39	1,42	1,16	0,915
993	22	08 00	0,65	0,86	0,96	0,64	0,54
991	22	10 45	0,63	0,72	0,75	0,49	0,35
989	22	14 20	0,68	0,82	0,86	0,65	0,525
974	23	05 00	1,20	1,36	1,54	1,33	1,00
974	23	09 00	0,87	1,00	1,14	0,98	0,685
974	23	15 00	1,36	1,47	1,66	1,53	1,10
973	24	06 50	1,22	1,29	1,41	1,14	0,92
973	24	10 17	0,81	0,93	1,06	0,80	0,50
973	24	14 20	1,30	1,40	1,47	1,14	0,86

Key:

1. Station 2. Date 3. GMT, h min

The maximum values of ρ_λ , exceeding 0.01, were in the spectral band between 530 and 570 nm, with an average of 550 nm.

Spectral brightness values, uncorrected for the influence of the sea surface, obtained from measurements made in 1981 and 1982 were compared with the suspended-matter concentrations determined according to method [48] and with the chlorophyll a and phaeopigment concentrations determined according to method [51]. The average concentrations for the surface layer from zero to 10 m were used, since this layer in the Baltic Sea is the most important in the process of water reflection. Measurements made only in the top surface layer are not representative, since during summer, the

maximum of suspended organic matter in the surface layers of the Baltic Sea frequently occurs at a depth of 3-5 m (due to the light obstruction of the primary productivity in the top 3-m layer [23]).

The relationship between the uncorrected brightness coefficients at a wavelength of 650 nm and the seston concentrations in the surface layer from zero to 10 m (Fig 4.6) can be represented in the following form:

$$\bar{S} = A \rho_{650}^B, \quad (4.2)$$

where $A = 14.24$ and $B = 0.565$ (correlation coefficient, 0.61).

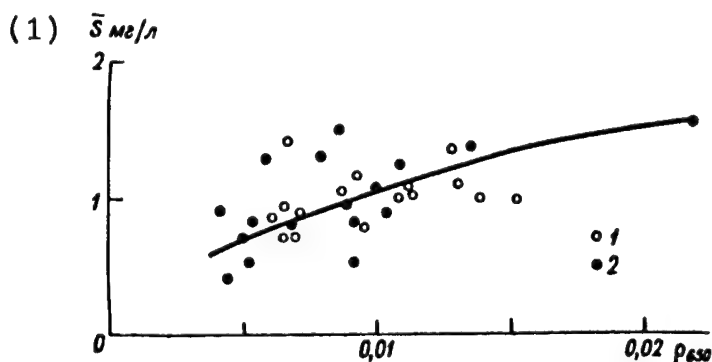


Figure 4.6. Ratio Between Seston Concentrations and Spectral Brightness Coefficients at a Wavelength of 650 nm, Based on Measurements Made in August 1981 (1) and April 1982 (2)

Key:

1. \bar{S} , mg/liter

Only a limited comparison of these results with the data of other authors is possible, due to the small range of measured seston concentrations. These concentrations (0.4-1.5 mg/liter) are lower than the average suspended-matter concentrations in the Baltic Sea surface layer [18]. The concentrations, according to data in analogous published works, in most cases is an order of magnitude higher.

Also investigated was the relationship between the seawater color index, ρ_{440}/ρ_{550} , and the average concentration of chlorophyll a and phaeopigments in the surface layer from zero to 10 m. A wavelength of 440 nm was selected because the absorption maximum of chlorophyll is in this spectral interval. The absorption minimum is at 550 nm. In addition, over 2/3 of the obtained spectral-brightness curves had a maximum in the interval 530-570 nm.

The following relationship was obtained for the total concentration of chlorophyll a and phaeopigments, C_{ch+p} , in the range 0.7-6.5 mg/m³:

$$C_{ch+p} = 1.58 (\rho_{440}/\rho_{550})^{-2.05}. \quad (4.3)$$

A comparison of this relationship with the regression equations obtained by other authors for different bodies of water unexpectedly resulted in a

correspondence (Fig 4.7). This is also true of other relationships not presented here.

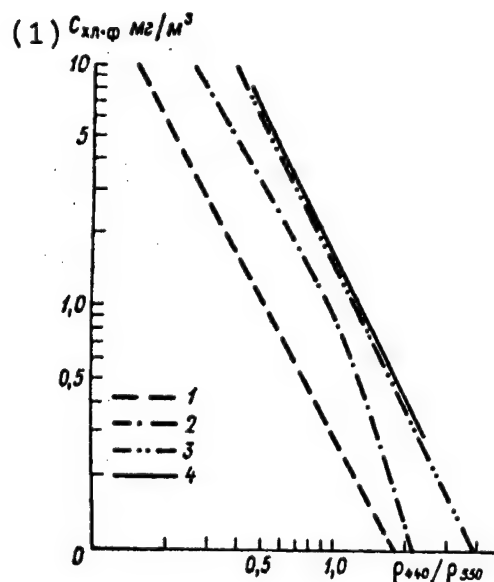


Figure 4.7. Relationship Between Chlorophyll a and Phaeopigment Concentrations and the Color Index:

- | | |
|------------------------------|------------------------------|
| 1. according to data in [60] | 3. according to data in [55] |
| 2. according to data in [41] | 4. present work |

Key:

1. C_{ch+p} , mg/m³

Reference [57] discusses three groups of spectral curves of spectral-brightness coefficients for the summer surface layer of the Baltic Sea, based on measurements made in August 1981. The difference in slope of these curves in the short wavelength region is caused by different concentrations of dissolved and suspended matter. A similar classification could not be made on the basis of measurements made during the joint subsatellite experiment, since different phases of phytoplankton bloom were observed in different areas of the Baltic Sea during this period.

4.3. Determination of the Sea Color Index From Measurements Made Through the Atmosphere

One simple method of analyzing a radiation spectrum is by the brightness ratio at two wavelengths. The selection of the wavelengths at which the brightness ratio is determined is arbitrary and depends on the goals of the investigation. In order to evaluate the biological productivity of waters, the brightness ratio used [32, 39] is that of light leaving vertically upward from the entire sea thickness, L_τ , in the spectral regions around $\lambda_1 = 450$ and $\lambda_2 = 550$ nm

$$I_{se} = L_{\tau\lambda_2} / L_{\tau\lambda_1} \quad (4.4)$$

The wavelengths in ratio (4.4), which is called the sea color index I_{se} , can vary somewhat, but a constant feature is that one of the wavelengths must be in the blue region (430-480 nm) and correspond to the absorption maximum of chlorophyll, while the other must be in the green region (520-550 nm) and correspond to the minimum. Often, a different determination of I_{se} is used: the ratio of the brightness coefficients at two wavelengths. This value differs from (4.4) by a factor equal to $E_{\lambda_1}/E_{\lambda_2}$, which in the general case is not unity.

The water color index observed in situ is a sensitive indicator of the presence of chlorophyll in water. Research in various parts of the world ocean have shown that, depending on the bioproductivity of the waters, the color index can range over more than two orders of magnitude [32]. With detailed study of a water body and with the obtaining of combined data on the chlorophyll content and the color indexes, the latter can be used to determine the chlorophyll concentration [7]. When a spectrophotometer is mounted on an airplane or a satellite, the color indexes can be remotely measured. In this case, the measured quantity is not the sea color index, but the color index of the ascending radiation. Measurements made simultaneously in situ and by above-surface photometers from a vessel or an airplane show that there is a difference between these two values [39]. As the thickness of the atmospheric layer between the sea surface and photometer increases, the information content of the color-index measurements sharply decreases. This is because at high altitudes, the brightness of the ascending radiation in the visible spectral region is formed mainly by the scattered atmospheric radiation and only 10-15 percent by radiation from the sea [11]. This ratio varies depending on the condition of the water medium and the atmosphere. The color index of scattered atmospheric radiation is close to the color index of direct solar radiation (for $\lambda_1 = 450$ nm and $\lambda_2 = 550$ nm, $I_{s,0} \approx 0.9$). To be more precise, the color index of atmospheric haze is somewhat less than this, since in clear atmosphere, Rayleigh scattering is predominant at high altitudes, which shifts the scattered-radiation spectrum toward the short wavelength region. When direct solar radiation propagates downward through the atmosphere, the color index increases an average of 1.14-fold. The value of $I_{s,0}$ increases to 1.05. We note that the color index increases by the same factor when radiation is propagated back from the sea surface to the upper boundary of the atmosphere. When radiation propagates in the water, the spectrum can change significantly, while the color index can have wide-ranging values, from hundredths of a unit to several tens of units (0.03-20) [32]. This depends on the component content of the seawater. Thus, when chlorophyll and dissolved organic matter are present, the proportion of blue-region radiation decreases greatly, and the color index increases. For pure water, it is the opposite: the color index is low, since the blue radiation predominates in the water. There are often cases when the sea color index is high and differs greatly from the atmosphere color index. Then, radiation with a low color index (scattered atmospheric radiation) greatly predominates in the ascending radiation at the upper boundary of the atmosphere, while radiation with the color index of the sea, which contains information about the sea medium, represents a small percentage. The sea color index measured from high altitudes is the color index of the atmospheric haze. How close this value is to the sea

color index being sought depends on a number of circumstances. The approximate formula (4.5) shows the relationship of the color index of radiation measured at an altitude of H , $I(H)$, with the sea color index at an altitude of $H = 0$, I_{se} :

$$I(H) = I_{se}(0) P(\lambda_2) \frac{L_{T\lambda_1}}{L_{h\lambda_1}} + I_h, \quad (4.5)$$

where $P(\lambda)$ is the transfer function of the atmosphere.

Formula (4.5) was obtained by simple transformations of the expression determining the color index:

$$I(H) = \frac{L_{\lambda_2}^h}{L_{\lambda_1}^h} = \frac{(L_{T\lambda_2} + L_{\lambda_2}) P(\lambda_2) + L_{\lambda_2}}{(L_{T\lambda_1} + L_{\lambda_1}) P(\lambda_1) + L_{\lambda_1}}. \quad (4.6)$$

Formula (4.5) is applicable for high altitudes because the brightness of the atmospheric haze, $L_{h\lambda_1}$, at $\lambda_1 = 450$ nm is great compared with the sea-thickness radiation brightness, $L_{T\lambda_1}$, and the sea-surface radiation brightness, $L_{s\lambda_1}$ (Table 4.7).

Table 4.7. Brightness of the Sea Thickness, the Sea Surface and the Atmospheric Haze for Three Situations, According to Data in [11], $W/(m^2 \cdot \mu m \cdot sr)$

	τ_0	L_T	L_s	L_h	Value of Expression (4.6)
Eutrophic waters, average haze	0.3	6.5	23	41	0.07
Oligotrophic waters, average haze	0.3	9	23	41	0.10
Oligotrophic waters, light haze	0.2	9	27	25	0.16

Note. τ_0 is the optical thickness of the atmosphere.

Table 4.7 shows that the approximation in which formula (4.5) was obtained is the most valid for the most interesting case: eutrophic waters (over 0.4 mg/ m^3 of chlorophyll) with average atmospheric optical thickness.

From formula (4.5) it can be seen that the color index $I(H)$ is represented in the form of two addends: the atmospheric-haze color index I_h and the sea color index $I_{se}(0)$ with a certain "weight." This "weight" for high altitudes even for the average case is much less than unity. Thus, the average transparency of the atmosphere for 550 nm is equal to 0.72, and the ratio $L_{T\lambda_1}/L_{h\lambda_1}$ for 450 nm very probably has a value of 1/7. Thus, the true sea color index has a "weight" of 0.1 in the sum (4.5); i.e., has 1/10 the weight of the atmospheric-haze color index. This is due to two factors: 1) the closeness of the values of $I(H)$ to unity; i.e., to the color index of solar radiation and to the scattering radiation of the atmosphere and 2) the small dynamic range of $I(H)$ compared with I_{se} .

The changes in the color index with observation altitude can be followed from spectral-survey data made using an MKF-6 camera and spectrophotometric measurements from various altitudes (Table 4.8).

Table 4.8. Change in the Color Index $I=L_{540}/L_{480}$ With Measurement Altitude

(1) Море	Высота измерения, м (2)					(3) Примечание
	0	1000	2000	3000	6000	
Каспийское, 1980 г. (4)	—	1,10	0,85	0,80	0,75	МКФ-6М (8) МКФ-6М (8) Авиационный спектрометр (9) [56]
Балтийское, 1982 г. (5)	1,10	1,00	—	0,95	0,85	
Балтийское, 1983 г. (6)	—	1,05	—	0,85	0,75	
Средиземное (7)	0,36	0,43	0,50	0,58	—	

Key:

- | | |
|----------------------------|--------------------------|
| 1. Sea | 6. Baltic, 1983 |
| 2. Measurement altitude, m | 7. Mediterranean |
| 3. Notes | 8. MKF-6M |
| 4. Caspian, 1980 | 9. Airborne spectrometer |
| 5. Baltic, 1982 | |

Table 4.8 shows that as light passes through the atmosphere, the color index decreases to 0.75-0.85; i.e., to a value characteristic of the color index of scattered light.

The second fact of note is that the difference in color indexes gradually decreases with an increase in the atmospheric-layer thickness, so that the radiation spectrum is characteristic not of the given sea region, but of the atmosphere.

When the color index is measured from a vessel, the range of values is also small due to the contribution to the radiation of light reflected from the water surface (Table 4.9). The color index values are close to 1, and range from 0.9 to 1.3. The values obtained by two different photometers differ somewhat. This is due to: 1) the difference in wavelengths at which the brightness ratios are determined (543/467 nm for LO GOIN and 550/480 nm for Institute of Oceanography, GDR AS) and 2) the distinguishing features of the measurement methodology.

4.4. Relationships Between Atmosphere Optical Thickness and a) the Horizontal Visibility Range and b) the Sky Radiation Brightness Under Various Atmospheric Conditions Above the Baltic Sea.

In accordance with the experiment program, the research vessel A. v. Humboldt was the platform for measuring the spectral brightness coefficient of the water surface, ρ_λ , and the atmospheric transmission, T_λ , for various spectral intervals in the visible and IR bands. The magnitude of ρ_λ was determined according to formula (4.1). The spectral optical thickness of the atmosphere, τ_λ , was calculated using data on τ_λ in accordance with the formula:

$$T_\lambda = \exp(-\tau_\lambda); \quad \tau_\lambda = \tau_{A\lambda} + \tau_{R\lambda} + \tau_o + \tau_{H_2O}, \quad (4.7)$$

where $\tau_{A\lambda}$ is the aerosol optical thickness of the atmosphere; $\tau_{R\lambda}$ is the Rayleigh optical thickness; τ_o is the ozone optical thickness and τ_{H_2O} is the water-vapor optical thickness.

Table 4.9. Color Indexes According to Vessel Spectrophotometer Measurements. April 1982.

(4)					(4)				
(1) Стан- ция	(2) Дата	(3) Время по Гринвичу, ч мин	Индекс цвета		(1) Стан- ция	(2) Дата	(3) Время по Гринвичу, ч мин	Индекс цвета	
			ЛО ГОИН (5)	ИМ АН ГДР (6)				ЛО ГОИН (5)	ИМ АН ГДР (6)
987	20	07 50	0,95	—	989		13 00	1,00	—
987		08 00	1,10	—	989		13 10	1,10	—
989		11 00	1,10	0,97	986		14 50	1,00	1,00
886		13 30	0,90	1,05	986		14 50	1,50	—
983		15 40	1,05	0,95	974	23	05 30	1,07	1,07
992	21	08 30	1,30	—	974		09 00	1,10	1,13
986		14 30	0,97	—	974		10 50	1,07	—
983		16 55	0,90	—	974		14 30	1,15	—
995	22	05 15	0,90	—	974		15 15	1,00	1,04
995		05 25	1,00	—	973	24	11 40	1,30	—
995		05 35	1,35	—	973		12 30	1,30	—
992		08 30	0,97	1,12	973		12 40	1,25	—
992		08 40	1,02	—	973		13 30	1,04	—
					973		13 40	1,07	1,00

Key:

- | | |
|---------------|--------------------------------------|
| 1. Station | 4. Color index |
| 2. Date | 5. LO GOIN |
| 3. GMT, h min | 6. Institute of Oceanography, GDR AS |

During the experiment, the meteorological visibility range, S , was estimated, with more precise determination made by shipboard radar. Measurements of the sky radiation brightness on an almucantar were made right after measurements of the atmospheric transmission, with a delay of not more than 5 min. Within the framework of the experimental research, the following problems were considered in this part of the work:

- 1) the function of the horizontal visibility range vs. the spectral optical thickness, τ ;
- 2) the relationship between the atmospheric optical thickness of a given spectral interval and the wavelength, λ , and
- 3) the relationship between the atmospheric spectral thickness and the spectral brightness of sky radiation at wavelengths of 443 and 777 nm.

The optical condition of the atmosphere above the sea is largely determined by the aerosol component of the optical thickness, $\tau_{A\lambda}$, which can be extracted using the following relationship:

$$\tau_{A\lambda} = -\ln T_{\lambda} - \tau_{R\lambda} - \tau_{O_2} - \tau_{H_2O}. \quad (4.8)$$

The values of τ_{O_2} and τ_{H_2O} can be evaluated graphically by analyzing the spectral change in the measured transmissions, T_{λ} , while the contribution of the Rayleigh component, $\tau_{R\lambda}$, is determined using the formula

$$\tau_{R\lambda} = 0,00879\lambda^{-4,09}. \quad (4.9)$$

It can be seen from Table 4.10 that for medium and long visibility ranges, S, (from 6 to 20 km), different values of transmission, T, or optical thickness, τ_{a} , correspond to the same values of visibility (Fig 4.8). Thus, the frequently proposed close relationship between horizontal visibility range and atmospheric optical thickness for Baltic Sea conditions apparently exists only in exceptional cases, when the aerosol vertical stratification coincides with the moisture-distribution profiles.

Table 4.10. Horizontal Visibility Range and Description of Atmospheric Masses. April 1982.

(1)	(2)	(3)	(4)	(5)	(8)	(9)	
№ изме- рения	Дата	Время по Гринвичу, ч мин	Высота Солнца	Координаты наблюдений		Горизон- тальная видимость, км	Характеристика атмосферных масс
				(6)	(7)		
1	14	6 05	15,7	54,9	13,5	18	Поступающие полярные мор- ские воздушные массы (10)
2	14	14 00	32,8	54,9	13,5	30	Поступающие полярные мор- ские воздушные массы (10)
3	15	15 15	23	54,1	14,0	7	Морские трансформированные воздушные массы (11)
4	15	15 43	19,3	54,1	14,0	6	То же (12)
5	16	7 03	25	54,1	14,2	38	Морские трансформированные воздушные массы, смешанные с континентальными (13)
6	17	6 20	21,5	55,4	18,6	10	Полярные арктические воздуш- ные массы за холодным фрон- том (14)
7	17	13 37	34,0	55,4	19,0	70	Неустойчивые полярные аркти- ческие воздушные массы за хо- лодным фронтом (15)
8	20	11 45	44,1	56,0	19,3	18	Полярные морские воздушные массы (16)
9	20	12 52	39,1	56,0	19,3	20	Нисходящие сухие полярные морские воздушные массы (17)
10	22	6 10	22,2	56,0	19,3	16	Полярные морские воздушные массы (16)
11	23	9 52	45,7	56,0	20,7	15	Морские воздушные массы (18)
12	24	10 05	46,3	56,0	19,3	17	То же (12)

Key:

- | | |
|----------------------|------------------------------|
| 1. Measurement No | 5. Observation coordinates, |
| 2. Date | 6. lat N |
| 3. GMT, h min | 7. long E |
| 4. Solar altitude, ° | 8. Horizontal visibility, km |
9. Description of atmospheric masses
 10. Arriving polar marine air masses
 11. Marine transformed air masses
 12. Same
 13. Marine transformed air masses mixed with continental
 14. Polar arctic air masses behind cold front
 15. Unstable polar arctic air masses behind cold front
 16. Polar marine air masses
 17. Descending dry polar marine air masses
 18. Marine air masses

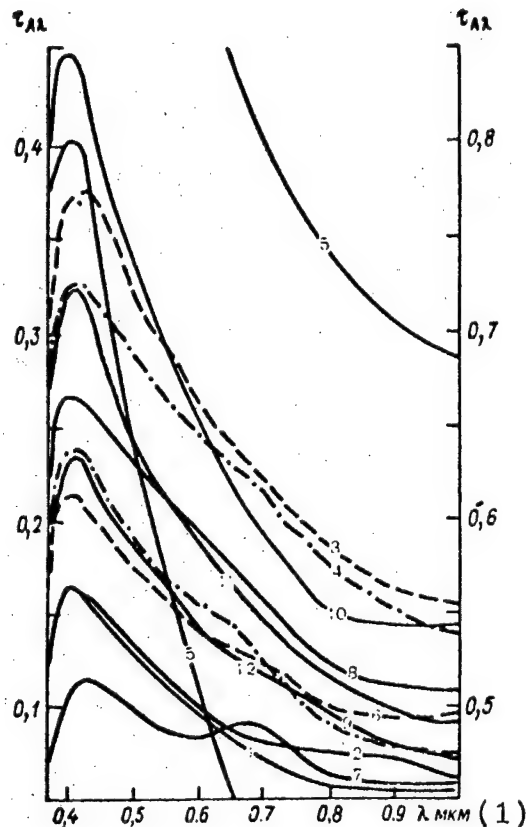


Figure 4.8. Spectral Dependence of Aerosol Optical Thicknesses, $\tau_{A\lambda}$, for Conditions Shown in Table 4.10.

Key:

1. λ , μm

In [65], measurements of the atmospheric transmission, T_λ , for two different sea regions (the Bermuda Region and the Gulf of Mexico) were used to determine parameters which in turn were used to determine the entire spectral curve, $\tau_A(\lambda)$, from the aerosol optical thickness at 670 nm:

$$\tau_A(\lambda) = a(\lambda/670)^{-b}. \quad (4.1)$$

From Fig 4.9 it can be seen that function (4.10) cannot be applied to our data, despite the sufficiently large volume. Most probably, function (4.10) is valid only if the air masses vary insignificantly; during the Baltic expedition, the air masses were constantly changing (Table 4.10), so that the optical characteristics--the horizontal visibility range and the turbidity factor (optical thickness)--correspondingly changed.

The data in Fig 4.10 clearly show that different horizontal visibilities might correspond to the same turbidity, T_λ . It can be noted that at wavelengths 553 and 777 nm at medium visibility, the haze layer at the water surface makes the horizontal visibility lower than above land (at the same turbidity values). The land measurements were made in the central GDR in 1979-1981.

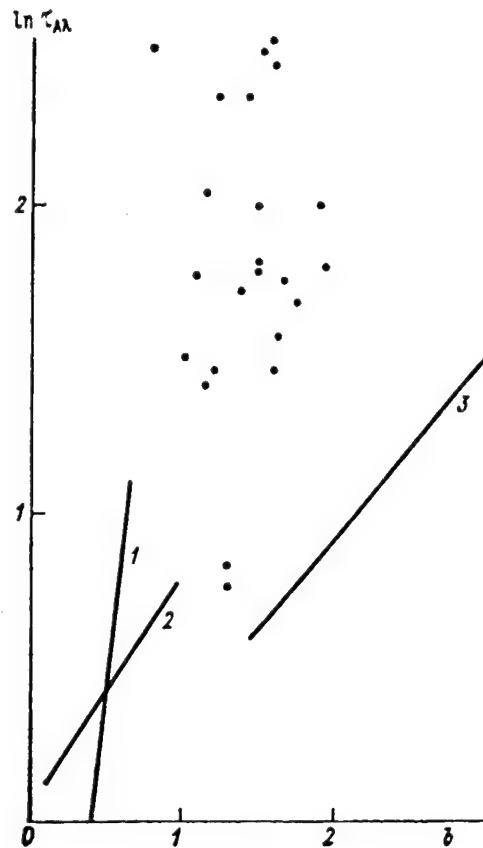


Figure 4.9. Parametric Representation of the Atmosphere Aerosol Optical Thickness, $\tau_{A\lambda}$, According to the Value of $\tau_{A\lambda}(670)$ and the Wavelength, λ :

1. according to the LOWTRAN-5 model
2. according to data in [65] for the Bermuda Islands region
3. according to data in [65] for the Gulf of Mexico

The points represent the authors' experimental data for the Baltic Sea.

As a result of the authors' research, a single-valued linear relationship was established between the differences in the spectral brightness of sky radiation measured at large scattering angles, γ , and the corresponding differences in the spectral optical thickness (Fig 4.11). The optical thickness for a different wavelength can be determined from the measured sky radiation brightnesses for various wavelengths and the optical thickness, τ , for one of these wavelengths. If a similar correlation function could be established between the brightness of the ascending radiation of the ocean-atmosphere system, L_{OA} , and the optical thickness, τ_λ , then, determining the optical thickness, τ_{760} , in the oxygen absorption band (about 760 nm) using the method proposed in [8] and using the radiation brightness measured in a different channel, the optical thickness in the 440 nm wavelength region could be found, in which the chlorophyll absorption band is located

$$L_{443OA}^i - L_{760OA}^i = a + b(\tau_{443} - \tau_{760}). \quad (4.11)$$

This procedure, in principle, could be useful for remotely determining the chlorophyll concentration in sea water.

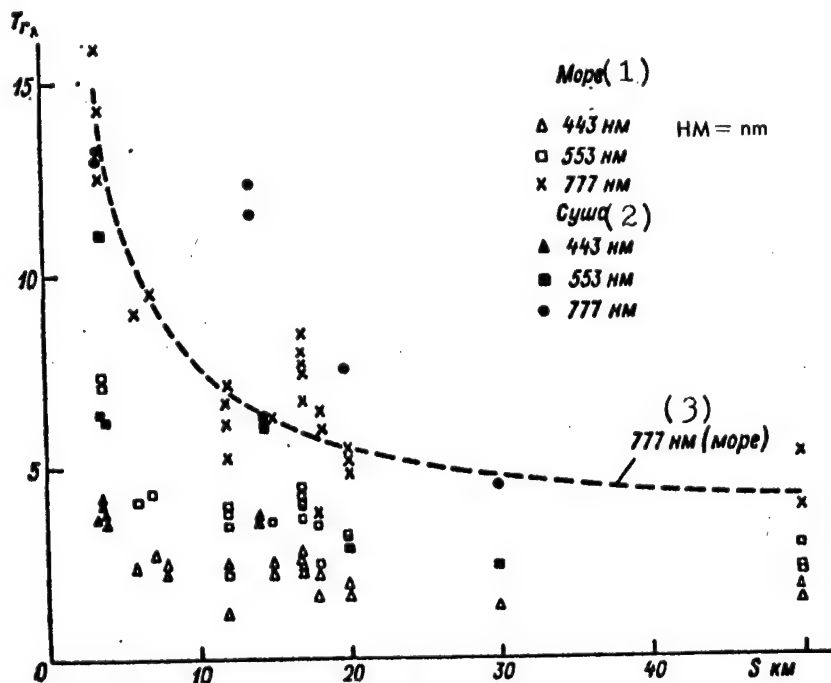


Figure 4.10. Function of Spectral Values of the Turbidity Factor $T_{\lambda} = (\tau_{\lambda A} + \tau_{\lambda R}) / \tau_{\lambda R}$ vs. the Horizontal Visibility

Key:

1. Sea

2. Land

3. 777 nm (sea)

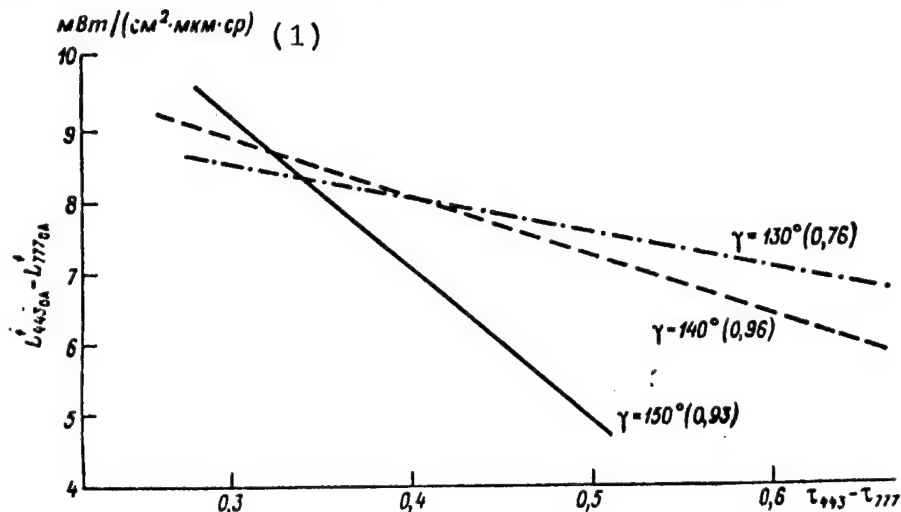


Figure 4.11. Relationship Between the Atmosphere Optical Thickness, τ , and the Sky Radiation Brightness Measured on an Almucantar for Scattering Angles of $\gamma = 130, 140$ and 150° :

The correlation coefficients are shown in parentheses.

Key:

1. $\text{mW}/(\text{cm}^2 \cdot \mu\text{m} \cdot \text{sr})$

4.5. Investigation of the Radiation Brightness Field of the Water+Atmosphere System from Satellite Images of the Baltic Sea.

During the experiment period, a series of images of the Baltic Sea in several spectral ranges was obtained from the Nos 30 and 31 Meteor satellites. The MSU-S camera (visible and near-IR bands) provided information on 16, 17 and 20-26 April and the Fragment camera provided information for 23 and 24 April (Table 4.11).

Table 4.11. List of Satellite Visible-Band Information from the No 30 Meteor Satellite. Fragment Camera. (Optical Part of the Experiment). April 1982.

(1)	Дата (2)	Время по Гринвичу, ч мин	Виток (3)	Кадр (4)	Канал (5)	Диапазон (6)	(7) Примечание
	23	09 46	10013	5313	1	0,5—0,6	Восточный виток, северная часть (8)
					4	0,6—0,7	То же (9)
					2	0,7—0,8	»
					3	0,8—1,1	»
		09 47	10013	5314	1	0,5—0,6	Восточный виток, южная часть (10)
					4	0,6—0,7	То же (9)
					2	0,7—0,8	»
					3	0,8—1,1	»
	24	09 55	10028	5	1	0,5—0,6	Западный виток, северная часть (11)
					4	0,6—0,7	То же (9)
					2	0,7—0,8	»
					3	0,8—1,1	»
		09 56	10028	6	1	0,5—0,6	Западный виток, южная часть (12)
					4	0,6—0,7	То же (9)
					2	0,7—0,8	»
					3	0,8—1,1	»

(13) Примечание. Имеются негативы и отпечатки (позитивы).

Key:

- | | |
|---------------|--|
| 1. Date | 8. Eastern pass, northern part |
| 2. GMT, h min | 9. Same |
| 3. Pass | 10. Eastern pass, southern part |
| 4. Frame | 11. Western pass, northern part |
| 5. Channel | 12. Western pass, southern part |
| 6. Band | 13. Note. Negatives and prints (positives) |
| 7. Notes | were obtained. |

The experiment participants had most of the data from the MSU-S camera only in the form of images (Fig 4.12) (negatives and positive prints). For technical reasons, high-quality reproduction of the satellite images in the present publication is impossible. This circumstance, as well as the distinguishing features of obtaining and photographically recording this information, necessitate limiting this presentation to only a qualitative description of the general structure of the brightness field of the water surface and atmosphere.



Figure 4.12. Frame from the MSU-S Camera Obtained from the No 30 Meteor Satellite on 23 April 1982 at 0946 GMT, Pass 10013, Channel 0.5-0.7 μm

The 17 April picture shows a strip (about 20-50 km wide along the eastern coast of the Baltic Sea from Kaliningrad northward, including Saaremaa and Hiiumaa Islands) which has a slightly higher water-surface brightness than the rest of the cloud-free sea.

From the image obtained on 20 April, this distinguishing feature is maintained in the region from Ventspils northward, including Saaremaa and Hiiumaa Islands, and somewhat farther north to the mouth of the Gulf of Finland. The region of the subsatellite vessel site is covered by clouds. The higher surface brightness of the Kurshskiy Gulf is very noticeable. The shallow waters of this gulf are frequently turbid because of wind action, which is the main reason for the anomalous brightness of this gulf on the satellite images in the 0.5-0.6, 0.6-0.7 and 0.5-0.7 μm bands. This circumstance makes it possible to use the Kurshskiy Gulf as a test area with specific optical properties.

In the 21 April picture, the subsatellite site is covered by clouds. The negatives of the cloud-free pictures of 22 and 23 April have low contrast, and only the brighter Kurshskiy Gulf can be distinguished. In the 24 April image, the sea surface is obscured by scattered cloudiness.

In the 25 April picture, there is local cloud formation which completely covers the coastal region from Gdansk almost to Liyepaya. The rest of the Baltic Sea surface is cloud-free (except the Gulf of Bothnia). Noteworthy are two regions of higher brightness: right near Riga (which is probably due to the entrance of turbid waters of the Daugava River into the Gulf of Riga) and north of Liyepaya by Cape Akmenrags. The dimensions of both areas do not exceed several kilometers. The areas are visible in the images in both bands of the MSU-S scanner.

In the 26 April image, the eastern and southeastern zones of the central Baltic Sea are covered with unbroken clouds. In the picture of the 0.5-0.7 μm band, there is a zone of higher brightness north of Bornholm. The contrast of this zone with the surrounding water surface is comparable to the contrast observed in the 17 April picture. It is difficult to interpret these contrasts without synchronous subsatellite measurements.

Thus, a qualitative analysis of the satellite images of the Baltic Sea surface made by the MSU-S camera during the subsatellite experiment did not find contrasts in the brightness field of the water+atmosphere system directly in the vessel site or in the experiment region.

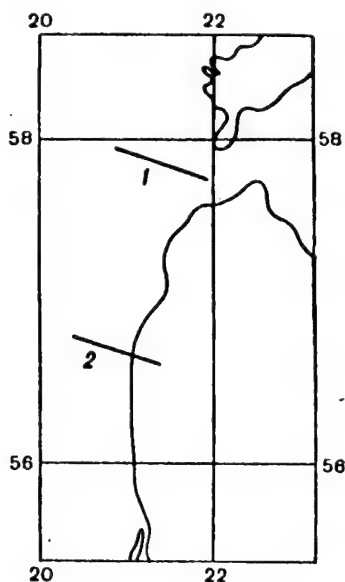


Figure 4.13. Map-Diagram of a Frame of the Fragment Camera, Obtained from the Meteor Satellite on 23 April 1982:

1, 2. brightness-field cross sections used for digital processing

The high-resolution Fragment camera images of the eastern and western Baltic Sea on 23 and 24 April 1982, respectively, were available not only

as negatives, but also in digital form. One frame of the Fragment camera covers only part of the sea (Fig 4.13). These images were digitally prefiltered to eliminate the banding effect. Then S.M. Sazhin, using the experimental computer system of GosNITsIPR, checked the hypothesis of homogeneity of the brightness field of the water+atmosphere system in the experiment region. The histograms obtained of the brightness distribution along individual selected cross sections (Fig 4.14) indicate the absence of significant differences in the brightness of individual elements of the water-surface images in the region of the subsatellite experiment during the experiment period.

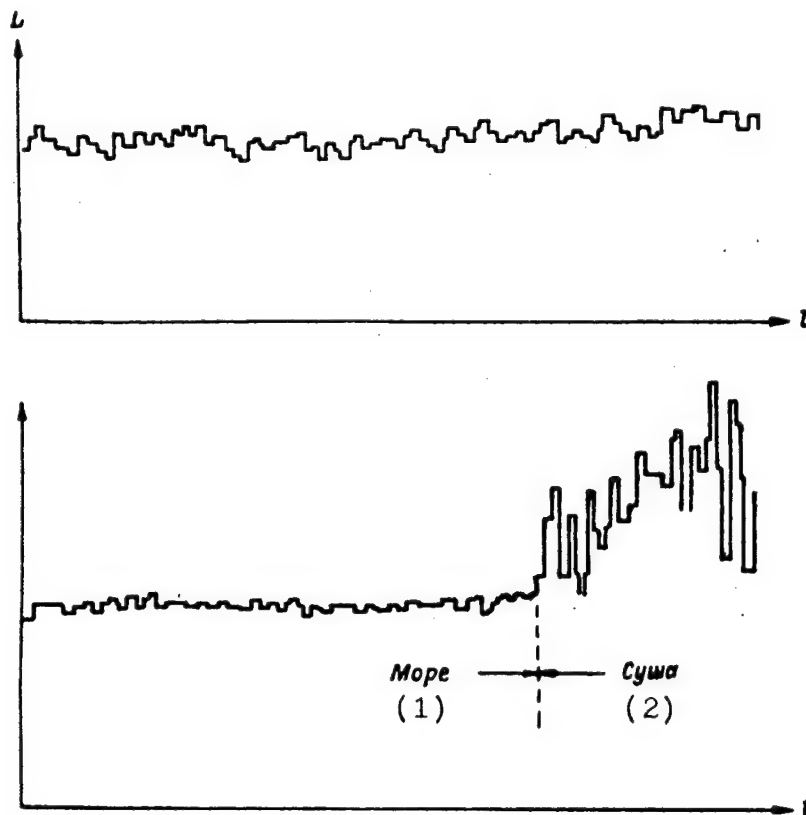


Figure 4.14. Histograms of the Brightness Distribution Along Individual Cross Sections

Key:

1. Sea

2. Land

4.6. Conclusion

The results obtained from the hydrooptical observations of the complex subsatellite experiment of the USSR and GDR indicate the great potential of using remote methods of sensing the sea in the visible band in conjunction with standard hydrooptical observations.

During the subsatellite experiment, the concentrations of suspended matter (seston), chlorophyll a and phaeopigments were determined on a site near

international station 9A. The concentration of dissolved matter and chlorophyll in the open sea was much lower than in the nearshore zone. The observed temporal changes in pigment concentrations were caused mainly by advective processes.

In the period from 10 through 26 April, the air masses above the sea changed constantly for a week during the experiment, which made it impossible to obtain valid observational data for establishing a function to determine the spectral dependence of aerosol optical thickness according to available measurements of this quantity at one wavelength (670 nm). Taking into account the rapid restructuring of the air masses over the Baltic, the time frames of future experiments should be expanded (for example, continuous observations of hydrooptical characteristics on the site should be made for two weeks). During the experiment, it was also established that a distinguishing feature of the Baltic is the absence of a close relationship between the horizontal visibility range and the atmosphere optical thickness; the only exception is the rare case when the vertical stratification of the aerosol coincides with the moisture distribution profile.

The satellite visible-band pictures showed no significant contrasts in the brightness field of the water-atmosphere system directly in the experiment region, although outside the site, for example, in the area of Bornholm and where the Daugava and Venta Rivers enter, such contrasts were noted. However, interpretation of these contrasts is difficult in the absence of synchronous subsatellite measurements in these regions.

In general, it must be emphasized that the data of the complex hydrooptical research show that at present, it is impossible to give a specific forecast of the time, duration and activity of phytoplankton for a separate small region of the Baltic Sea (commensurate with the subsatellite site of 1982). Therefore, further research must be done to obtain a large amount of subsatellite observation data on the space-time variability of the hydrooptical characteristics of the Baltic Sea. This last point is especially important for the interpretation of satellite data, since a satellite picture taken practically instantaneously can show various phases of phytoplankton bloom in different parts of the sea.

5. Complex Research on the Baltic Sea Temperature Field

5.1. Distribution of Thermodynamic Temperature of the Water in the Experiment Region According to Measurements Made on the Vessel A. v. Humboldt

The hydrological conditions in the region of the subsatellite experiment near international station 9A were characteristic of the thermal condition of the waters in the deep parts of the Baltic Sea. The water temperature distribution largely depends on the heat exchange at the sea surface; it has a definite annual pattern and has great temporal and spatial variability.

Detailed research, performed by different authors, is available on the average seasonal temperature variability in the open part of the Baltic Sea. The thermal conditions at station 9A are discussed in [52].

The distribution of the sea-surface-layer temperature (T_{ssl} , TSSL) depends on the heat flux through the sea surface and also on heat exchange with deeper layers. In the southern Gotland Basin, there is an insignificant annual variation in temperature to a depth of 100 m.

The annual variation is especially pronounced in the low-salinity layer right down to a depth of 50 m. This layer is almost homogeneous from early December to the end of April. The average minimum of 1.2°C at the sea surface occurs in mid-March.

In late April, thermal stratification begins. This is caused by the establishment of the summer heated homogeneous nearsurface layer, the lower boundary of which is a thermocline. Below 40-70 m is a cold intermediate layer. The average maximum water temperature, 17.2°C , occurs in late August. The thermal discontinuity layer is at a depth of 20-30 m. Only with the reduction of the strong summer thermal stratification does heat begin to penetrate to great depths. In the southern Gotland Basin, the average maximum water temperature at a depth of 50 meters, 5.4°C , occurs in early December.

Relatively warm water lies below the salinity discontinuity layer. The temperature of this water is mainly determined by advection processes. Sporadic inflows of brackish waters from the North Sea bring in water masses of different temperatures.

Besides the periodic annual variation, there is also a relatively weak daily temperature change in the nearsurface layers, depending on the daily variation of the thermal-balance components. However, there are only a few published works on the daily variation. Research done with floating beacons in the open part of the Baltic Sea [40] established that the daily variation in water surface temperature also has an annual cycle. In April and May, this average daily variation reaches about 0.3 K. Research done in the Bornholm Basin [54] showed that daily changes caused by heat exchange at the sea surface under certain conditions (strong radiation, absence of waves) can be rather large (in this case, 2 K in 7 h).

Besides these periodic changes, significant aperiodic changes in the water temperature are observed in the southern Gotland Basin, as in other regions of the Baltic Sea. These changes are especially pronounced in the summer at the thermocline level. Spatial thermal unevennesses are also linked with these aperiodic changes. For example, [4] reports on research on the synoptic variability of the water temperature and other physical factors near the region of the subsatellite experiment. A wavelike variation of temperature-distribution disruption with amplitudes of 2-2.5 K and dimensions of 20-25 km has been discovered in the homogeneous nearsurface layer. At the thermocline depth (20 m), the amplitudes increased to 5 K. The time ranges of these low-frequency processes varied from several days to tens of days. Similar temperature changes near the subsatellite experiment region are also reported in [36].

A possible reason for these water temperature unevennesses might be moving eddies caused by Rossby topographic waves [4, 44] or the breaking of internal waves on the lower boundary of the thermocline [36]. The authors of

[45] describe short-term changes in the surface temperature in the experiment region due to erosion of the thermocline when the wind causes short-period waves to break. They observed temperature changes of 3.5 K in 12 h.

The horizontal gradients linked with temperature-field unevennesses reach 0.5 K/km [38]. The development of fronts might be limited by a nearshore zone several kilometers wide [58, 60]. Statistical research on horizontal temperature gradients in the Baltic Sea was also conducted in [34], although due to the use of data obtained at individual stations, this research cannot be the basis for conclusions on the characteristics of synoptic-scale processes.

During the subsatellite experiment, no significant distinguishing features in the surface-temperature distribution were observed. According to existing maps of the average water temperatures for 1902-1956 [50], the average sea surface temperature in April is about 2.5° C, reaching 3.0° C closer to shore (near station 974). The average-temperature map does not show any large horizontal gradients in this region. A more detailed processing of available data [54] for international station 9A (102 series of measurements during 1924-1973) shows that the average multiyear sea surface temperature is 2.6° C for 19 April (beginning of the subsatellite experiment) and 3.1° C for 26 April (end of the experiment). At this station, the multiyear absolute maximum surface temperature is 4.0° C, while the minimum is 1.0° C (during the above period).

According to present representations [53], the surface layers of the water masses in the site are still homogeneous in April. If the criterion

$$T_{ssl} - T_{dep} > 0.5K$$

is used as an indicator of stratification, then on average, stratification develops below a depth of 40 m only after 24 April. In the upper 10-m layer of water, stratification appears only in mid-May.

The sea surface temperatures measured by the research vessel A. v. Humboldt during the experiment were in the range 2.6-3.5° C, which is only slightly above the average values (Table 5.1). At nearshore station 974 (about 35 km from the coast), the values of TSSL were 3.4-6.0° C, while at station 973, they ranged from 3.5 to 4.8° C. These significant temporal changes in temperature at stations 974 (2.6 K in 10 h) and 973 (1.2 K in 12 h) require additional research.

On the site, the very top layer of water to a depth of 10 m was homogeneous during the entire experiment period almost without exception; gradients exceeding 0.1 K/10 m occurred in only 7 percent of all measurements. The vertical thickness of the homogeneous layer, determined using the criterion

$$T_{ssl} - T_{dep} \leq 0.5K,$$

in most observations exceeded 30 m. Noticeable temperature gradients in the upper 10 m occurred only at stations 974 and 973 when radiation was significant and in the absence of wave mixing. Under these conditions, a maximum of 1.2 K/m was observed, which for the layer 0-10 m totalled 2.5 K/10 m.

Table 5.1. Water Temperature (0-2 m Horizon) at Individual Stations of the Site, °C. 1982.

(1) Станция	(2) 9 апреля		(3) 20 апреля		(4) 21 апреля	
	Время, ч мин (5)	T _{псм} (6)	Время, ч мин (5)	T _{псм} (6)	Время, ч мин (5)	T _{псм} (6)
9A(995)	5 30	2,87	4 15	2,84	—	—
992	7 40	2,55	6 38	2,53	—	—
989	9 54	2,61	9 07	2,70	9 52	2,87
986	11 49	2,59	12 13	2,70	13 50	2,58
983	14 30	2,67	16 06	2,88	15 38	2,76
980	16 31	2,75	17 41	2,88	17 49	2,74
977	18 21	2,68	—	—	19 17	2,65

Станция	(7) 22 мая		(8) 25 апреля		(9) 26 апреля	
	Время, ч мин (5)	T _{псм} (6)	Время, ч мин (5)	T _{псм} (6)	Время, ч мин (5)	T _{псм} (6)
9A(995)	4 15	2,94	4 15	2,84	4 06	3,52
992	8 35	2,71	6 46	3,44	6 43	3,23
989	11 57	3,00	9 01	3,32	8 20	3,62
986	13 46	2,88	12 23	3,02	10 12	2,90
983	17 01	2,84	14 33	3,26	12 43	2,80*
980	18 41	2,88	16 35	3,38	14 48	3,11*
977	20 12	2,94	18 41	3,25	—	—

(10) Примечание. * Из-за волнения глубина измерений 3,0 м; время измерений по Гринвичу.

Key:

- | | |
|---------------------|---|
| 1. Station | 7. 22 April |
| 2. 19 April | 8. 25 April |
| 3. 20 April | 9. 26 April |
| 4. 21 April | 10. Note. *Due to rough conditions, the |
| 5. Time, h min | measurement depth was 3.0 m; |
| 6. T _{ssl} | measurement times, GMT |

Horizontal temperature gradients in the surface layer on the site were insignificant during the entire experiment and varied between 0.3 and 0.8 K.

The homogeneity of the sea-surface temperature field was also confirmed by temperature IR pictures from the Il-14 airplane.

The homogeneity of the temperature field, determined from vessel measurements in the subsatellite experiment site, made it possible to obtain reliable reference information for comparison with satellite measurements of water surface temperature.

5.2. Analysis of Sea Surface Layer Temperature (TSSL) in the Test Areas

Measurements of TSSL from Vessels and at GMS's [hydrometeorological stations]. Three test areas were used to evaluate the satellite measurements of the TSS:

- 1) the site of the Soviet-German experiment (measurements by the research vessel A. v. Humboldt;

2) the Gulf of Riga (GMS observations) (Fig 5.1) and

3) the southern part of the Baltic Sea (measurements by vessels of opportunity) (Fig 5.2). Every day, 5-10 observations were made in this area quasi-synchronously with the satellite measurements.

The Gulf of Riga was selected, firstly, because it has a sufficiently developed network of hydrometeorological stations and, secondly, because variance analysis showed that the data from the Gulf of Riga GMS's can be considered as representative for comparison with the satellite data, as opposed to the data from other GMS's, which do not satisfy the criterion of variance homogeneity (Table 5.2).

Observation data were processed using variance analysis methods. The following conditions are prerequisite for the variance analysis:

- 1) the observation results must be mutually independent random values and
- 2) the measurements must have normal distribution and the same variance.

Since in this situation, the observation subjects (TSSL measurements from vessels and stations) can be considered as randomly selected, because each subject is measured individually, therefore it is entirely acceptable to assume that the first condition is fulfilled.

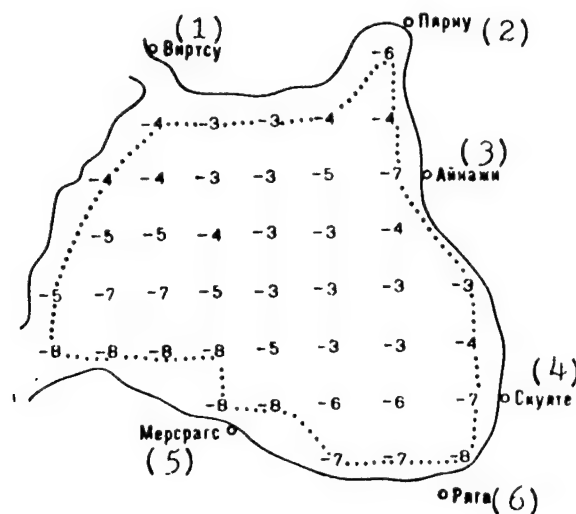


Figure 5.1. Portion of a Map of Radiative Temperature ($^{\circ}\text{C}$) Obtained in the Gulf of Riga from the No 7 Meteor-2 Satellite on 24 April 1982, 0100 GMT:

The dots indicate the nearshore zone.

Key:

- | | |
|------------|-------------|
| 1. Virtsu | 4. Skulte |
| 2. Pyarnu | 5. Mersrags |
| 3. Aynazhi | 6. Riga |

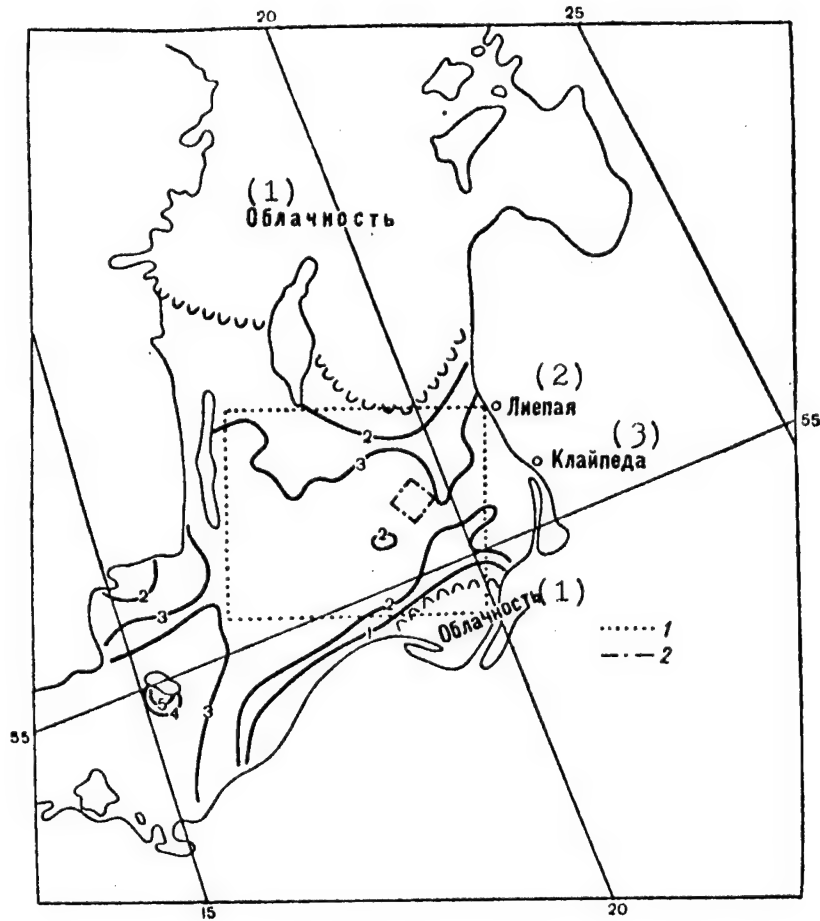


Figure 5.2. Surface Temperature of the Baltic Sea ($^{\circ}\text{C}$) from Data of the No 7 Meteor-2 Satellite. 17 April 1982, 1200 GMT:

1. southern test area
2. site of the research vessel A. v. Humboldt

Key:

1. Clouds
2. Liyepaya
3. Klaypeda

A verification of the second condition of the variance analysis requires the use of specially developed mathematical methods. We will verify this condition for a set of observation data on the TSSL obtained from 16 through 25 April 1982 at 0600 GMT at shore stations of the Gulf of Riga (Table 5.2).

Verification of Variance Homogeneity

a) homogeneity of station variances

Using the Cochran test, the hypothesis of whether the greatest variance value differs from the other values is tested. For this, the following ratio is calculated

$$S_{i \max}^2 / \sum_{i=1}^{12} S_i^2 = 3,3/21,7 = 0,15.$$

Table 5.2. TSSL Measured at Hydrometeorological Stations of the Gulf of Riga at 0600 GMT, °C

(1) Номер станции	(2) Апрель										\bar{T}_{1*}	s_i^2
	16	17	18	19	20	21	22	23	24	25		
1	3	3	3	3	2	0	2	3	3	3	2,5	0,9
2	3	5	4	2	3	0	2	2	2	3	2,6	1,0
3	2	5	3	2	3	0	2	2	2	2	2,3	1,6
4	4	6	3	3	2	1	1	2	6	4	3,2	3,3
5	2	5	2	2	0	0	1	4	4	3	2,3	1,8
6	3	5	3	4	5	1	2	6	4	5	3,8	2,4
7	2	4	2	2	1	0	0	2	4	3	2,0	2,0
8	1	2	3,6	2	0	1	1	2	6	4	2,3	2,7
9	1	2	2	2	0,5	1	2	3	4	5	2,3	2,0
10	3	3	3	2	2	2	3	3	4	5	3,0	0,8
11	3	4	4	3	2	1	4	3	5	3	3,2	1,3
12	1	2	2	2	1	1	1	2	4	5	2,1	1,9
\bar{T}_{*j}	2,3	4,0	2,9	2,4	1,8	0,7	1,8	2,8	4,0	3,8		
S_j^2	1,0	1,7	0,5	0,4	2,1	0,5	1,1	1,4	1,6	1,1		
j	1	2	3	4	5	6	7	8	9	10		

Key:

1. Station number

2. April

The upper 1-percent critical value for the 12 variances is equal to 0.25 when the number of degrees of freedom of each evaluation is $k = 9$ [16]. Since this exceeds the calculated value, there is not sufficient basis for rejecting the hypothesis of variance equality.

b) homogeneity of daily variances

$$S_{j \max}^2 / \sum_{j=1}^{10} S_j^2 = 2,1/11,4 = 0,18.$$

The upper 1-percent critical value for 10 variances is equal to 0.26 at $k = 11$ [6], which also exceeds the calculated value.

Thus, for the set of measurements under consideration, the assumption of variance homogeneity for the variance analysis can be accepted.

Test of Normal Distribution of Measured Values of TSSL. The hypothesis that the TSSL has a normal distribution function is tested by using the Pearson test (the χ^2 test). For this set of data, the calculated value is $\chi^2 = 8$. The critical upper and lower values of χ^2 (for the number of degrees of freedom $k = n-3$, where n is the number of intervals, $n = 5$), determined for the level of test significance of $q = 1$ percent, are equal to: $\chi_1^2 = 9,2$ and $\chi_2^2 = 0,02$. Since $\chi_2^2 < \chi^2 < \chi_1^2$, the hypothesis of normal distribution of the random value is accepted.

Thus, the prerequisites of variance analysis are fulfilled; consequently, we can move on, properly, to performing the analysis. The goal of the research will be to determine the possible differences between groups of data; i.e., between measurements of TSSL at one station, but on different

days, or between TSSL measurements for the specified period at different stations. The influence of two factors simultaneously affecting TSSL is studied: the main-level factor, D, ("days") and the second factor, C, ("stations," subgroup level).

There are $v = 10$ levels of factor D and $r = 12$ levels of factor C, and each cell contains one observation. Then, one observation can be represented in the form (it is assumed that there is no interaction between the factors):

$$T_{ij} = \mu + \gamma_i + g_j, \quad (5.1)$$

where μ is the overall mean; γ_i is the effect from the i -th level of factor C and g_j is the effect from the j -th level of factor D.

Hereinafter, we will designate \bar{T}_i as the mean of the observations of factor C on the i -th level and \bar{T}_j as the mean of the observations of factor D on the j -th level. The evaluations of μ , \bar{T}_i and \bar{T}_j are, respectively, the overall mean

$$\bar{T} = \frac{1}{rv} \sum_{i=1}^r \sum_{j=1}^v T_{ij}$$

and the level means

$$\bar{T}_{i*} = \frac{1}{v} \sum_{j=1}^v T_{ij}; \quad \bar{T}_{*j} = \frac{1}{r} \sum_{i=1}^r T_{ij}.$$

The overall variance (S^2) and its components (S_1^2 , S_2^2 , S_3^2) are determined using the formulas:

$$S^2 = \frac{1}{rv-1} \sum_{i=1}^r \sum_{j=1}^v (T_{ij} - \bar{T})^2 = \frac{Q}{rv-1}, \quad (5.2)$$

where Q is the total sum of the squares of the deviations of individual observations from the overall mean;

$$S_1^2 = \frac{1}{r-1} v \sum_{i=1}^r (\bar{T}_{i*} - \bar{T})^2 = \frac{Q_1}{r-1}, \quad (5.3)$$

where Q_1 is the sum of the squares of the differences between the row-wise means and the overall mean;

$$S_2^2 = \frac{1}{v-1} r \sum_{j=1}^v (\bar{T}_{*j} - \bar{T})^2 = \frac{Q_2}{v-1}, \quad (5.4)$$

where Q_2 is the sum of the squares of the differences between the column-wise means and the overall mean and

$$S_3^2 = \frac{1}{(r-1)(v-1)} \sum_{i=1}^r \sum_{j=1}^v (T_{ij} - \bar{T}_{i*} - \bar{T}_{*j} + \bar{T})^2 = \frac{Q_3}{(v-1)(r-1)}, \quad (5.5)$$

where Q_3 is the residual sum of the squares, which characterizes the influence of other factors not taken into consideration.

The results of variance analysis using formulas (5.2)-(5.5) are given in Table 5.3. The overall mean of the observations is $\bar{T} = 2.6^{\circ} \text{C}$.

Table 5.3. Results of Variance Analysis of TSSL Observations at Hydrometeorological Stations of the Gulf of Riga on 16-25 April 1982, 0600 GMT

<u>Variance Component</u>	<u>Sum of Squares</u>	<u>Number of Degrees of Freedom</u>	<u>Evaluations of Variance, K^2</u>
Between row-wise means (factor C)	33	11	0.3
Between column-wise means (factor D)	126	9	12.6
Residual	91	99	0.9
Total	250	119	2.1

In order to ascertain the significance of the influence of factors D and C on the investigated characteristic, the factor-wise variances must be compared with the residual variance. The statistics $F_c = S_1^2/S_3^2$ are calculated with $k_1 = r - 1 = 11$ and $k_2 = (v - 1) \cdot (r - 1) = 9 \cdot 11 = 99$ degrees of freedom, as well as $F_D = S_2^2/S_3^2$ with $k_1 = v - 1 = 9$, $k_2 = 99$.

$$F_c = 0.3/0.9 = 0.33; \quad F_D = 12.6/0.9 = 14.$$

For a level of significance of $\alpha = 0.05$, tables [16] are used to determine the critical value $F_{\alpha, k_1, k_2} : F_{0.05, 11; 99} = 1.88; F_{0.05, 9; 99} = 1.97$.

$F_c < F_{\alpha, k_1, k_2}$; consequently, it can be confirmed that the difference between stations does not significantly affect the determination of TSSL of the Gulf of Riga. The value of \bar{T} determined in this manner can be used as a standard for comparison with the satellite data, and the gulf itself can be considered an acceptable test area (from the point of view of the correctness of comparing TSSL and T_r).

$F_D > F_{\alpha, k_1, k_2}$; i.e., the influence of factor D is significant, and a satellite-data correction determined from in situ observations made on one particular day cannot be applied to other days.

A study of the data of in situ measurements of TSSL at nearshore stations of the Baltic Sea itself showed that the daytime observations of GMS's during this period are not representative (Tables 5.4 and 5.5) from the point of view of using them to evaluate the precision of satellite measurements: in light of the heating of the narrow nearshore zone, the GMS measurements differed from the TSS measurements made from the Il-14 airplane in that same nearshore zone by 4-5 K. Thus, for example, aerial measurements in the Gulf of Riga made by SZ UGKS [not further identified] during the day on 25 April recorded a temperature field of 3-5 $^{\circ}$ C with a maximum of 6 $^{\circ}$ C in the Gulf of Pyarnus, while the GMS daytime observations give TSSL values of 6-10 $^{\circ}$ C. At the same time, the TSSL measurements from vessels in the open sea differed from the airplane TSS measurements by not more than 1 K. Therefore, the daytime GMS observations were not used in

further analysis of the precision of satellite TSS measurements or in the evaluation of ΔT from subsatellite observations. However, in the Gulf of Riga, GMS information was used on observations made only at 0600 GMT, when the influence of daytime heating is still insignificant.

Table 5.4. Values of TSSL Measured at GMS's of the Gulf of Riga at 1200 GMT, °C

(1) Номер станции	(2) Апрель										\bar{T}_{l*}
	16	17	18	19	20	21	22	23	24	25	
1	3	3	5	4	2	3	5	5	10	10	5
2	7	6	5	4	3	4	5	6	8	10	5,8
3	7	7	2	4	4	5	5	7	8	6	5,5
4	—	—	4	5	6	8	8	8	12	10	7,6
5	4	4	3	5	4	3	7	8	11	10	5,9
6	3	3	2	3	4	5	5	5	8	6	4,4
\bar{T}_{*j}	4,8	4,7	3,5	4,1	3,8	4,7	5,8	6,5	9,5	8,7	

Key:

1. Station number
2. April

Table 5.5. Values of TSSL Measured at GMS's in the Southern Part of the Baltic Sea at 1200 GMT, °C

(1) Номер станции	(2) Апрель									
	16	17	18	19	20	21	22	23	24	25
1	6	5	4	5	5	3	9	8	10	7
2	6	5	5	4	5	3	6	6	8	6
3	8	6	6	4	4	3	—	9	9	8,6
4	—	—	—	5	4	3	8	10	8	8
5	6	9	6	—	6	—	6	8	—	—
6	9	5	5	4	3	1	5	6	7	5

Key:

1. Station number
2. April

5.3. Analysis of the TSS Measurements by Airborne IR Radiometer on the Sea Test Area

During the entire experiment, LO GOIN's Il-14 airplane laboratory performed a temperature survey on test areas, the dimensions of which were commensurate with the resolution element of the satellite camera. On 18, 19, 24 and 26 April, the work was performed on a site south of the point long 19° E, lat 56° N (see Fig 2.5). On 23 April, the flights covered a square directly adjacent to the coastline (see Fig 2.6). In order to evaluate the influence of the daily TSS variation on the measurements, several flights were made in the same square on 18 and 23 April (see Figs 2.5 and 2.6). The goal of this experiment was to obtain reliable data for evaluating the precision of satellite measurements; it was necessary to determine the optimum number of flight legs needed to evaluate the average TSS over the test area (\bar{T}_0).

Table 5.6 gives the results of measurements obtained on 24 April 1982 using an airborne IR radiometer. These results were processed using a parametric model with fixed levels of the factor L (the factor "flight legs"). The influence of the selection of various legs on the magnitude of \bar{T}° was investigated. The prerequisites for variance analysis were considered to be fulfilled.

Table 5.6. TSS Measurements by an Airborne IR Radiometer on the Test Area on 24 April 1982, 1100-1300 GMT

(1) Галсы	(2) ТПМ, °C												
1	3,7	3,6	3,7	3,5	3,7	3,2	3,2	3,5	3,0	2,8	3,2	2,2	
2	3,3	3,8	3,6	3,7	3,7	3,6	3,3	3,5	3,3	3,5	3,8	3,5	3,2
3	3,5	3,6	3,8	3,2	3,5	3,2	4,0	3,0	3,1	3,3	3,0	2,7	3,5
4	3,5	3,6	3,2	3,3	3,7	2,9	3,3	3,3	3,4	3,0	3,0	3,0	2,9
5	3,0	3,1	3,0	3,2	3,5	3,0	3,3	3,0	3,1	3,3	3,0	3,4	2,9
6	3,7	3,6	3,3	3,7	3,3	3,8	3,6	3,6	3,3	3,5	3,8	3,7	3,5
7	3,7	3,8	3,8	3,7	3,6	3,3	3,5	3,1	3,5	3,2	3,3	3,2	2,9
8	2,7	2,8	2,6	3,2	3,0	3,0	2,6	2,8	2,6	2,6	3,0	2,9	

(1) Галсы	(2) ТПМ, °C											\bar{T}_{t*}	$\bar{T}^\circ C$
1												3,3	3,2
2	3,3	3,0	3,3	3,2								3,4	
3	2,6	2,8	3,3	2,7	3,0	3,3	2,9	3,0				3,2	
4	2,9	2,7	2,4	2,8	2,6							3,1	
5	2,6	3,0	2,7	2,7	2,9							3,0	
6	3,5	3,6	3,3	3,5	3,4	3,5	3,6	3,3	3,1	3,5	3,2	3,5	
7	3,2	2,7	2,9	2,9	2,7	2,7	2,6	2,8	3,4	3,1	3,0		
8									3,0	2,9		3,15	
												2,8	

Key:

1. Leg

2. TSS, °C

We use the parametric model

$$T_{ti} = \mu + \gamma_t + Z_{ti}, \quad (5.6)$$

where Z_{ti} is the random remainder; μ is the overall mean; γ_t is the effect caused by the influence of the t -th level of the factor; $i=1, \dots, n_t$; $t=1, 2, 3, \dots, 8$; $n_1=12$; $n_2=18$; $n_3=22$; $n_4=19$; $n_5=19$; $n_6=28$; $n_7=24$; $n_8=12$; $N=154$.

The mean square between legs is equal to

$$(k-1)^{-1} \sum_{t=1}^k n_t (\bar{T}_{t*} - \bar{T})^2 = 0,57 \text{ K}^2.$$

The mean square within legs is equal to

$$(N-k)^{-1} \sum_{t=1}^k \sum_{i=1}^{n_t} (T_{ti} - \bar{T}_{t*})^2 = 0,1 \text{ K}^2.$$

Table 5.7. TSS Measured by Airborne IR-Radiometer on the Test Area,
19 April 1982, 1230-1450 GMT

(1) Гача	(2) ТПМ, °C													\overline{T}_t^*
	1,4	1,4	1,3	1,6	1,5	1,5	1,4	1,5	1,6	1,6	1,3	1,6	1,6	
1	1,4	1,4	1,3	1,6	1,5	1,5	1,4	1,5	1,6	1,6	1,3	1,6	1,6	1,5
2	1,2	1,3	1,3	1,6	1,5	1,3	1,1	1,5	1,2	1,4	1,6	1,4	1,6	1,4
3	1,2	1,4	1,4	1,1	1,4	1,4	1,1	1,3	1,4	1,4	1,4	1,4		1,3
4	1,5	1,5	1,2	1,2	1,3	1,3	1,3	1,4	1,4	1,4	1,4			1,35
5	1,2	1,2	1,3	1,2	1,3	1,4	1,4	1,3	1,4	1,4	1,3	1,4		1,3
6	1,6	1,7	1,6	1,7	1,4	1,7	1,4	1,4	1,3	1,3	1,1	1,3	1,3	1,4
7	1,6	1,7	1,6	1,7	1,6	1,4	1,4	1,4	1,4	1,4	1,4	1,4		1,5
8	1,4	1,5	1,5	1,4	1,2	1,1	1,2	1,3	1,4	1,4	1,5	1,2		1,3

Key:

1. Leg

2. TSS, °C

Results of Variance Analysis

\overline{T}^*	1.40 C
Mean square between flight legs	0.09 K ²
Mean square within flight legs	0.02 K ²
Ratio of mean squares	F = 4.5

$F_{7; 96; 0.999} = 3.7$

$F > F_{7; 96; 0.999}$

The ratio of standard deviations is equal to 5.7. The critical value of the F-distribution with k-1 and N-k degrees of freedom and a significance level of $\alpha = 0.001$ is found from table [16]: $F_{7; 146; 0,999} = 3,7$.

Since $5,7 > F_{7; 146; 0,999}$, the zero hypothesis on the absence of differences between the legs is rejected, and there is a strict difference. Similar conclusions were obtained in the processing of observations for 18, 19 and 26 April (Table 5.7). Consequently, when determining \bar{T}^0 from airborne measurements, the flight legs should not be arbitrary, but should rather be an optimum number according to a certain constant pattern. An analysis of all the measurements made showed that an undistorted evaluation of \bar{T}^0 with minimum time expenditure is obtained with flights along legs 1-6-5. Thus, Z-shaped routes over the site are most suitable for determining \bar{T}^0 .

In order to determine the significance of the daily variation in temperature (factor F, representing "flights") on the investigated characteristic, \bar{T}^0 , airborne measurements obtained on 18 and 23 April were processed using two-factor variance analysis (Tables 5.8-5.11). On 23 April, measurements were made in the nearshore region, where the daily variation would be expected to have the greatest influence on the temperature-survey results. Two flights (2nd and 3rd) were made over a Z-shaped path on 23 April; the survey was completed in 1.5 h. Two flights were also made on 18 April, but the survey consisted of 6 legs and required 4.5 h.

Table 5.8. TSS Measurements by Airborne IR Radiometer Over the Test Area on 23 April 1982, $^{\circ}\text{C}$

(1) Залеты	(2) Галсы			\bar{T}_{i*}
	1	4	6	
2	3,8	4,5	3,8	4
3	3,8	4,0	3,7	3,8
\bar{T}_{*j}	3,8	4,25	3,75	3,9

Key:

1. Flight

2. Leg

Table 5.9. Results of Variance Analysis of TSS Data Obtained by an Airborne IR Radiometer on 23 April 1982

<u>Variance Component</u>	<u>Sum of Squares, K^2</u>	<u>Number of Degrees of Freedom</u>	<u>Evaluations of Variance, K^2</u>
Row-wise	0.06	1	0.06
Column-wise	0.31	2	0.155
Residual	0.07	2	0.035
Total	0.44	5	0.09

Table 5.10. TSS Measurements by Airborne IR Radiometer Over the Test Area on 18 April 1982, °C

(1) Залеты	(2) Галсы						\bar{T}_{ls}
	1	2	3	4	5	6	
1	6,3	5,5	5,0	4,6	4,0	6,0	5,2
2	5,1	5,2	5,5	5,5	5,3	5,0	5,3
\bar{T}_{*j}	5,7	5,35	5,25	5,05	4,7	5,5	5,25

Key:

1. Flight

2. Leg

Table 5.11. Results of Variance Analysis of TSS Data Obtained by Airborne IR Radiometer on 18 April 1982

Variance Component	Sum of Squares, K ²	Number of Degrees of Freedom	Evaluations of Variance, K ²
Between row-wise means (factor F)	0.03	1	0.03
Between column-wise means (factor L)	1.29	5	0.26
Residual	2.66	5	0.53
Total	3.98	11	0.36

$$F_F = 0,03/0,53 = 0,004$$

$$F_{\alpha(F)} k_1 - 1, k_2 - 5 = 6,61$$

$$F_L = 0,26/0,53 = 0,24$$

$$F_{\alpha(L)} k_1 - 5, k_2 - 5 = 5,05$$

$$F_F < F_{\alpha(F)}$$

$$F_L < F_{\alpha(L)}$$

The sums of the squares Q_1 , Q_2 and Q_3 and the evaluations of the variances were found using formulas (5.2)-(5.5). The significance of the influence of factors F and L ("flight legs") were determined by calculating the statistics $F_L = S_2^2/S_3^2$; $F_F = S_1^2/S_3^2$;

$$F_F = 0,06/0,035 = 1,7; F_L = 0,155/0,035 = 4,4.$$

For a level of significance $\alpha = 0.05$ and a number of degrees of freedom of $k_1 = 1$ and $k_2 = 2$, the critical value of the F -distribution is $F_{\alpha(F)} = 18,51$; $k_1 = k_2 = 2$ $F_{\alpha(L)} = 19,0$. Consequently, $F_F < F_{\alpha(F)}$, $F_L < F_{\alpha(L)}$.

Thus, the zero hypothesis on the equality of the row-wise means is not rejected; i.e., the influence of factor F on the investigated characteristic is insignificant. The influence of factor L is also insignificant. Consequently, measurements can be made on a site in the nearshore zone over 1.5 h without the daily temperature variation significantly influencing the value of \bar{T}^0 .

In the open sea, the influence of factor F on the investigated characteristic (\bar{T}^0) is also insignificant, although the measurements were

conducted over 4.5 h. In general, the airborne measurements over the subsatellite site showed that Z-shaped routes are sufficient to reliably determine the average surface temperature of this area, and quasi-synchronous information can be used for comparison with satellite data: the time interval between the airborne and satellite measurements can be as long as 4 h. It must be taken into account that during the experiment period, there was practically no thin-film effect; during other seasons, the temperature variability in the thin film might reduce the permissible time interval between airborne and satellite measurements.

The same time interval between measurements was selected for comparing research-vessel and satellite data: when determining the mean difference between vessel and airborne observations, all vessel temperature measurements, T_v , made less than 4 h before or after the airplane overflight above a given point were considered. The resulting mean difference $(T_v - T_{ob})$ (where T_{ob} designates the airborne temperature measurements quasi-synchronous with the research-vessel measurements) was then added to the mean radiative temperature obtained on the site by the airborne IR radiometer, $\overline{T^0}$. Then the quantity $\overline{T^0} + (T_v - T_{ob})$ was directly compared with the average value of the satellite radiative temperature, $\overline{T_{sat}}$, on the site.

Thus, the atmospheric correction for the Meteor satellite was determined as: $\Delta T_s = \overline{T^0} + (T_v - T_{ob}) - \overline{T_{sat}}$. In the case that there were no airplane flights on a given day, then the correction ΔT_s for the site was determined only according to the measurement data taken by the research vessel A. v. Humboldt within ± 2 h of the satellite overflight (Table 5.16).

5.4. Analysis of the Influence of the Atmosphere on the Measurements of the Baltic Sea Surface Temperature According to Aerological Sounding Data and Climatic Data

We will evaluate the actual influence of the atmosphere on IR measurements using another independent type of observation: aerological sounding of the atmosphere.

The transformation of radiation in the atmosphere can be evaluated using the transfer function P_λ [31]:

$$P_{\Delta\lambda} = \int_{\lambda_1}^{\lambda_2} \varphi_\lambda I_\lambda d\lambda / \int_{\lambda_1}^{\lambda_2} \varphi_\lambda B_\lambda(T_{ss}) d\lambda = I_{\Delta\lambda}(T_r) / B_{\Delta\lambda}(T_{ss}), \quad (5.7)$$

where φ_λ is the spectral characteristic of the IR radiometer; I_λ is the outgoing radiation of the earth-atmosphere system; B_λ is Planck's function; T_{ss} is the temperature of the underlying surface and T_r is the radiative temperature of the earth-atmosphere system.

Another possible evaluation of the influence of the atmosphere on radiation is the quantity $\Delta T = T_{ss} - T_r$, which is the temperature correction to the satellite-measured value of T_r .

The radiation intensity I_λ in (5.7) can be calculated using the radiation transfer equation [25], for which it is necessary to know the vertical distribution of absorbing substances in the atmosphere and their spectral

properties (i.e., a radiation model). We will select several atmosphere models to evaluate radiation transformation in the atmosphere. For a description of the actual atmospheric condition, we use radiosonde observations under clear-sky conditions (model 1, Table 5.12) performed by a coastal GMS on 23 and 25 April 1982 near the time of the satellite measurements. For the climatic version (model 3, Table 5.12), we use climatic data on the vertical profiles of temperature, $T_{cl}(p)$, and specific humidity, $q_{cl}(p)$, at standard levels, p , in the atmosphere for April at a point with coordinates of lat 55° N, long 20° E [26]. Models 2 and 4 (Table 5.12) combine the vertical profiles of $T(p)$ and $q(p)$ according to climatic and radiosonde T_{rs} and q_{rs} data. For all four atmosphere models, average climatic data were used on the ozone content at that point [27], and the influence of aerosol was not taken into account. The radiation model for calculations of $P_{\Delta\lambda}$ is described in detail in [28, 30].

Table 5.12. Atmospheric Transfer Function, $P_{\Delta\lambda}$, for Various Atmosphere Models and Various Spectral Characteristics, $\varphi(\lambda)$, of the IR Radiometer

(1) Номер модели	(2) Модель атмосферы	$\varphi(\lambda) = 1$			φ_I			φ_{II}		
		H ₂ O	O ₃	H ₂ O, O ₃	H ₂ O	O ₃	H ₂ O, O ₃	H ₂ O	O ₃	H ₂ O, O ₃
23 апреля 1982 г. 12 ч 16 мин по Гринвичу (3)										
1	T_{rs}, q_{rs}	0,9740	0,9538	0,9289	0,9804	0,9499	0,9315	0,9806	0,9496	0,9315
2	T_{cl}, q_{rs}	0,9788	0,9547	0,9344	0,9840	0,9509	0,9360	0,9843	0,9507	0,9359
3	T_{cl}, q_{cl}	0,9772	0,9547	0,9329	0,9829	0,9509	0,9348	0,9831	0,9507	0,9348
4	T_{rs}, q_{cl}	0,9714	0,9538	0,9264	0,9783	0,9499	0,9296	0,9786	0,9496	0,9296
25 апреля 1982 г. 10 ч 20 мин по Гринвичу (4)										
1	T_{rs}, q_{rs}	0,9816	0,9491	0,9318	0,9842	0,9509	0,9362	0,9844	0,9510	0,9364
2	T_{cl}, q_{rs}	0,9796	0,9501	0,9310	0,9825	0,9518	0,9355	0,9826	0,9520	0,9358
3	T_{cl}, q_{cl}	0,9816	0,9501	0,9329	0,9843	0,9518	0,9372	0,9844	0,9520	0,9374
4	T_{rs}, q_{cl}	0,9837	0,9491	0,9338	0,9861	0,9509	0,9379	0,9862	0,9510	0,9382

Key:

- | | |
|---------------------|----------------------------|
| 1. Model number | 3. 23 April 1982, 1216 GMT |
| 2. Atmosphere model | 4. 25 April 1982, 1020 GMT |

This set of models used in the calculations of $P_{\Delta\lambda}$ makes it possible to evaluate the influence of variability of atmospheric weather parameters $q(p)$ and $T(p)$ relative to their climatic values on the temperature correction and to determine the contribution of each.

Several versions of the calculations $P_{\Delta\lambda}$ were made for the four atmospheric models, taking into account the influence of the IR-radiometer spectral characteristic and the influence of various atmospheric absorbers atmosphere (H_2O and O_3) on the reconstruction of the water surface temperature (Table 5.12). The atmospheric transfer function under real conditions (model 1, $\varphi(\lambda)=1$) is 0.929 and 0.932. The calculations show that the main contribution to radiation transformation is made by ozone, not water vapor. This is due to the low water-vapor content ($\omega = 1.1$ cm on 23 April and $\omega = 1.4$ cm on 25 April). The variations of weather parameters relative to the climatic values (models 2 and 4) make an insignificant contribution to radiation transformation. For this reason, the transfer functions for actual conditions and climatic conditions practically coincide. No significant changes were caused by taking into account the spectral characteristics of the two operating IR radiometers (I and II) in the calculation of $P_{\Delta\lambda}$ (see Table 5.12). In addition, the calculations showed that the spectral characteristics of the two IR radiometers were nearly the same.

We will now calculate the temperature correction, ΔT , on the basis of the data in Table 5.12 as a function of the radiative temperature $T_r = (-1) - (+10)^\circ C$, measured by satellite (Table 5.13 and Fig 5.3). The actual value of the correction, determined from radiosonde data for 23 and 25 April 1982 is in the range 3.6-4.3 K, depending on T_r . According to the climatic data, this correction is equal to 3.4-4.1 K. The quantity ΔT also is in this range when taking into account the spectral characteristic $\varphi(\lambda)$ for IR radiometer II, which was used in an on-line mode to obtain the basic sea surface temperature maps.

Table 5.13. Calculated Value of ΔT . 1982

$T_r, ^\circ C$	(1) 23 апреля		(2) 25 апреля	
	(3) Модель 1	(4) Модель 3	(3) Модель 1	(4) Модель 3
$\varphi(\lambda) = 1$				
-1	3,8	3,6	3,5	3,5
0	3,8	3,6	3,5	3,5
2	3,8	3,6	3,6	3,6
4	3,9	3,7	3,7	3,6
6	4,0	3,8	3,8	3,7
8	4,2	4,0	3,9	3,8
10	4,3	4,1	4,0	3,9
φ_{II}				
-1	3,6	3,4	3,5	3,4
0	3,8	3,6	3,6	3,6
2	3,8	3,6	3,6	3,6
4	3,8	3,6	3,6	3,6
6	4,0	3,8	3,8	3,8
8	4,2	3,9	4,0	3,9
10	4,3	4,0	4,1	4,1

Key:

1. 23 April
2. 25 April

3. Model 1
4. Model 3

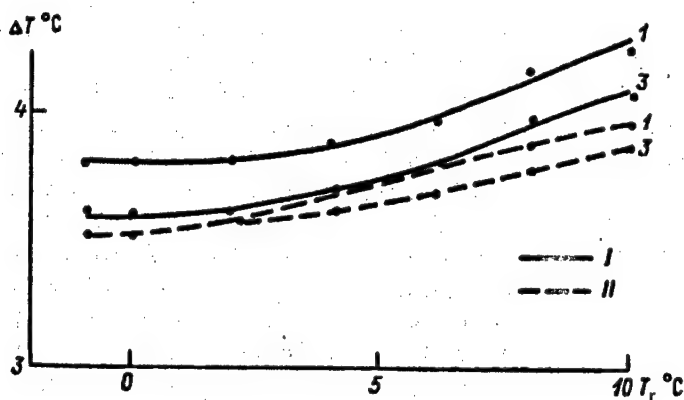


Figure 5.3. Temperature Correction for Different Atmosphere Models (1, 3) as a Function of the Sea-Surface Radiative Temperature:

I. 23 April 1982

II. 25 April 1982

5.5. Analysis of Satellite Measurements of the Temperature Field of the Baltic Sea Surface with an Evaluation of the Atmospheric Corrections

This section uses satellite observation data on sea test areas to analyze satellite TSS (for the selection of test areas and a description of the measurement devices, see paragraphs 2.1-2.4 and 5.2).

Satellite maps were obtained from the No 5 Meteor-2 satellite (time of overflight over the experiment region, 1200 GMT) and from the No 7 Meteor-2 satellite (time of overflight over the experiment region, about 0200 and 1100 GMT). In all, during the experiment period of 15-26 April 1982, 29 TSS maps were received (including 10 maps from Meteor-2 No 5 and 8 daytime maps from Meteor-2 No 7).

From these maps, 8 were selected as suitable for comparative analysis of the Gulf of Riga. The selected maps had no cloudiness over the gulf; the time intervals between the measurements by the two satellites was 1 h. The analysis established that the data for the gulf in each map could be divided into two groups: the nearshore zone (block 1) and the central zone (block 2); each group contained 21 measurements (see Fig 5.1). These groups of data have significant differences in average TSS values, due to heating of the nearshore zone during the day and the possible partial inclusion of the warmer shore in the radiometer field of vision (TSS values differing from the average by more than 3σ were considered spurious and were rejected). The results were processed according to a randomized block design. It was considered that the TSS satisfies the assumptions accepted for the variance analysis of random quantities (the validity of the assumption of variance homogeneity was determined using the Cochran test).

The measurement and variance-analysis results are given in Tables 5.14 and 5.15.

Table 5.14. Values of \overline{T}_r ($^{\circ}\text{C}$) Determined for the Gulf of Riga According to IR Radiometer Readings from Meteor-2 Satellites. April 1982

(1) „Meteor-2“	(2) Блок	(3) Дата			
		19	20	23	25
(4) 5-й ИСЗ	1	-3,0	-3,9	0,4	1,2
	2	-4,9	-4,0	-1,4	-0,7
(5) 7-й ИСЗ	1	-1,0	-2,0	1,5	1,7
	2	-2,5	-2,0	-0,2	-0,25

Key:

- | | |
|-------------|-------------------|
| 1. Meteor-2 | 4. Satellite No 5 |
| 2. Block | 5. Satellite No 7 |
| 3. Date | |

Table 5.15. Results of Variance Analysis of \overline{T}_r Data for the Gulf of Riga from Meteor-2 Satellites

Source	Sum of Squares, K^2	Number of Degrees of Freedom	Evaluation of Variance, K^2
Blocks	4/3	1	4/3
Days	30/13	3	10/4.3
Residual	1/4	3	0.3/1.3
Total	35/20	7	5/3

Note. Numerator, satellite No 5; denominator, satellite No 7

In order to check the comparability of data from both satellites, the residual variance values must be compared. The statistic $F = 4.3$ is calculated and compared with the critical value of the F -distribution with (3; 3) degrees of freedom. At a significance level of $\alpha = 0.05$, $F_{0.05; 3; 3} = 9.28$ and $F < F_{0.05; 3; 3}$; consequently, the measurements of these satellites can be considered comparable with one another. The agreement of the results is tested by finding out whether the measurements of these satellites lead to identical results. Overall, the higher evaluations of TSS obtained from Meteor-2 No 7 were not taken into account, since this fact simply indicates that the IR radiometers of the satellites have different filters, and the atmospheric correction which must be added to the IR radiometer readings of Meteor-2 No 5 is larger than that for No 7. Both satellites observed a warmer water surface on 25 April and colder water on 19 and 20 April. These results correspond also with the observations of nearshore stations given in Table 5.2.

When determining the corrections to the daytime satellite measurements on the basis of GMS measurements in the Gulf of Riga, evaluations were used of the average satellite temperature in the central zone (block 2) and the average temperature according to GMS measurements at 0600 GMT.

These measurements were considered quasi-synchronous, since it was shown above that in the open sea, the change in average surface temperature over 4 h was insignificant, while the morning measurements by nearshore stations can be applied to the open-sea regions (since solar heating has not yet had a significant effect on the TSSL).

Table 5.16 gives the corrections determined according to satellite measurements on the site (for the airplane test areas, see Figs 2.5 and 2.6; these areas include from 2 to 9 satellite measurements). A correction for atmospheric attenuation is preliminarily included in the airborne measurements. This correction was obtained on the basis of a comparison with the data from the IR radiometer on the research vessel A. v. Humboldt. On those days when there were no satellite observations on the site, the reference point for comparison was the in situ observations of the A. v. Humboldt.

Table 5.16. Determination of Corrections to Satellite TSS Measurements According to the Results of Synchronous Subsatellite Observations on the Baltic Sea from 17 through 25 April 1982, °C

(1) Дата	(2) Рижский залив			(3) Полигон					(4) Южная часть моря				ΔT
	T_{sat}	T_{GMS}	ΔT	T_{sat}	\bar{T}°	T_v	$T_v - T_{ab}$	ΔT	T_{sat}	T_v	\bar{T}°	ΔT	
17	—	—	—	—	—	—	—	—	-2/ -1	3	—	5/ 4	5/ 4
19	-4,9/-2,5	2,4	7,3/4,9	-4/-1	1,4	2,6	1,1	7/ 4	-4/ -1	3,5	—	7,5/4,5	7/4,5
20	-4,0/-2,0	1,8	5,8/3,8	-4/—	—	2,6	—	6,6/—	-4/ —	3,4	—	7,4/—	7/ 4
21		0,7		-/-2,5	1,8	2,8	1	-/ 5	- /-1,5	3,0	—	-/4,5	-/ 5
23	-1,4/-0,2	2,8	4,2/3	-1,0/ 1,3	4	4	0	5/ 3	-1,2/ 1,0	3,5	—	4,7/ 3	4,5/ 3
24	-1,5/ —	4,0	5,5/—	-1,0/-0,5	3,2	4	1	5/4,5	-1,5/ -1	3,5	3,5	5/4,5	5/4,5
25	-0,7/-0,25	3,8	4,5/4,05	-1/-1	2,1	3,1	1	4/ 4	-0,4/-0,4	—	3,5	4/ 4	4/ 4

Note. T_{sat} is the radiation temperature determined from data of the Meteor-2 satellites (numerator, satellite No 5/denominator, satellite No 7); T_{GMS} is the temperature measured at the GMS; T_v is the temperature measured by vessels; \bar{T}° is the temperature measured from the IL-14 airplane; ΔT is the correction to the TSS measurements by the Meteor-2 satellites (numerator, No 5 satellite/denominator, No 7).

Key:

- | | |
|-----------------|-----------------------------|
| 1. Date | 3. Site |
| 2. Gulf of Riga | 4. Southern part of the sea |

Table 5.16 also gives the corrections based on vessel observations in the southern part of the sea (southern test area, see Fig 5.2). For this, the value of \overline{T}_{sat} , obtained as the average of 100 or more satellite measurements and the value of \overline{T}_v obtained as the average of 5-10 vessel measurements from vessels of opportunity were compared. On 24 and 25 April, the data of SZ UGKS aerial surveys were used.

The total correction (Table 5.16) was obtained as the average for three test areas. The calculated values of ΔT were introduced into the satellite measurements. As a result, TSS maps were constructed with correction for atmospheric absorption on the basis of subsatellite observations (see Figs 5.2, 5.4 and 5.7).

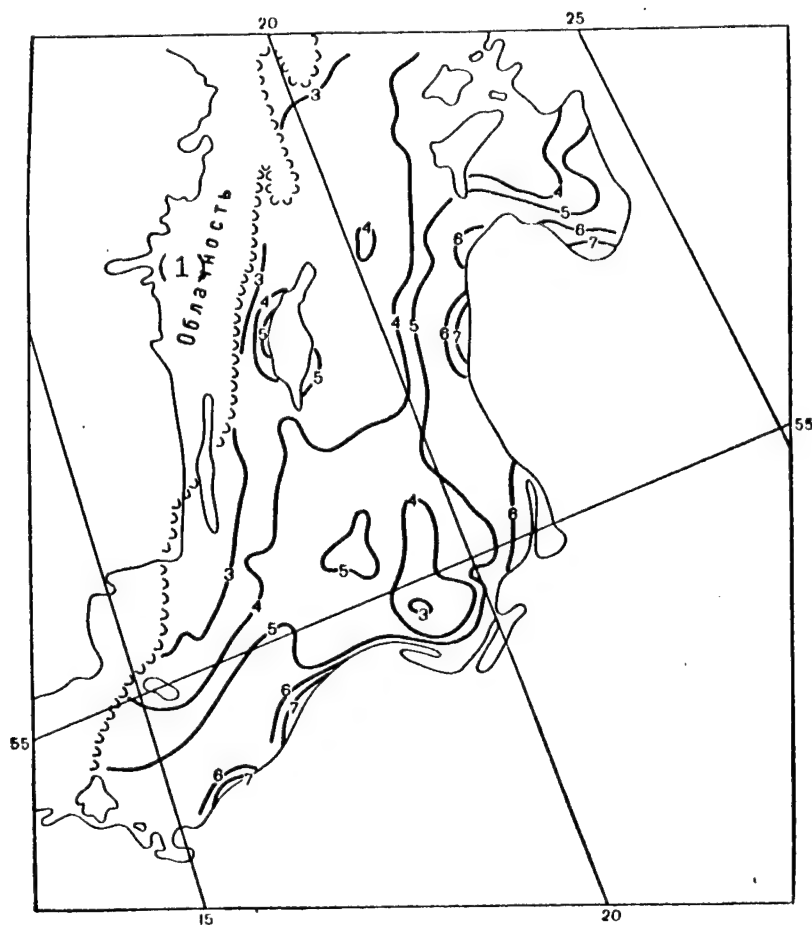


Figure 5.4. Surface Temperature of the Baltic Sea ($^{\circ}\text{C}$) According to Data from the No 5 Meteor-2 Satellite. 23 April 1982, 1100 GMT

Key:

1. Clouds

Figures 5.5 and 5.6 show TSS maps constructed taking into account the atmospheric correction using average climatic data [28].

As can be seen from Table 5.16, the atmospheric correction for the experiment period, determined from subsatellite observations, was 4-7 K for Meteor-2 No 5 and 3-5 K for Meteor-2 No 7. The correction calculated according to the average climatic data is equal to 4 K; i.e., the data from Meteor-2 No 7 (which has been in orbit for less than a year) can be successfully corrected using the average climatic method. The data from Meteor-2 No 5 (which had been operating over 2 years at the start of the experiment) need a significantly larger correction, which is due, as was indicated above, to a possible change in the spectral characteristics of its optics and to reduced sensitivity of its radiation detector. Obviously, changes in the mechanical functioning of the instrument over the operating period must be taken into account (for example, by artificially aging a camera in a laboratory or by other methods involving orbital

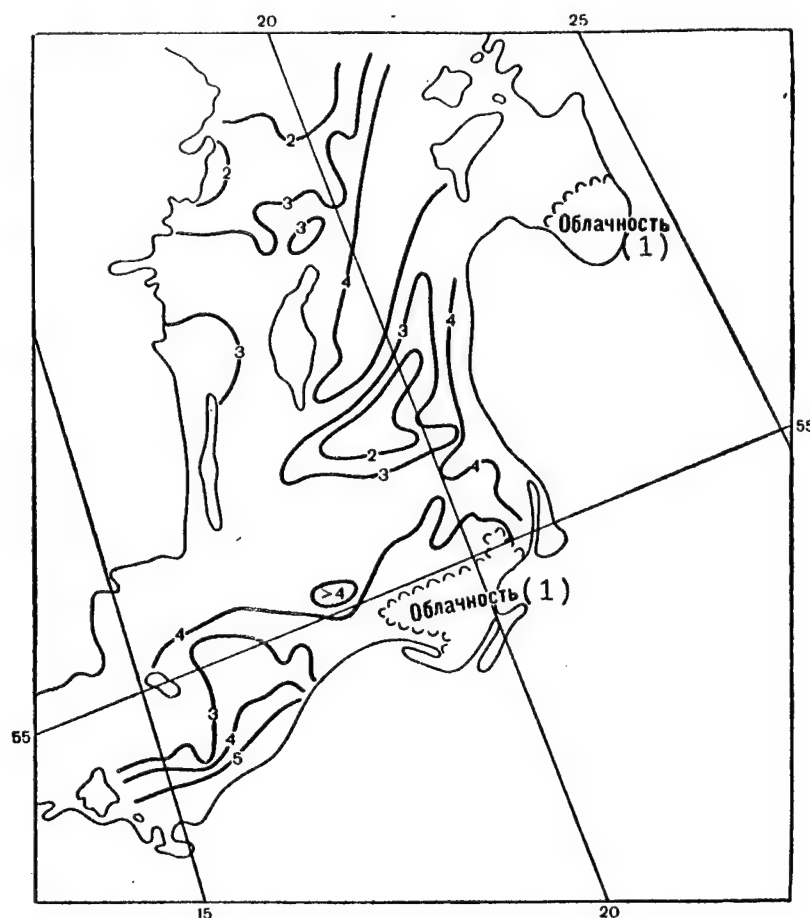


Figure 5.5. Surface Temperature of the Baltic Sea ($^{\circ}\text{C}$) According to Data from the No 5 Meteor-2 Satellite. 25 April 1982, 0100 GMT

Key:

1. Clouds

tests). The configuration of the isolines constructed from the data of both satellites also differed significantly; to some degree, this might be due to the high level of instrument noise. In sum, the data of the Meteor-2 satellites should be used for qualitative analysis of the processes: determining latitudinal change and seasonal variability. It is unfeasible to do precise quantitative analysis using the present statistical methods (as was done, for example in [151]) due to the high noise level and the insufficient spatial resolution: there are only 2-4 temperature measurements made by Meteor-2 satellites for the site. Figure 5.8 shows an example of a TSS map obtained from a NOAA satellite on the experimental APPI [not further identified] of LO GOIN and LPI [not further identified] on 23 April 1982. There are already 84 TSS values for this site, which made it possible to use the following processing procedure: the atmospheric correction of satellite data ($\Delta T = 2$ K) was made by histogram analysis of TSS data obtained from the satellite and from the LO GOIN airplane. The method of evaluating the true temperature from the "thermal" side of the histogram, proposed in [59], was used in the

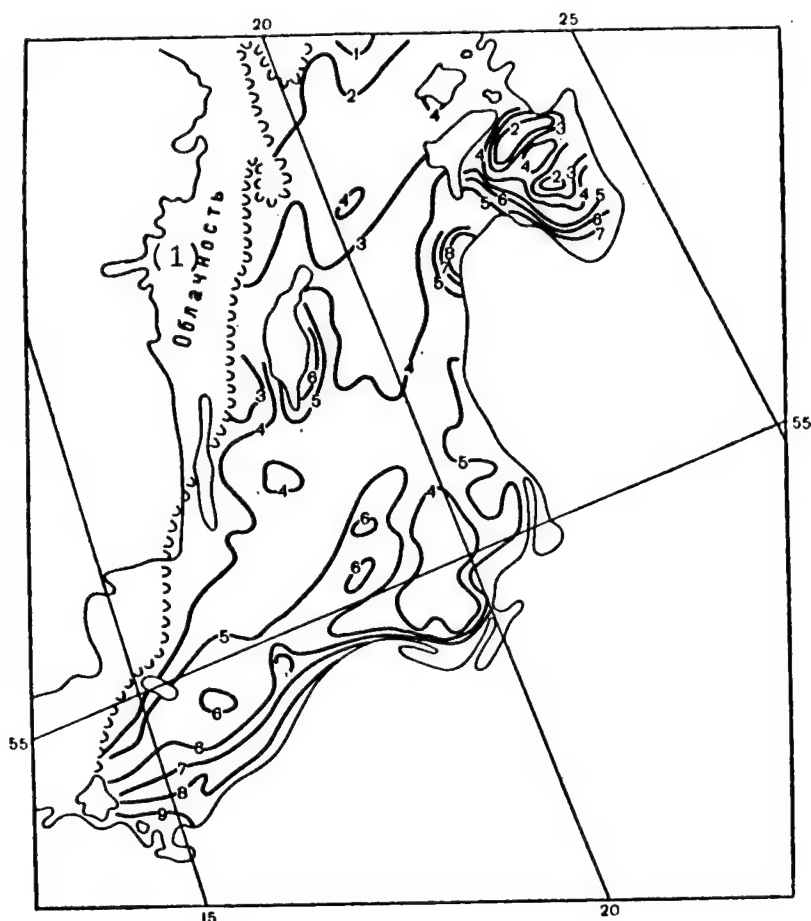


Figure 5.6. Surface Temperature of the Baltic Sea ($^{\circ}\text{C}$) According to Data from the No 7 Meteor-2 Satellite. 23 April 1982, 1200 GMT

Key:

1. Clouds

analysis, taking into account the fact that the temperature field of the site was homogeneous; i.e., the intrinsic natural variability of the TSS field was small, while the instrument noise levels of the satellite IR radiometers and of the airborne IR radiometer were comparable. The site cannot be analyzed in this manner using Meteor-2 data due to the insufficient number of satellite observations of the site.

5.6. Conclusion

Overall, the totality of information from all levels and with different spatial resolutions shows the following picture of the thermal processes on the Baltic Sea surface: uneven heating is observed, linked with the significant latitudinal change in the incoming solar radiation in spring. In the southern part of the sea, the surface waters are 5-7° C warmer than in the northern part of the Gulf of Riga. Data from the high-resolution satellite IR radiometer showed that there are areas of warm water ("spotty" formations in the TSS field) 10-15 km in diameter with a gradient of

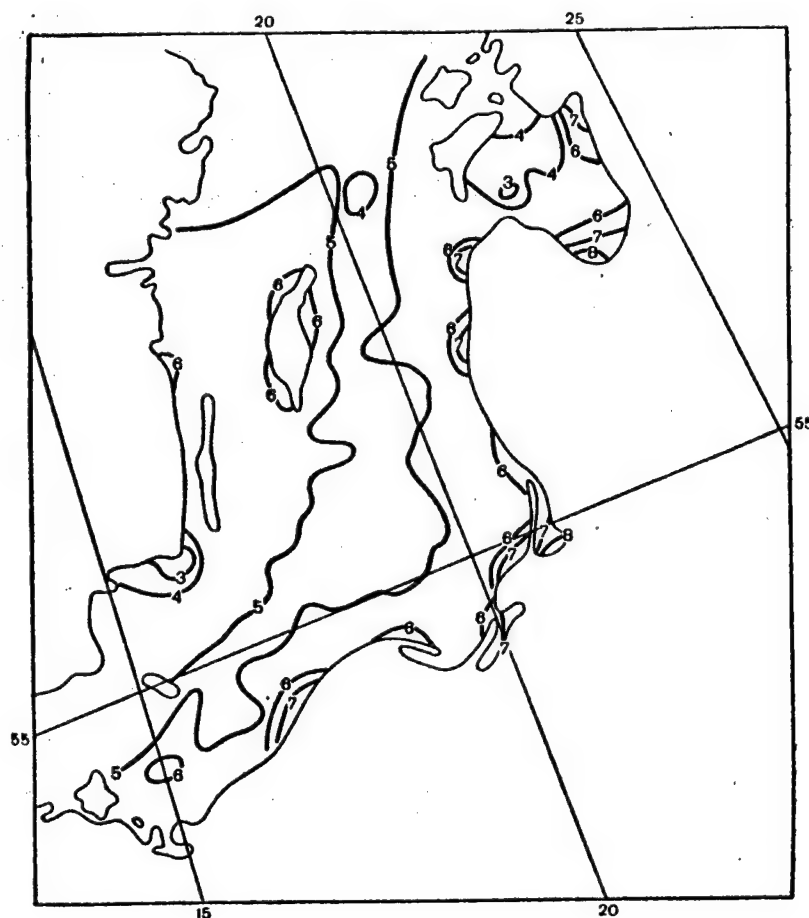


Figure 5.7. Surface Temperature of the Baltic Sea (°C) According to Data from the No 5 Meteor-2 Satellite. 25 April 1982, 1100 GMT

1°C/km in the southern part of the sea. In the open sea at the latitude of Klaypeda, there is an elongated region of cold waters (100 km across; temperature, 3°C), which is recorded on the maps from satellites with different resolutions (see Figs 5.4 and 5.8) and on the aerial-survey map of radiative temperature made during this period (Fig 5.9). The coldest waters are in the northern part of the Gulf of Riga: $T_{ss} = 2^{\circ}\text{C}$, according to both satellite and aircraft data.

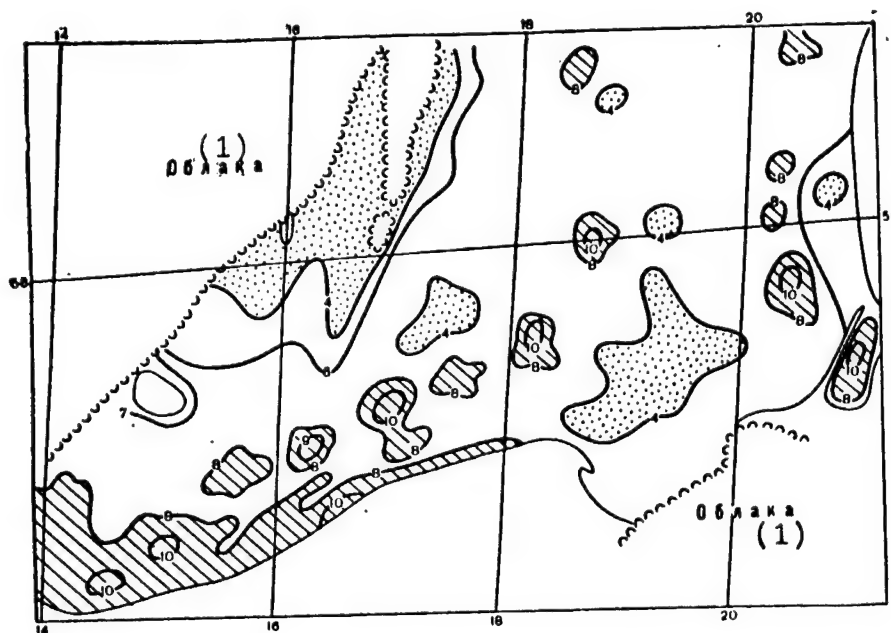


Figure 5.8. Surface Temperature of the Baltic Sea ($^{\circ}\text{C}$) According to NOAA-6 Satellite Data. 23 April 1982. Projection Close to the Projection of the Satellite Photograph

Key:

1. Clouds

The reliability of the satellite information also is qualitatively confirmed by the results of TSSL measurements by thermistors towed by the research vessel Akademik Kurchatov for a short 3-h route in the southern Baltic as an auxiliary to the experiment program. The towed-sensor data were kindly provided by K.N. Fedorov and A.S. Kazmin, and are shown in Fig 5.10. According to the thermistor data, the water surface temperature along the route varied in the range $2.7\text{--}3.9^{\circ}\text{C}$, having a general tendency to increase from northwest to southeast. The satellite information notes the same trend in TSS (Figs 5.6 and 5.8), although according to the high-resolution radiometer data, the range of temperature variations on the same cross section is somewhat larger than the range given by towed-sensor data. It must be noted that a simple comparison of the satellite data with the towed-sensor data cannot be considered adequate, in view of the distinguishing methodological features of measuring TSSL using towed sensors.

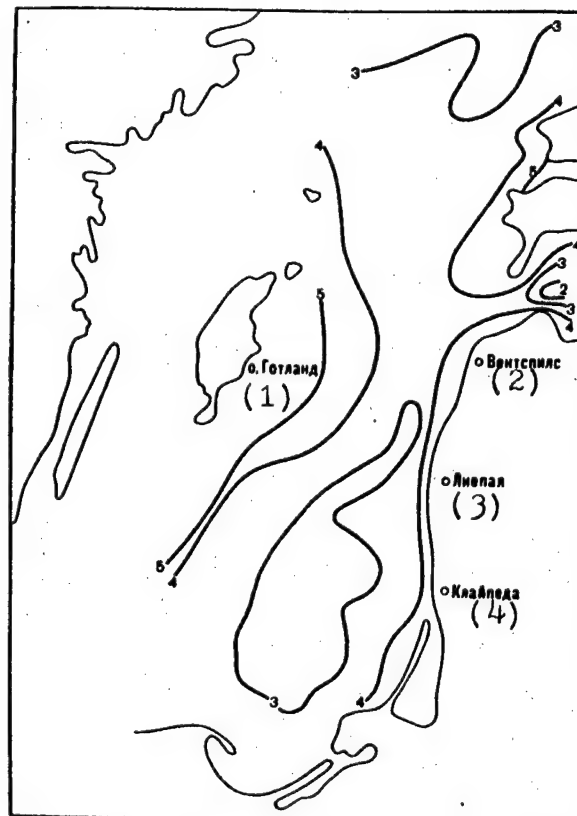


Figure 5.9. Radiative Temperature of the Baltic Sea ($^{\circ}\text{C}$) According to SZ UGKS Aerial Survey Data. 24-25 April 1982

Key:

1. Gotland 2. Ventspils 3. Ljupaya 4. Klaypeda

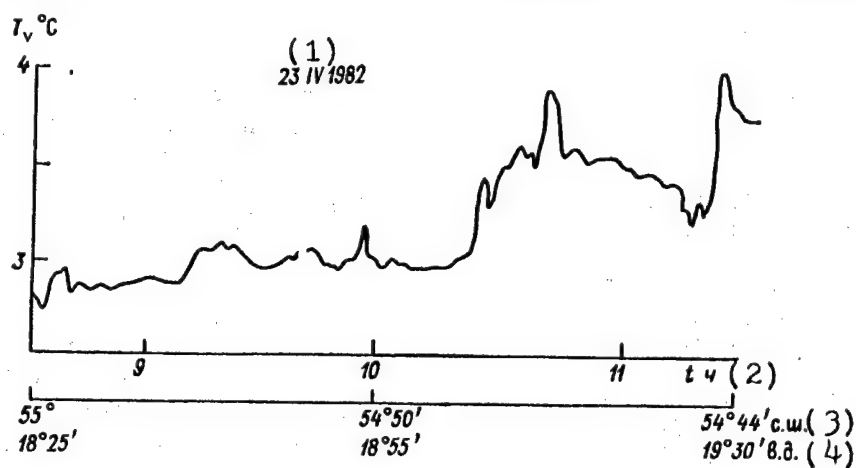


Figure 5.10. Baltic Sea Temperature According to Towed-Sensor Data

Key:

1. 23 April 1982 2. t, h 3. lat N 4. long E

According to the high-resolution satellite data, there is a warm nearshore front with surface temperature gradients of $0.5-1^{\circ}\text{C/km}$ along the south shore of the Baltic. The width of the strip of heated nearshore waters ranges from 30 to 50 km in the southern sea (according to high-resolution satellite IR radiometer data) to 100 m along the Latvian Coast (according to airborne-survey data). The existence of warm nearshore waters leads to the formation of warm air masses near the coasts, which in turn affects the representativeness of the water-temperature measurements by coastal GMS's for the atmospheric correction of remote TSS measurements. As was indicated above, during the experiment, the data of GMS's located on the eastern shore of the Baltic sea were considered unrepresentative for making atmospheric corrections of satellite IR radiometer data. Local air warming and the presence of nearwater inversions in the air layer (for example, on 23 April 1982) can also make unreliable the atmospheric correction of satellite data using aerological sounding data from coastal GMS's. Thus, on 23 April, the correction according to aerological data was 1°C above the correction determined according to the results of measurements on open-sea test areas (see Tables 5.13 and 5.16). It is clear that more reliable data could be obtained from aerological sounding from island GMS's or directly from research vessels.

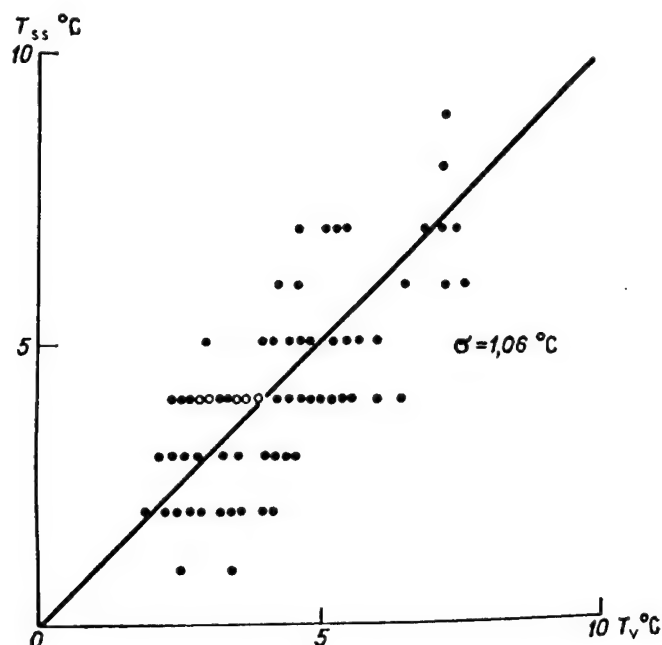


Figure 5.11. Regression Function T_{ss} (T_v) According to Satellite Remotely Sensed Data (T_{ss}). The Total Number of Cases of Synchronous Measurements is $N = 116$:

Open dots represent towed-sensor data on 23 April 1982 from the research vessel Akademik Kurchatov.

The precision of establishing the TSS according to satellite data from Meteor-2 satellites was evaluated during the experiment period. The

measure of precision was the standard deviation of TSS established from satellite measurements (T_{ss}) from the temperature measured by in situ methods from the vessel (T_v) within the permissible time interval of measurements (± 2 h from the time of satellite overflight). During the entire experiment period, 116 pairs of T_{ss} and T_v were obtained. Figure 5.11 gives a regression function of $T_{ss}(T_v)$ for this sample. The standard deviation of the difference $T_{ss} - T_v$ was 1.3° C. This conclusion coincides with the evaluation of precision of the satellite IR radiometer data collected for the Baltic Sea in June 1978.

Overall, this subsatellite experiment showed that single-channel satellite data for the Baltic Sea during a transition season can be corrected for atmospheric effects using vessel-airplane measurements on a specialized subsatellite site located in a zone with a homogeneous TSS temperature field. It should be noted that the joint-experiment site in this case can be considered a satisfactory test area for determining the necessary atmospheric correction for satellite measurements.

In order to introduce corrections into the satellite measurements, GMS data can also be used if the data are preliminarily subjected to variance analysis to reject stations with extreme TSSL variances. In certain cases, GMS aerological sounding data and open-sea vessel data also can be used. However, in each specific case, the actual condition of the air masses above the sea and near the shore must be taken into account. Therefore, it is feasible when determining atmospheric corrections in the future to use several test areas for this purpose, in order to determine the possible latitudinal variation of corrections caused by the presence of different air masses. In the present experiment, the corrections obtained on all three test areas gave comparable results, which permitted the use of a unified correction for the satellite data, without taking into account the latitude of the location. However, realistically, it might be necessary to differentiate the corrections according to latitudinal (or other) zones.

In principle, the corrections determined according to the computer catalog of climatic data can also be used. However, they must be differentiated depending on the spectral characteristics of the specific satellite radiometers, taking into account the distinguishing features of camera aging. In addition, it must be kept in mind that the climatic catalog, naturally, cannot take into account the actual synoptic variability of the atmospheric processes.

6. Basic Results of the Experiment

The present work is an attempt to discuss the range of questions linked with the organization of complex subsatellite experiments necessary for the correct use of satellite data for the study of a specific semi-enclosed sea: the Baltic Sea. It should be noted that the problems of using satellite information in oceanography--given the limited nature of this information at the present stage--have been insufficiently investigated. This relates both to oceanographic work in general and to regional investigations. This is absolutely the case with the Baltic Sea as well. Soviet and foreign publications lack regular articles on the use of satellite information for the study of this sea, although in recent years

the number of such efforts has been gradually increasing. In general, the existing experience (mainly foreign) of using satellite data in regional research is limited in nature.

As a subject of study using satellite information, the Baltic Sea is exceptionally complicated, from the point of view of general processing and interpretation of the data.

The irregularity of the coastline and the meridional elongation of the sea cause difficulties for automated geographic location of data with specific precision. The interpretation of satellite measurement data is difficult because of: 1) the relatively small-scale nature of the processes, 2) the strong influences of river drainage and of water exchange between the parts of the sea, 3) the shallowness of the water, 4) the greater temporal variability of the oceanographic parameters than in the ocean and 5) the great frequency of cloud situations and the rapid restructuring of atmospheric processes which are characteristic of the Baltic.

There is sufficient justification for considering the last decade as the beginning of a significant increase in international and national Baltic-Sea research, in which satellite data is important.

Data from satellite remote sensing of the earth can make a noticeable contribution to the solution of such fundamental problems of the Baltic Sea as: 1) research on the principles of the movement of "passive" admixtures (heat, salinity, turbidity, biological and selected chemical elements and contaminants) in the Baltic Sea; 2) research (including full-scale) and a mathematical description of the characteristics of variability and unevenness of hydrological, hydrochemical and contamination fields in the Baltic Sea. It can also provide information for the mathematical description of biochemical processes and for the study of the structural and functional principles of biological ecosystem communities of the Baltic Sea. Satellite oceanographic research must be based on the presently established bank of integrated characteristics of the Baltic Sea and in turn must be one of the sources of data for this bank.

Problems of studying the vertical and horizontal mass-, energy- and momentum-exchange of the Baltic Sea are extremely urgent. The role of satellite data is significant also in the study of eddies and eddy-like formations of the Baltic Sea. The occurrence of these phenomena is not linked with any particular time of the year; they can be observed during the entire year. Tracers for observing eddy currents can be specific lines of plankton bloom fields (in spring and summer) or sea surface temperature fields.

An analysis of the data obtained by a number of Soviet and foreign expeditions using the latest means of obtaining and methods of processing information leads to the conclusion that synoptic-scale phenomena (such as nonsteady-state circulation, eddies, internal waves and upwellings) are especially significant in the Baltic Sea, with its layers, complicated morphometry and bottom relief and irregular coast line. The surface manifestations of these phenomena, in the form of inhomogeneities in: 1) water-mass temperature fields and optical properties or 2) the sea state,

have attracted the close attention of researchers very recently. The problem has been called the "spottiness of the Baltic Sea" and was the subject for discussion at a special conference of seven Baltic countries (Tallinn, 22-23 March 1983) within the framework of the International Council for the Exploration of the Sea.

This problem can only be solved by the wide use of satellite information with the organization of complex vessel-airplane experiments on the sea during various seasons. Subsatellite experiments are a necessary element in verifying satellite data and make it possible to reconstruct a three-dimensional picture of the hydrophysical fields and study the space-time variability of these fields. It is namely this path that USSR and GDR oceanographers have followed in organizing the joint work to study the Baltic Sea by remote means. Two complex USSR-GDR experiments have now been conducted in the Baltic Sea: in April 1982 and in June 1983.

The first experiment, which is described in fairly great detail in the present book, gave researchers a large volume of synchronous experimental data from satellites, airplanes and a vessel. These data characterize the thermal and optical properties of the Baltic Sea water masses. Specialists of the Operational Control Group, the crews of the vessel and airplanes, scientists, engineers and technicians have accumulated much experience in joint research and have worked out a number of specific interaction arrangements for complex subsatellite oceanographic experiments.

Compared with the first experiment, the second subsatellite experiment, conducted in May-June 1983, featured an expanded spatial scale of synchronous measurements, a longer operating period and a larger number of participating vessels, as well as a different working area. The research vessels A. v. Humboldt (GDR AS), Ayu-Dag (Estonian AS) and Rudolf Samoylovich (State Committee on Hydrometeorology and Environmental Control) participated in the experiment, conducting hydrological, hydrochemical, hydrobiological and hydroptical research. An Il-14 airplane with an IR radiometer and an An-30 airplane with equipment including an MKF-6M and a spectrophotometer also took part. During the experiment, the vessel equipment of the participating parties was intercalibrated.

The results of the synchronous subsatellite experiments and an analysis of the satellite data, make it possible with assurance to confirm the possibility of using satellite information to study synoptic processes and, when information is obtained regularly, to investigate the seasonal variability of Baltic Sea hydrophysical fields.

The data of the subsatellite experiments show the necessity of further improving the system of collecting reference data, including oceanographic parameters, atmospheric characteristics and accompanying hydrometeorological characteristics, based on optimizing the aggregate of vessel and airborne information-measurement systems and on automating the processing of experimental data. It should be emphasized that on-line processing of information directly during the experiment makes it possible, if necessary, to change the work program, control the spatial position of individual measurement devices or flexibly restructure the measurement cycles depending on changing meteorological or other conditions.

In conclusion, we note that the methodological results obtained in the course of the preparation and execution of the complex subsatellite oceanographic experiments on the Baltic Sea can be used in the planning of similar subsatellite experiments on other water bodies.

BIBLIOGRAPHY

1. Ablyazov, V.S., et al., "Future Multipurpose Radiophysics Laboratory Based on an Il-18 Airplane," *IZV. VUZOV "GEODEZIYA I AEROFOTOSYEMKA,"* No 2, 1982, pp 11-24.
2. Avanesov, G.A., Barinov, I.V., and Glazkov, V.D., "Multispectral Scanning System in an Airborne Experiment to Investigate the Earth's Resources," *METEOROLOGIYA I GIDROLOGIYA*, No 4, 1974, p 35.
3. Avanesov, G.A., Barinov, I.V., Glazkov, V.D., et al., "Modeling a Satellite Experiment Using an Airplane Laboratory," in: "Kosmicheskiye issledovaniya zemnykh resursov" [Satellite Investigation of Earth Resources], Vol 1, Moscow, 1976, pp 280-287.
4. Aytsam, A., et al., "Synoptic Variability of Physical Fields in the BOSEX Site in the Central Part of the Baltic Sea," in: "Trudy XII Konferentsiy Baltiyskikh okeanografov" [Works of the 12th Conference of Baltic Oceanographers], Leningrad, 1981, pp 27-41.
5. Allabert, A.V., et al., "On the Problem of Investigating Sea Surface Radiative Temperature Fields from an Airplane Over Experimental Subsatellite Sites," in: "Pervaya Vsesoyuznaya konferentsiya 'Biosfera i klimat po dannym kosmicheskikh issledovaniy' (Tezisy Doklady)" [First All-Union Conference "Biosphere and Climate According to Satellite-Research Data" (Abstracts of Reports)], Baku, 1982, pp 320-322.
6. Allakhverdov, F.M., and Kallinikov, Yu.V., "Problem of Constructing Marine Subsatellite Information Measurement Systems," *ISSLEDOVANIYE ZEMLI IZ KOSMOSA*, No 1, 1982, pp 110-115.
7. Afonin, Ye.I., et al., "Evaluation of the Chlorophyll Content in the Upper Layer of the Sea According to the Change in the Color Index," in: "Svetovyye polya v okeane" [Light Fields in the Ocean], Moscow, 1981, pp 191-196.
8. Badayev, V.V., and Malkevich, M.S., "Integrated Method of Remote Determination of Ocean Brightness and Atmospheric Optical Parameters," in: "Tezisy dokladov XI Vsesoyuznogo soveshchaniya po aktinometrii. Ch. 6. Distantсионное зондирование атмосферы и подстилающей поверхности" [Abstracts of Reports to the 11th All-Union Conference on Actinometry. Part 6. Remote Sounding of the Atmosphere and the Underlying Surface], Tallinn, 1980, pp 79-82.

9. Belyayev, M.M., et al., "Experimental Oceanographic Sites," in: "I syezd sovetskikh okeanologov. Tezisy dokladov" [1st Conference of Soviet Oceanographers. Abstracts of Reports], No 1, Moscow, 1977, pp 173-174.
10. Berestovskiy, I.F., Brosin, H.-J., and Viktorov, S.V., "USSR-GDR Oceanographic Subsatellite Experiment," ISSLEDOVANIYE ZEMLI IZ KOSMOSA, No 1, 1983, pp 121-122.
11. Burenkov, V.I., et al., "Brightness Spectra of Ascending Radiation and Changes in These Spectra with Observation Altitude," in: "Opticheskiye metody izucheniya okeanov i vnutrennikh vodoyemov" [Optical Methods of Studying the Oceans and Inland Water Bodies], Novosibirsk, 1979, pp 41-58.
12. Viktorov, S.V., "Airborne Equipment Systems for Oceanographic Research in the Optical Band," in: "Optika okeana i atmosfery (Tezisy dokladov)" [Optics of the Ocean and Atmosphere (Abstracts of Reports)], Baku, 1980.
13. Viktorov, S.V., and Tishchenko, A.P., "Principles of the Organization of a Reference Data Bank for Use in Interactive Systems of Processing Satellite Information About the Ocean," TRUDY GOIN, No 166, 1982, pp 24-29.
14. Vinogradov, V.V., and Koprova, L.I., "Use of IR Information from Meteor Satellites to Evaluate Hydrological Processes on the Baltic Sea Surface," TRUDY GOIN, No 157, 1982, pp 132-146.
15. Vinogradov, V.V., Bychkova, I.A., and Grigoryev, V.V., "Possibility of Using IR Information from Meteor Satellites to Evaluate Oceanographic Processes on the World Ocean Surface," TRUDY GOIN, No 166, 1982, pp 54-60.
16. Johnson, N., and Lyon, F., "Statistics and Planning of Experiments in Engineering and Science. Experiment Planning Methods," Moscow, Mir, 1981.
17. Drabkin, V.V., Allabert, A.V., and Florenskaya, M.L., "Tasks and General Principles of Organizing Oceanographic Aerial-Satellite Sites," TRUDY GOIN, No 166, 1982, pp 30-36.
18. Yemelyanov, Ye.M., and Pustelnikov, O.S., "Suspended Matter, Its Composition and the Balance of Residual Material in Baltic Sea Waters," in: "Geologiya Baltiyskogo morya" [Geology of the Baltic Sea], Vilnyus, 1976, pp 159-186.
19. Yemelyanov, Ye.P., and Stryuk, V.P., "Aquatic Suspended Matter," in: "Osadkoobrazovaniye v Baltiyskom more" [Sediment Formation in the Baltic Sea], Moscow, 1981, pp 79-106.
20. Zernova, V.V., "Seasonal Changes in Baltic Sea Phytoplankton," in: Ibid., pp 64-73.

21. Ziman, Ya.L., Sazhko, M.Yu., and Tsitovich, V.S., "Airplane Laboratories and the Experience of Using Them in the Development of Methods and Means for Remote Investigation of Earth Resources," in: "Kosmicheskiye issledovaniya..." op. cit., pp 275-279.
22. Ismailov, T.K., "Development of Methods and Means for Subsatellite Observations," ISSLEDOVANIYE ZEMLI IZ KOSMOSA, No 1, 1980, pp 35-39.
23. Kaiser, W., and Siegel, H., "Experiments to Determine the Capability of Baltic Sea Phytoplankton for Light Adaptation," in: "Trudy XII Konferentsii..." op. cit., pp 433-438.
24. Koblents-Mishke, O.I., and Konovalov, B.V., "Primary Product and Chlorophyll in the Baltic Sea in the Summer of 1978," in: "Osadkoobrazovaniye ..." op. cit., pp 45-64.
25. Kondratyev, K.Ya., and Timofeyev, Yu.M., "Meteorologicheskoye zondirovaniye atmosfery iz kosmosa" [Meteorological Sounding of the Atmosphere From Space], Leningrad, Gidrometeoizdat, 1978.
26. Koprova, L.I., "Catalog of Global Apriori Information for On-Line Processing of Spectrophotometric Measurements from Satellites," TRUDY GOSNITSIPR, No 4, 1977, pp 62-66.
27. Koprova, L.I., "Global Distribution of Ozone for Various Seasons," TRUDY GOSNITSIPR, No 9, 1978, pp 94-100.
28. Koprova, L.I., and Solovyev, V.I., "Metodicheskiye rekomendatsii. Voprosy sputnikovoy meteorologii. Opredeleniye temperatury vodnoy poverkhnosti po IK-izmereniyam s ISZ 'Meteor'" [Methodological Recommendations. Problems of Satellite Meteorology. Determining the Water Surface Temperature from IR Measurements Made by Meteor Satellites], Moscow, Gidrometeoizdat, 1983.
29. Koprova, L.I., Utkin, Ye.F., and Bakhmatov, A.Ye., "Results of a Test of the Methods of Determining the Water Surface Temperature from Meteor Satellites," METEOROLOGIYA I GIDROLOGIYA, No 7, 1981, pp 61-69.
30. Koprova, L.I., and Utkin, Ye.F., "Global Distribution of the Transfer Function in the 8-12 m Atmospheric Window," TRUDY GOSNITSIPR, No 12, 1982, pp 45-60.
31. Malkevich, M.S., "Opticheskiye issledovaniya atmosfery so sputnikov" [Optical Atmospheric Research From Satellites], Moscow, Nauka, 1973.
32. Neuymin, G.G., Solovyev, M.V., and Martynov, O.V., "Several Results of Measuring the Color Index of Waters in Regions of the World Ocean," in: "Opticheskiye metody..." op. cit., pp 27-38.
33. Poletayev, Yu.I., Popov, A.A., and Nistoglo, S.A., "Means and Organization of Aerial Surveys," in: "Vozdushnyy transport" [Air Transport], Moscow, 1978.

34. Pomeranets, K.S., "Spatial Variability of Water Temperature in the Baltic Sea," TRUDY GOIN, No 110, 1972, pp 37-44.
35. "Samolet AN-30. Kratkiye svedeniya" [AN-30 Airplane. Brief Information], Moscow, Voenizdat, 1973.
36. Sustavov, Yu.V., Chernysheva, Ye.S., and Mikhaylov, A.Ye., "Hidden Eddies of the Baltic Sea," TRUDY GOIN, No 152, 1980, pp 17-37.
37. Khodarev, Yu.K., et al., "Use of Satellite Means to Study Earth Resources and Monitor the Environment. Airplane Experiment," METEOROLOGIYA I GIDROLOGIYA, No 4, 1974, pp 25-29.
38. Aitsam, A., et al., "Preliminary Results on the Study of Spatial and Temporal Characteristics of the Synoptic Variability of the Baltic" in: "The Investigation and Modelling of Processes in the Baltic Sea, P. 1," Tallinn, 1981, pp 70-98.
39. Clarke, G.L., Ewing, G.C., and Lorenzen, G.J., "Spectra of Back-Scattered Light from the Sea Obtained from Aircraft as a Measure of the Chlorophyll Concentration," Science, Vol 167, No 3921, 1970, pp 1119-1121.
40. Dietrich, G., "Der jährliche Gang der Temperatur- und Salzgehaltsschichtung in der britischen Randmeeren und in der Nord- und Ostsee, Univeröff. wiss.," Bericht, Deutsches Hydrograph. Institut, Hamburg, 1948, pp 16-22.
41. Højerslev, N.K., "Bio-Optical Properties of the Fladen Ground: 'Meteor' FLEX 75 and FLEX 76," J. CONS. INT. EXPLOR. MER., Vol 40, 1982, pp 272-290.
42. Kaiser, W., and Schulz, S., "On the Causes for the Difference in Space and Time of the Commencement of the Phytoplankton Bloom in the Baltic," KIELER MEERESFORSCHUNGEN, Sonderheft 4, 1978, S 161-170.
43. Kaiser, W., Renk, H., and Schulz, S., "Die Primärproduktion der Ostsee," GEODAT. GEOPHYS. VERÖFF, R IV, H 33, 1981, S 27-52.
44. Kielmann, J., "Mesoscale Eddies in the Baltic," in: "Proc. XI Conf. Baltic Oceanogr.," Rostok, Vol 2, 1978, pp 729-755.
45. Krauss, W., "The Erosion of a Thermocline," J. PHYS. OCEANOGR., Vol 11, No 4, 1981, pp 415-433.
46. Leiterer, U., Weller, M., Händel, H., and Bischoff, K.-H., "Das Spektralfotometer BAS für Messaufgaben in Rahmen der Fernerkundung der Erde," FEINGERÄTETECHNIK, Bd 31, 1982, S 291-293.
47. Leiterer, U., and Markgraf, H., "Zur Strahldichtekalibrierung des Spektralfotometers BAS," FEINGERÄTETECHNIK, Bd 32, 1982, S 164-167.

48. Lenz, J., "Zur Methode der Sestonbestimmung," KIELER MEERESFORSCHUNGEN, Bd 27, 1971, S 180-193.
49. Lenz, J., "Phytoplankton," in: "Assessment of the Effects of Pollution on the Natural Resources of the Baltic Sea," Helsinki, 1981, pp 295-312.
50. Lenz, W., "Monatskarten der Temperatur der Ostsee dargestellt für verschiedene Tiefenhorizonte," DEUTSCHE HYDROGR. Z. ERG.-H., No 11, 1971, 147 S.
51. Lorenzen, C.J., "Determination of Chlorophyll and Phaeopigments: Spectro-Photometric Equations," LIMNOL. OCEANOGR., Vol 12, 1961, pp 343-346.
52. Matthäus, W., "Zur mittleren jahreszeitlichen Veränderlichkeit der Temperatur in der offenen Ostsee," BEITR. MEERESKUNDE, Bd 40, 1970, S 117-155.
53. Matthäus, W., "Mittlere thermische Schichtungsverhältnisse im Oberflächenwasser der offenen Ostsee," BEITR. MEERESKUNDE, Bd 42, 1979, S 123-131.
54. Matthäus, W., Sturm, M., and Francke, E., "Einige Aspekte des thermischen Regimes der Ostsee im Sommer 1975 am Beispiel der Bornholmsee," METEOROL. Z., Bd 20, No 6, 1976, S 360-372.
55. Morel, A., and Prieur, L., "Analysis of Variations in Ocean Color," LIMNOL. OCEANOGR., Vol 22, 1977, pp 709-722.
56. Morel, A., "In-Water and Remote Measurements of Ocean Color," BOUND-LAYER METEOROLOGY, Vol 18, No 2, 1980, pp 177-202.
57. Siegel, H., et al., "Some Preliminary Results of Investigations on the Spectral Reflectance in the Baltic Sea," in: "Proc. XIII Conf. Baltic Oceanogr.," Helsinki, 1982, pp 628-643.
58. Shaffer, G., "Baltic Coastal Dynamics Project--The Fall Downwelling Regime of Askö," CONTRIBUTIONS ASKÖ LABORATORY OF STOCKHOLM, No 7, 1975, 61 p.
59. Smith, W.L., Rao, P.K., Koffler, R., and Curtis, W.R., "The Determination of Sea Surface Temperature from Satellite High Resolution Infrared Window Radiation Measurements," MONTHLY WEATHER REVIEW, Vol 98, 1970, pp 604-611.
60. Sturm, B., "Selected Topics on CZCS-Data Evaluation," in: "Summer School on Remote Sensing Application in Marine Science and Technology," Dundee, 1982.
61. Sturm, M., and Helm, R., "Zur raum-zeitlichen Variabilität der horizontalen Wärmeadvektion in der westlichen Ostsee," BEITR. MEERESKUNDE, Bd 48, 1983, S 9-22.

62. Victorov, S.V., Vinogradov, V.V., and Terziev, F.S., "Studies of the Baltic Sea with the Help of IR-Diapason 'Meteor-2' Information," in: Proc. XIII Conf. Baltic Oceanogr., Helsinki, 1982, pp 732-741.
63. Walin, G., "Some Observations of Temperature Fluctuations in the Baltic," TELLUS, Vol 24, No 3, 1972, pp 187-198.
64. Wennerberg, G., "Användning av vädersatellitdata för att studera ytattentemperatur," SMHI, HB, REPORT NR 41, Norrköping, 1980.
65. Wilson, W.N., "Measurements of Atmospheric Transmittance in a Maritime Environment," SPIE, Vol 195, ATMOSPHERIC EFFECTS ON RADIATIVE TRANSFER, 1979, pp 153-159.

COPYRIGHT: Gosudarstvennyy komitet SSR po gidrometeorologii i kontrolyu prirodnoy sredy (Goskomgidromet), 1985

12595

CSO: 8144/3462

- END -